

# **The Design, Characterisation and Application of an Accelerated Drill Test for Cutting Tool Development**

A thesis submitted in fulfilment of the requirements for the degree of  
Master of Applied Science by Research

Jimmy Timothy Toton BSc

School of Applied Sciences  
College of Science, Engineering and Health  
RMIT University  
June 2014

## **Acknowledgements**

I would firstly like to thank my supervisors Dr Steve Dowey and Professor Edward Doyle for all their support, encouragement and most of all patience.

Special thanks also go to Dr Antony Pilkington and André Rousseau for all their guidance, support and experience. It was always a pleasure to work and learn from them.

I would also like to thank my parents and grandparents, for helping to shape who I am and always supporting me with my academic endeavours.

In addition, I would like to thank RMIT University and the DMTC for the funding which allowed me to learn so much, I am truly grateful.

Finally, I would like to thank the employees of Sutton Tools, particularly Michael Grogan, Guy Stephens and Fred Peters for all their support and expertise. I gained so much valuable experience working at Sutton Tools Thomastown, it was a privilege. All workpiece materials, cutting tools and access to coating and metrology facilities are appreciated.

## Declaration

I certify that except where due acknowledgement has been made, the work is that of the author alone; the work has not been submitted previously, in whole or in part, to qualify for any other academic award; the content of the thesis is the result of work which has been carried out since the official commencement date of the approved research program; any editorial work, paid or unpaid, carried out by a third party is acknowledged; and, ethics procedures and guidelines have been followed.

Signed.....

Jimmy Timothy Toton

17/06/2014

## Abstract

Metal cutting has been shown by other researchers, as well as within this work, to be a stochastic process with many complex behaviours and sources of variance which detrimentally affects the scatter in tool life results. Empirical testing is still the preferable method for cutting tool development especially in an industrial environment, as models are currently unable to replicate the complex interaction between cutting tool and workpiece as tool wear is the result of several mechanisms working simultaneously. The use of low value Jobber drills has been used as a vehicle for cutting tool development beyond the scope of specific drill design features, specifically for the purpose of coating research and development.

The need to quantify differences in sample groups and make sound statistical inference's about their populations is crucial for any large scale tooling manufacturer to manage the level of quality, as well as to continually improve their products. This is highlighted in the cutting tool market as end users are continually demanding longer tool lives, low variance and no early tool life failures, as large amounts of overhead costs are incurred in partially manufactured components, with sudden tool failure resulting in substantial costs to a business. Accepting that the drive for productivity is constant and universal, manufacturers must not only continually increase the productivity and quality of their manufacturing capability but their research and development methods as well. Hence within the arena of cutting tool manufacturing a robust, sensitive, rapid and low cost cutting tool test was found to not only be necessary but essential. The objective of this research was to design and develop a destructive accelerated drill test.

It was found, that although sources of machining complexity and variance which affects the scatter in tool life data, specifically in context of drill testing, have been identified within the literature; specifically the effect of plate hardness, a solution to deal with it has not yet been provided. Using a systems approach facilitated the management of the complex behaviours so a machining regime could be identified which offered a repeatable and mono-modal tool failure, a robust test, as well as, where possible, to minimise and empirically model the effect of machining variance on tool life scatter, a sensitive test. A statistical approach was also adopted for the drill test methodology so tool life data generated would be able to resolve differences in tool life, using small samples, so that conclusions could be made with a high level of confidence on the population of drills. The notion of a universal drill test which can adequately resolve tool life differences for all design features was not possible because the application of the cutting tool would need to be taken into consideration before conducting a drill test.

D2 cold work tool steel was able to offer a low tool life standard deviation and a mono-modal tool failure mode. In stark contrast P20 plastic mould steel showed a larger standard deviation and a bi-modal failure mode. Therefore, D2 was able to fulfil the robustness

requirement that the drill test was identified to need. This work also showed that for accelerated testing of HSS cutting tools, which are thermally sensitive, an abrasive wear test is preferable over a thermo-chemical wear type.

Pre inspection of drill geometries for the rejection of Jobber drills outside of tolerance was found to be less of an issue when distinguishing the difference between sample means. It was assumed that the drills outside of tolerance would be randomly distributed, along with their effect on tool life. It was important however to determine, that the drills outside of tolerance, would have a small effect on the standard deviation in tool life, relative to the sample size and relative to the sample means so statistically significant results could be determined.

It was found that the specific torque value may be used to describe a drills performance because it was shown to vary little over the steady state phase of life, however, further work would need to be conducted to test this hypothesis. This methodology may allow drill testing to be stopped once the steady state region has been reached. At which point the drilling torque can be compared with a reference or base line to distinguish if a design feature has made a change.

An extended Taylor's tool life model was generated which modelled the effect of batch to batch mean plate hardness between the range of 467HLD to 511HLD for annealed D2 cold work tool steel. This work showed that the life of uncoated M2 HSS 6.35mm Jobber drills is sensitive to small changes in plate hardness. At a cutting speed of 25m/min an increase in plate hardness from 467HLD to 492HLD, an increase of 5.3%, decreased drill life by 70.9%. The complexity of machining imposes limitations on the justification for how many machining factors should be modelled using empirical methods. An alternative solution to empirical modelling is the use of a large population of reference test drills which could be sampled each time a new test plate or batch of test plates were supplied. This methodology would allow a constant reference to be used to correct for the difference in plate hardness.

# Table of Contents

## The Design, Characterisation and Application of an Accelerated Drill Test for Cutting

Tool Development .....	i
Acknowledgements .....	ii
Declaration .....	iii
Abstract .....	iv
Glossary of terms .....	x
Nomenclature Drill Features .....	xi
<b>1 Introduction .....</b>	<b>1</b>
1.1 Cutting Tool Testing .....	1
1.2 Drill Testing Methodology .....	2
1.3 Variance in Drill Testing .....	3
1.4 Complex Behaviours.....	4
1.5 Summary .....	5
<b>2 Literature Review.....</b>	<b>6</b>
2.1 Introduction .....	6
2.2 Drill Design.....	7
2.3 Cutting Tool Testing.....	8
2.3.1 Drivers of Cutting Tool Development .....	8
2.3.2 Destructive Versus Non-Destructive Cutting Tool Testing.....	9
2.4 Metal Cutting.....	12
2.4.1 Chip Formation .....	12
2.4.2 Wear Mechanisms.....	14
2.4.3 Tool Wear Evolution.....	18
2.5 Metal Cutting as a System .....	20
2.6 Tool Life Modelling .....	24
2.7 Statistical Methods.....	26
2.8 PVD Technology .....	32
2.8.1 Substrate Cleaning.....	32
2.8.2 Cathodic Arc Deposition.....	32
2.9 Metrology Tools .....	34

2.9.1	Alicona Infinite Focus Microscope .....	34
2.9.2	Tool Maker's Microscope.....	38
2.10	Summary .....	41
<b>3</b>	<b>Experimental Design, Development and Application of an Accelerated Drill Test....</b>	<b>43</b>
3.1	Drill Test Design.....	43
3.2	A Statistical Analysis Comparing Tool Life and Failure Modes from Accelerated Drill Tests in P20 and D2 Steel Plate .....	47
3.2.1	Introduction .....	47
3.2.2	Experimental Procedure.....	48
3.2.2.1	Workpiece Material D2 and P20 .....	48
3.2.2.2	Drilling Conditions in D2 and P20 Steel .....	49
3.2.2.3	R40 Drill Hardness.....	49
3.2.2.4	Statistical Analysis methods.....	49
3.2.3	Results.....	50
3.2.3.1	P20 and D2 microstructure and hardness.....	50
3.2.3.2	R40 Drill Hardness.....	52
3.2.3.3	Tool life results .....	52
3.2.3.4	Weibull Failure Mode Analysis.....	55
3.2.4	Discussion .....	60
3.2.5	Conclusions.....	62
3.3	Examining Sources of Tool Life Variability and Torque and Thrust Response to Cutting Parameters in Drilling of D2 Steel.....	64
3.3.1	Introduction .....	64
3.3.2	Experimental Procedure.....	65
3.3.2.1	Jobber Drill Geometry .....	65
3.3.2.2	Workpiece Material & Hardness.....	66
3.3.2.3	Accelerated Cutting Conditions.....	66
3.3.2.4	Torque and Thrust Measurements .....	67
3.3.3	Results.....	68
3.3.3.1	Jobber Drill Geometry .....	68
3.3.3.2	Workpiece Material.....	71
3.3.3.3	Torque and Thrust Results .....	72

3.3.4	Discussion .....	76
3.3.5	Conclusions.....	78
3.4	Applying the Drill Test to a Surface Engineering Case Study.....	79
3.4.1	Introduction .....	79
3.4.2	Experimental Procedure.....	80
3.4.2.1	Drag Polishing.....	81
3.4.2.2	Surface Roughness Analysis.....	82
3.4.2.3	Coating Thickness Measurements .....	83
3.4.2.4	Drill Test .....	84
3.4.3	Results.....	85
3.4.3.1	Coating Thickness .....	85
3.4.3.2	Surface Analysis .....	85
3.4.3.3	Tool Life Results.....	89
3.4.4	Discussion .....	93
3.4.5	Conclusions.....	95
3.5	Modelling the Effect of Batch to Batch Plate Hardness on Tool Life for Uncoated Jobber Drills using Empirical Methods.....	97
3.5.1	Introduction .....	97
3.5.2	Experimental Procedure.....	98
3.5.2.1	Workpiece Material.....	99
3.5.3	Results.....	99
3.5.3.1	Workpiece Material.....	99
3.5.3.2	Taylor’s Tool Life Model .....	99
3.5.3.3	Extended Taylor’s Tool Life Model .....	102
3.5.4	Discussion .....	103
3.5.5	Conclusions.....	104
<b>4</b>	<b>Discussion: The Developed Accelerated Drill Test.....</b>	<b>105</b>
<b>5</b>	<b>Conclusions and Recommendations for Further Work .....</b>	<b>110</b>
5.1	Conclusions.....	110
5.2	Recommendations for Further Work .....	112



<b>Appendix A – VMC Setup and Programming for Drill Testing.....</b>	<b>113</b>
Programming a VMC Using G and M Code with Global and System Variables .....	113
Network Infrastructure .....	116
<b>Appendix B - Designing an Automated Drill Test and DAQ System for Spindle Current Collection.....</b>	<b>117</b>
Automated Drill Testing .....	117
DAQ System for Spindle Current Collection .....	118
<b>Appendix C – Chapter 3.2 Data .....</b>	<b>123</b>
<b>Appendix D – Chapter 3.3 Data.....</b>	<b>125</b>
<b>Appendix E – Chapter 3.4 Data &amp; Results .....</b>	<b>134</b>
<b>Appendix F – Chapter 3.5 Data &amp; Results .....</b>	<b>153</b>
<b>References.....</b>	<b>156</b>

## Glossary of terms

ANOVA	Analysis of Variance
BUE	Built-Up-Edge
CNC	Computer Numerical Control
DAQ	Data Acquisition (System)
DOE	Design of Experiment
HLD	Hardness Leeb D
HRC	Hardness Rockwell C
HSS	High Speed Steel
HV <sub>30</sub>	Hardness Vickers 30Kg Load
ICMCTF	International Conference on Metallurgical Coatings and Thin Films
L <sub>c</sub>	Cut off wavelength
MRR	Material Removal Rate
NAF	Nylon Abrasive Filament
NAS	National Aerospace Standard
PVD	Physical Vapour Deposition
QA	Quality Assurance
R&D	Research and Development
SEM	Scanning Electron Microscope
SOP	Standard Operating Procedure
S	Standard deviation
VB <sub>B</sub>	Flank wear
VB <sub>BMax</sub>	Flank wear maximum limit
VMC	Vertical Milling Centre
WC Co	Tungsten Carbide Cobalt
X	Sample mean
XRF	X-Ray Fluorescence
$\sigma$	Population standard deviation
$\mu$	Population mean
2.5xD or 3xD	2.5 times the Diameter or 3 times the Diameter of a drill
3D	3 Dimensions

# Nomenclature Drill Features

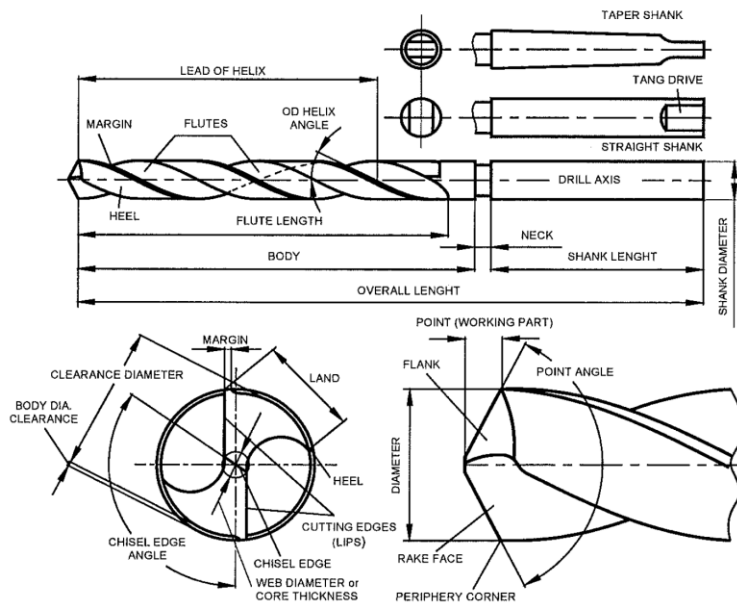


Figure N.1. A schematic of the design features for Jobber drills [1], with kind permission from Springer Science+Business Media.

Table N.1. The following terms have been copied from the 'Geometry of Single-point Turning Tools and Drills' as a point of reference for terminology on drill features used throughout this work [1], with kind permission from Springer Science+Business Media.

Axis	The imaginary straight line which forms the longitudinal centre line of the drill.
Back taper	A <i>slight!</i> decrease in diameter from front to back in the body of the drill.
Body	The portion of the drill extending from the shank or neck to the periphery corners of the cutting lips.
Body diameter clearance	That portion of the land that has been cut away to prevent its rubbing on the walls of the hole being drilled.
Chip packing	The failure of chips to pass through the flute during the cutting action.
Chisel edge	The edge at the end of the web that connects the cutting lips.
Chisel edge angle	The angle included between the chisel edge and the cutting lip, as viewed from the end of the drill.
Clearance	The space provided to eliminate undesirable contact (interference) between the drill and the workpiece.
Cutting tooth	A part of the body bound by the rake face and flank surfaces and by the land.
Drill diameter	The diameter over the margins of the drill measured at the periphery corners.
Flute length	The length from the periphery corner of the lips to the extreme back end of the flutes.

Flutes	Helical or straight grooves cut or formed in the body of the drill to provide cutting lips, to permit removal of chips, and to allow cutting fluid to reach the cutting lips.
Galling	An adhering deposit of nascent work material on the margin adjacent to the periphery corner of the cutting edge.
Helix angle	The angle made by the leading edge of the land with the plane containing the axis of the drill.
Land	The peripheral portion of the cutting tooth and drill body between adjacent flutes.
Land width	The distance between the leading edge and the heel of the land measured at right angles to the leading edge.
Lead	The axial advance of a helix for one complete turn or the distance between two consecutive points at which the helix is tangent to a line parallel to the drill axis.
Lip (major cutting edges)	A cutting edge that extends from the drill periphery corner to the vicinity of the drill centre.
Lip relief	The relief made to form flank surface. There can be several consecutive relieves as the prime relief, secondary relief etc. made to clear the lip as well as to prevent interference between the flank surface and the bottom of the hole being drilled.
Margin	The cylindrical portion of the land which is not cut away to provide clearance.
Periphery corner	The point of intersection of the lip and the margin.
Relative lip height	The difference in indicator reading between the cutting lips.
Web	The central portion of the body that joins the lands. The extreme end of the web forms the chisel edge on a two flute drill.

# 1 Introduction

## 1.1 Cutting Tool Testing

At the 2011 International Conference on Metallurgical Coatings and Thin Films (ICMCTF), Dr. S. Veprek; after his acceptance lecture for the R.F Bunshah award, was asked “what is the best way of testing coatings for cutting tools?” He answered that the only relevant way was “...to apply it on a cutting tool”. Kopac in 1996 also argues that experimental research has advantages over metal cutting models [2] “the experimentally-obtained specifics with respect to heterogeneity of the workpiece material can” using quick stop devices “be presented in the form of reliable results, which could otherwise, on the basis of theoretical models and calculations, hardly be done in such a clear way”. The specifics Kopac refers to are aspects of the cutting process such as, chip thickness, shear plane angle, crystal grain deformation and the effect BUE formation. In 2001 he recognised that considerable effort in modelling had taken place, citing that molecular dynamic models have been used to simulate the cutting process. However, the models “considerably simplify” the cutting process as tool wear is the result of several mechanisms working simultaneously, hence, it is difficult to analyse [3] (Figure 2.2). Shaw [4] goes a step further with respect to cutting tool development and states that “it is not possible to use non-cutting tests to evaluate cutting tools” as the temperatures and pressures play such an important and complex role. Therefore at the time of writing in 2014 it is still preferable, from a scientific standpoint, to test cutting tools directly.

It is estimated that 15% of the value of all mechanical components manufactured worldwide are derived from machining (incidentally, 36% of all machining operations comprised hole making [5]). The worldwide cutting tool revenue in 1999 was estimated to be \$18.3B US dollars, with HSS cutting tools making up \$5B [6]. By 2015 the market is estimated to grow to \$20.44B, with HSS cutting tools growing to \$6.2B [7]. Cutting tools are consumed by machine tools and this market follows global economic cycles [8] and technology advances. So, far from being a simple object, frozen in its design, the ‘cutting tool’ reflects, drives and is driven by machine tool development and consumption.

Hole making can be broadly defined as operations which make holes in materials. Atkins [9] uses an unorthodox example of hole making by burning a hole through wood with a red hot poker from the fire, this method can be thought of as the ancestor of hole making. While at the time of writing this thesis one of the most advanced methods of hole making, using cutting tools, is helical milling. Helical milling has been shown by Iyer [10], through experimentation, that it is able to offer, higher productivity, tool life and surface finish compared to drilling using specifically designed drills in the difficult to machine application of hole making in hardened D2 at 60HRC. However, hole making using drills is still a

significant operation as the Gardner Tooling and Workholding survey of 2010 [11] revealed that in 2011 drills made up 12% of the entire US cutting tool market.

This work is therefore well justified both scientifically and economically. The work in this thesis was undertaken to further refine and develop a drill test methodology at the partner organisation's workplace (Sutton Tools Pty Ltd), which was used to empirically model drill life and further optimise and develop cutting tool features and design attributes – i.e. with wider application than drills alone.

## 1.2 Drill Testing Methodology

There are three main reasons why cutting tool testing is conducted by the partner organisation. The first is to perform quality assurance testing; so that a level of quality may be managed. The second is benchmarking; where performance measures such as tool life, surface integrity and productivity are compared against competitor products. The third is in the application of product engineering; testing different design features such as macro geometries, micro geometries, surface treatments and coating compositions and architectures (for tool life or productivity improvements). Sutton Tools make and test many cutting tool products but as this work concentrates on twist drill testing, albeit with application to other cutting tools, tools such as end mills and cutting or forming taps will not be explicitly described.

The ability of a drill test to provide experimental conclusions in product engineering experiments will be explored in later chapters, indeed it is the motivation for this thesis. However, it is important to introduce the basics of a drill and a drill test method at this point.

A drill is [1] “an end point cutting tool for machining holes having one or more major cutting edges, and having one or more helical or straight chip removal flutes”. The prime cutting motion is rotation applied to the drill or workpiece or to both and the feed motion is applied along the longitudinal axis of the drill to the drill or workpiece.

Vogel and Bergmann [12] in 1986 reported a method of drill testing where a number of Jobber drills are consumed in a machining centre at accelerated machining parameters. The drills are driven by the VMC to failure over a number of holes, which are drilled into a prepared 42CrMo4 steel plate. Failure is simply determined by catastrophic failure of the drills. This is indicated by a loud screech, or occasionally a drill may shatter or melt. This is a destructive test, suited to testing low value tools. High value drills made from tungsten carbide cobalt (WC Co) for example are typically not tested destructively. The carbide drill will be consumed (i.e. wear) until a predefined wear or force limit has been reached (Figure 2.10). This allows the tool to be recovered by re-grinding. Carbide drills could be tested to destruction but this will likely consume large quantities of test material, as it is more wear resistant (physically and thermo chemically) than HSS [13, 14].

### 1.3 Variance in Drill Testing

It is clear when a single drill has failed destructively, however not all drills will fail at the same time. The life of a population of drills will have some distribution. Typically, wear-out processes follow a normal distribution compared to fatigue failure which has a highly skewed distribution [15]. Notwithstanding, depending on the type and number of wear and failure modes in operation, the distribution may be non-normal and multi-model. It is therefore necessary to define sources of variance in drilling which effect tool life variance as well as the theory of central limit theorem which is the basis for inferential statistical tests used to estimate population parameters using sample statistics.

Statistics offers a tool to estimate population parameters. This work will make multiple references to confidence and significance. Both words have a particular meaning when used in statistical analysis. Confidence means that a population mean (a constant) can be estimated to lie in a range applied to the sample mean (a variable) at a particular limit. This limit is the significance level, the probability that the cause behind the change in population (in this work a change in tool life) has occurred due to a particular design change or fault. If the researcher uses a significance limit of 5% they are allowing a 5% chance that they are wrong, that the change in tool life was due to some other cause besides the change that they have applied to a sample. Incidentally, the central limit theorem is what allows levels of confidence to be applied to a population estimate. Central limit theorem describes the population of means. The population of means is the combination of an infinite number of individual means from a sample size of  $N$  randomly sampled from a large population. Regardless of the type of distribution of the original large population, the population of means curve will increasingly approximate the shape of a normal curve 'bell shaped' as the large population is repeatedly sampled.

A source of variance that effects the distribution of tool life results and hence the ability to determine if a change has occurred is the workpiece. This can be in the form of plate hardness variation within a single plate or batch to batch. Vogel and Bergmann [12] determined the effect of plate hardness on the tool life for Jobber drills tested to screech failure in 42CrMo4 steel. They showed that between 28-36 HRC an exponential fall in the number of holes drilled (tool life) occurs. The batch to batch plate hardness variation is usually outside the control of the researcher, with only limited options for control, such as expensive heat treatment or excluding sections of plate which fall outside a specific tolerance. In this instance it is therefore justified to empirically model this effect in order to develop a robust drill test which can compare tool life results over time.

The variance in macro geometry features is another significant source of tool life variance. According to the American National Aerospace Standard for split point drill design [16] the primary lip relief, lip height variation and chisel edge centrality are key features which require repeatability and uniformity in manufacture. Firstly, if these features deviate from required specifications and/or are non-uniformly ground, the dimensional accuracy and tool

life performance will be significantly lowered [17]. Secondly, if the repeatability of the grinding process varies across a production run, then the tool life distribution will likely reflect this variance [18]. This last statement is exactly what a quality assurance (QA) drill test should be able to resolve, on the other hand, a product engineering experiment aimed at distinguishing if there is a difference in tool life between two coatings or surface treatments, will require this source minimised (preferable eliminated altogether). These concepts are universal to all cutting tool design features with varying levels of significance on tool life between them. Galloway [19] reported that for the point angle a 50% difference in drill life was observed when drilling En 10 steel between the angles of 80-90 degrees. Additionally, a 65% difference in drill life can be obtained when the primary relief angle varies between 4-12 degrees.

Vogel and Bergmann [12] reported the results of a drill test and reiterated a well-known characteristic that a PVD TiN coating can increase the mean tool life of HSS drills [20-22]. Supplementary to this finding was the unexpected result that a high quality coating can reduce the tool life variance. Their findings represent a goal in quality product engineering, increasing the mean and reducing the variation in a products intrinsic life.

In the context of cutting tool testing, a low standard deviation is also preferable, as it may allow hypotheses to be answered with a high level of confidence. According to Eq. 3 (page 30), the two main factors that can minimise the confidence intervals and maximise the ability to distinguish a difference between the mean tool lives of two populations; are the denominator  $n$  (sample size) and the numerator  $S$  (standard deviation). Typically, time and cost constrain the sample size  $n$ . However, if  $n$  is small it will result in an increase in  $t$ , which will have a detrimental effect on the confidence interval (further discussed in chapter 2.7).

Therefore, the standard deviation  $S$  needs to be as small as possible. The numerator in the equation for 'S' (Eq. 4 page 30) reveals that the significant factor which can reduce  $S$  is minimising the difference between a tool life result and the mean tool life. The need to minimise  $S$  is therefore the objective of the modifications to the drill test.

## **1.4 Complex Behaviours**

Sources of variance are not the only element which needs to be addressed when designing a test which can correctly distinguish tool life differences between sample groups. Complex behaviours within the machining system need to be managed. Astakhov [1] published a report discussing the mismanagement of the gun drill in the automotive and mould-making industry. A survey completed by members in this industry showed, among other points that the gun drill was not being used at the correct cutting parameters 52% of the time and was not being used (consumed) to the correct tool life capacity 57% of the time. He followed this survey by using a systems approach to identify the factors of the gun drill system. He identified sources of complex behaviours and variance within the gun drill system and



stated that “that only when there is system coherency will we be able to achieve productive use of cutting tools”, however, a solution to this problem was not provided.

The complex behaviour of the wear mechanisms interacting with the cutting tool has been introduced. Notwithstanding, another source of complex behaviour which requires management is exhibited by the workpiece material. The crystal phase structure [23] thermal conductivity and carbide distribution [24] for example, will influence a materials ability to resist cutting i.e. machinability. This intrinsic resistance to be cut can be observed by measuring the cutting forces, rate of tool wear or life at failure during machining (further discussed in chapter 2.4).

A further source of complex behaviour is the machine tool interaction with the cutting tool and workpiece [1] i.e. machining system. For example, the dynamic and static rigidity of the spindle and workpiece fixturing are sources of complex vibration during machining. This thesis will not be directly investigating this source of complex behaviour; however, it is relevant to introduce it, as steps were taken during the preliminary drill test design phase to reduce this influence on tool life.

## **1.5 Summary**

Empirical testing is still the preferable method for cutting tool development, especially in an industrial environment, as machining has been shown to be a stochastic process with many complex behaviours and sources of variance [12, 25, 26]. Drill testing can be used as a vehicle for cutting tool development beyond the scope of specific drill design features [12]. Vogel and Bergmann identified that a drill test is sensitive to changes in plate hardness [12]. Astakhov, using a systems approach identified the sources of variance in the application of gun drilling. However, a solution to dealing with these sources of machining variance which affects tool life data in the context of drill testing has not yet been provided. Therefore, the objective of this research is to apply a systems approach to designing and developing a destructive accelerated drill test. Managing the complex behaviours and minimising and empirically modelling their source of variance on tool life will allow a drill test to be able to resolve differences in cutting tool failure data and be compared over multiple tests as the scatter in tool life results will be minimised. So as to allow decisions to be made, by statistically analysing tool life data with a level of significance applied.

Managing the complex behaviours found in machining leads to a concept of robustness. In the context of drill testing this means that it must be able to offer a repeatable failure mode over time. This will be achieved by determining a machining strategy which can offer a predominate and repeatable wear/failure mode, i.e. a regime of ‘stable complexity’. Minimising and modelling sources of machining variance on tool life leads to the concept of a sensitive test. Hence, it is possible to have a robust yet sensitive test without it being a contradiction of terms.

## 2 Literature Review

### 2.1 Introduction

The machining system has a series of complex interactions working simultaneously [1, 13, 25]; furthermore, these interactions have their own source of variance [1]. These sources of complex behaviour and their related sources of variance will have an effect on the measures of central tendency and dispersion of tool life results [1, 19]. Therefore, in order to design a drill test in which conclusions may be drawn with a level of confidence, these complex behaviours will need to be firstly identified using existing literature as well as experimentally investigated for a particular drilling system, with the aim of managing the complex behaviours for a repeatable and mono-modal failure mode, additionally, minimising or empirically modelling their source of variance on tool life (scatter) so small changes in life may be distinguished.

The following subchapters review work completed by other researchers in the areas of drill design, cutting tool testing, metal cutting and tool life modelling. It also covers the tools used in order to complete this work such as, statistical test methods for machining data analysis, PVD coating technology used for drill sample production, tool maker's microscope and the Alicona Infinite Focus Microscope (IFM) used to determine the geometry and surface roughness of cutting tools.

## 2.2 Drill Design

Cutting tool design is a combination of tool material such as HSS or WC-Co, macro and micro geometry and surface and coating engineering. According to Davim [13] cutting tool geometry is of prime importance because it directly effects; chip control, productivity of machining, tool life, direction and magnitude of cutting forces and surface integrity. This thesis uses Jobber drills as a vehicle for cutting tool development. Therefore, the test must be able to correlate tool design and performance at accelerated cutting conditions; hence the author sees it as fundamental to understand the basic cutting actions and design features of a Jobber drill which is discussed throughout this work.

A drill is “an end point cutting tool for machining holes having one or more major cutting edges, and having one or more helical or straight chip removal flutes” [1]. The prime cutting motion is rotation applied to the drill or workpiece or to both and the feed motion is applied along the longitudinal axis of the drill to the drill or workpiece. There are many different types of drill designs, for this work the standard Jobber drill will be introduced, also known as a twist drill [16]. The Jobber drill is a homogenous drill, made of one piece of tool material such as HSS or carbide, making holes in solid workpieces without previously made holes. It may have a straight shank, taper shank or a tang drive, which may or may not have the same diameter of the body of the drill. The jobber used in this study is of regular length, having a length-to-diameter ratio not exceeding 10 [1]. Two flutes are used for chip removal with no special means for coolant supply. According to Astakhov [1] the jobber drill is a ‘transiently-balanced drill’ meaning that only the margins support the radial direction. This description by Astakhov is only accurate when the drill is fully engaged into the workpiece, meaning, when the outer corner/s of the cutting edge are engaged in the workpiece. Prior to this point the drill is not transiently-balanced as the chisel edge causes the drill to ‘wander’ which affects dimensional accuracy and hole straightness. Drill ‘wandering’ was first overcome by drilling a pilot hole using a small diameter drill. The split point drill was designed which provides secondary cutting edges near the centre of the drill. Radhakrishnan [27] reports that a split point drill not only does reduces wandering but also reduces thrust forces during drilling.

## 2.3 Cutting Tool Testing

### 2.3.1 Drivers of Cutting Tool Development

A significant aim of cutting tool development is to design tools which can work faster, Sandvik have published data [28] showing that only 1% saving in total costs can be achieved from 50% increases in life or tooling cost, whereas a 20% increase in a tools productivity provides a 15% reduction in part or component cost. In machining, an increase in productivity is achieved by increasing the material removal rate (MRR). Therefore, cutting tool testing is used to optimise tool design, because the best tools can increase productivity. Productivity (not tool life) is the only means of control that a cutting tool user has to substantially modify the cost of a good. Although productivity is significant in industry, it is difficult and time consuming to test for directly. Taylor [29] provided a solution to determining the productivity of a cutting tool by determining the relationship of Time (tool life) versus cutting speed in his work 'On the Art of Cutting Metal'. Why is the productive use of cutting tools important? There has been a continuous drive throughout history to make a profit and provide a service; it is summed by the mandate, faster, cheaper, lighter and stronger.

As end users apply pressure for development of products industries have responded by using more application driven materials with specific mechanical and chemical properties. For example, high strength to weight ratio titanium alloys for the aerospace industry, corrosion resistant stainless steels in the maritime industry and high temperature oxidation resistant nickel super alloys in the aerospace and automotive industries.

The adoption of new application driven materials by manufacturers has come at the price of machinability and therefore productivity. Materials such as titanium alloys and nickel based super alloys cause reductions in tool life and productivity [30, 31], due to their high rate of work hardening, their low thermal conductivity and an affinity to adhere to the tool.

Cutting tool manufacturers have sought solutions to these problems. In fact Smith [32] highlighted the properties a cutting tool should have in modern machining, namely, hot hardness, toughness, oxidation resistance, thermal shock resistance and a non-affinity to work piece material. Considerable research has been conducted into producing materials capable of sustaining high hardness at high temperatures, examples of which are HSS alloyed with cobalt [33], powder metallurgy HSS [34] and micro-grain carbide [35]. Significant research has also been conducted into the mass application of PVD coatings [21, 36, 37]. Such coatings offer abrasive wear resistance, low coefficient of friction and some act as a thermal barrier. This allows the cutting speeds and feed rates to be increased significantly compared to their uncoated counterparts.

This has led cutting tool manufacturers to no longer be just a cutting tool provider, but a source of expert knowledge in the machining of these 'difficult to machine materials' and the

associated cutting tool technologies. This knowledge and expertise, however, requires considerable investment into research and development as the testing of mass manufactured cutting tools becomes complex as there are many design features, such as tool macro geometries, cutting edge micro geometries, surface treatments and coating composition and architectures. All of which must be optimised for machining particular materials and part geometries, as well as characterising the optimal cutting conditions for primarily, productivity and secondary, life time improvements.

### **2.3.2 Destructive Versus Non-Destructive Cutting Tool Testing**

As Davim writes “tool life is not an absolute concept” [13]. A tool may be considered to have failed depending on the tool life criterion. Generally in finishing operations, surface integrity and dimensional accuracy are of prime concern, while in roughing operations excessive wear and cutting forces are the limiting factors [13]. It is not the aim of this thesis to examine different machining operations; however an appraisal of the different failure criteria and testing methods used by researchers must be conducted so the type of tool failure used throughout this work is clearly justified.

There are two cutting tool testing methodologies used by the partner organisation, a destructive method and a non-destructive method with two different failure criteria. The first methodology comprises of testing a small number of tools (1 or 2) at the cutting conditions and in the material for which the tool is designed. The evolution of tool life is characterised by either measuring flank wear or the cutting forces periodically over the life of the tool until a predefined wear or force limit is reached. This method can be graphically shown in Figure 2.10 and coincides with ISO standard 3685 [38] known as non-destructive testing, this method is typically used but not limited to high value tools. However, this method gathers limited information about the variance in manufacturing capability and no information to calculate an estimate of the populations tool life performance, unless this method of testing is applied to a larger sample set. However, this would significantly increase the work and time involved.

The second method used comprises of testing a small batch of cutting tools usually 2-4 at accelerated cutting conditions to catastrophic failure (destructive testing) or to a predefined length of cut or number of holes close (non-destructive). For example in a quality assurance test for drills, iron oxide treated drills would need to drill 40 holes at accelerated conditions before considered ‘passed’ while PVD coated drills would need to drill 120 holes before achieving the pass criteria. This methodology is known in industry as a ‘go, no go’ test, as the drill will either pass or fail. This criterion of failure censors the data to the right, therefore no information of the tool life variance is acquired and only limited information of the manufacturing variance. It is necessary to compare the industrial sponsor’s current testing methodologies to others in the field of metal cutting.

One of the first empirical studies of metal cutting and cutting tool testing started in 1880 by Frederick Winslow Taylor. As steel replaced cast iron as the predominate material of choice during the 2<sup>nd</sup> industrial revolution [39] the cutting conditions needed to work this material productively soon needed to be characterised. Taylor, a foreman at the Midvale Steel Company, observed that the workers there were not functioning efficiently, and this was limiting the number of parts produced per day (train tyres). He believed that the workers could be more productive, in his own words, Taylor [29]:

“He found, however, that his efforts to get the men to increase their output were blocked by the fact that his knowledge of just what combination of depth of cut, feed and cutting speed would in each case do the work in the shortest time, was much less accurate than that of the machinists who were combined against him.”

Put simply, no one knew the best practice until Taylor asked the questions and conducted the experiments, as the introduction of steel brought about its own challenges (its own complex behaviours).

There are many test methods for hard wear resistant PVD coatings, for example, the scratch test [40], pin on disk [36] and ball crater [37]. These tests have been used by PVD coating researchers to characterise the fracture toughness, wear, and adhesion strength respectively. Some of these coatings are then tested on cutting tools to determine if they can increase tool life or productivity. If a cutting tool test was developed that was timely, low cost and sensitive to small changes in life, then the aforementioned tests would not be needed in the context of developing better coatings for metal cuttings operations. None of these tests simulate the unique forces, thermal gradients and chip-tool-workpiece interactions which are found along the cutting edge/s and the principle cutting faces in machining operations. Vogel and Bergmann [12] assisted in the development of such a drill test for Guhring and Balzers. The effect of cutting conditions on tool life were characterised over wide range for coated and uncoated drills as well as the effect of plate hardness on tool life so as to eliminate this source of variance from tool life data. This type of cutting tool test can fulfil the three reasons why the partner organisation conducts tests for low value tools, as it would allow QA of products, benchmarking against competitors and experimental design performance verification.

Posti and Nieminen's work characterising the effect of coating thickness of TiN coated HSS turning and planning tools [41] used the combination of catastrophic failure criterion (destructive testing) with non-destructive methods, measuring the flank wear periodically. This methodology allowed the characterisation of tool life/wear evolution and also characterising the three stages of life, however, as this method is time/work intensive it was only applied to one tool per sample group and therefore not accounting for the variability in tool life performance.

A cutting tool test was developed by the Australian and New Zealand standards committee of 1994 for drills[42]. The cutting conditions and depth of holes are supplied for drill diameters between 3mm-75mm. The cutting speed remains fixed through all diameters, however, the penetration rate (mm/min) decreases as the diameter increases while the depth of holes follows an inverse of this relationship. The steel workpiece is also recommended, it must have a hardness value between 200-215 Brinell, a chemical composition with Carbon between 0.6-0.65%, Silicon between 0.15-0.30% and Manganese between 0.6-0.7 percent. The failure criterion used in this test is a "go, no go" where drills are tested to a particular limit and they pass or fail depending if they have reached it. Just like the partner organisations QA test this test censors the test to the right, therefore fails to provide information of the tool life variability or an indication of the manufacturing variance.

By examining the partner organisations testing methods, current industry standards as well as scientific published work, the choice of cutting tool testing methodology has been found to depend on a number of factors. One factor being the aim of the test such as, quality assurance, benchmarking or experimental verification. Another being the information required, pass or fail (censored data), measures of central tendency and/or dispersion and sample size and lastly, time and budgetary constraints.

## 2.4 Metal Cutting

Drilling produces chips using a number of cutting edges which are exposed to a variable cutting velocity and rake angle from the centre to the outer corner [1], therefore, it can be considered as a more complex machining operation than single point turning. This section will introduce and discuss the complex behaviours and sources of variance within metal cutting, the simplest cutting models will be used. The following subchapters first introduce the chip-formation process using a 2-D orthogonal single shear plane model. Next the type of wear mechanisms involved in metal cutting will be defined, followed by the evolution of tool wear which determines the life of a cutting tool.

### 2.4.1 Chip Formation

Metal cutting covers all manufacturing operations which produces shapes out of materials through the generation and removal of chips [4, 14]. Modern machining technology has its roots from the production of the steam engine in the 1760's, where easy to machine cast iron, brass and bronze as well as difficult to machine wrought iron were used and machined using basic hardened high carbon tool steel [14].

The simplest explanation of metal cutting is the 2-D orthogonal cut, which can be reasonably represented, in figure 2.1, as a hard large angled wedge (two faces, rake face and clearance face) which is fed into a work material to remove a thin layer through shear deformation [14]. The concentrated shear region has been observed, through orthogonal cutting experiments, to be localised along a shear plane starting at the cutting edge and heading up at an angle until the free surface, the angle and width of the shear plane is dependent on the cutting tool, workpiece and cutting parameters [1, 4, 14]. The newly created chip is then forced over the rake face under high compressive stresses, the underside of the chip undergoing further shear deformation [5, 14, 23, 43, 44].

An early and well known shear plane model was the Merchant single shear plane model [45]. This model was able to calculate the shear stress encountered along the shear plane during chip formation and the friction between the chip-tool interface. From this work Merchant concluded that the shear strength of the material is the only relevant characteristic showing the material's resistance to cut (machinability).



Figure removed due to copyright reasons.

Figure 2.1. schematic diagram of an orthogonal cut as used by Ernst and Merchant in their single shear plane model. It shows an area of undeformed material about to undergo high strain, high strain rate deformation along a shear plane producing a chip [14].

The assumptions of this model include [4, 45]:

1. The tool is perfectly sharp and there is no contact along the clearance face.
2. The shear surface is a plane extending upward from the cutting edge.
3. The cutting edge is a straight line extending perpendicular to the direction of motion and generates a plane surface as the work moves past it.
4. The chip does not flow to either side but behaves as a plane strain.
5. The depth of cut is constant.
6. The width of the tool is greater than the workpiece.
7. The work moves relative to the tool with uniform velocity.
8. A continuous chip is produced with no built up edge.
9. The shear and normal stresses along the shear plane and tool are uniform.

There are some fundamentals of the chip formation process, such as the chip separation criteria and contact conditions at the chip-tool interface that are not well understood. For example, does the chip separate via the formation of micro cracks ahead of the tool [46, 47] or should the deformation of the material be treated as plastic flow around the cutting edge [14]. Contrasting views for the chip-tool interaction are, does seizure contact explain the interactions between the chip and rake face [48] rather than intimate contact with relative movement [4, 44].

Turley and Doyle [23] examined the chip formation process during orthogonal cutting from the behaviour of the microstructure during machining. They concluded that chip formation is dictated by how the phase, size and orientation of the materials microstructure reacts under highly localised shear strain. They concluded that shear band formation was the fundamental microstructural mechanism defining the geometry of the chip along the shear plane. They observed that in machining copper in which the primary deformation mechanism is slip, acrystallographic shear bands do not form until high levels of strain are developed, this finding correlated with copper having a low shear plane angle. Whereas, in 70/30 brass acrystallographic shear bands form at lower levels of shear strain and hence give rise to a higher shear plane angle. This work highlights that the complex behaviour of the material being cut is specific for a particular material grain structure and cutting parameters and will affect the cutting forces necessary to generate chips.

## 2.4.2 Wear Mechanisms

During service, metal cutting tools are put under harsh conditions of high forces, high contact pressures, high temperatures and chemical attack [49]. Referring to figure 2.2, regions of wear and their corresponding wear mechanism are shown. A significant feature of machining steels is Built-up-edge (BUE) formation. This is another form of wear shown in shown in figure 2.8. BUE does not appear when machining pure metals, only alloyed materials with a two phase structure predominantly found in steels [14], as this work deals with drilling steels, BUE must be defined as it is a source of complex behaviour and its effect on tool life and cutting forces will be discussed in chapter 2.5.

Wear limits tool life by restraining productivity, increasing surface roughness and decreasing dimensional accuracy of the machined component. The mechanisms that cause tool wear at these regions are abrasion, adhesion, plastic deformation, fracture, oxidation and diffusion. What type of wear mechanism and the region it will operate in depends on a number of factors of the machining system, such as tool material, tool geometry, workpiece material and cutting parameters such as cutting speed, feed rate, depth of cut and cutting fluids.

Figure removed due to copyright reasons.

Figure 2.2. A schematic representation of an orthogonal cutting tool, depicting different potential mechanisms of tool wear operating at particular regions. Which may work simultaneously, highlighting the complexity of the metal cutting system [25].

Soderberg [50], Hogmark [49] and Barrow [51] each discuss wear as the combination of mechanism and region, depending on the above mentioned machining factors. This was found by the author to provide a more holistic interpretation of the wear mechanisms and their effect on tool life evolution. Stressing the evolution of wear at different phases of tool life which may change in severity or mechanism entirely, an example of this is the evolution of crater wear (see below). Davim [13] has published the wear mechanisms guide by Sandvik, this guide however, did not discuss wear as a dynamic process which evolves over time as the tool wears or if the machining parameters change. A description of the wear mechanisms and which region it predominantly operates in is defined.

## Abrasive wear

Abrasive wear operates on the flank and rake face (flute face) surfaces and is characterised by the mechanical removal of tool material from the tool surface due to the ploughing/scratching action of hard particles in the workpiece material. Abrasive wear is counteracted by increasing the hardness and the volume of carbides inside the cutting tool.

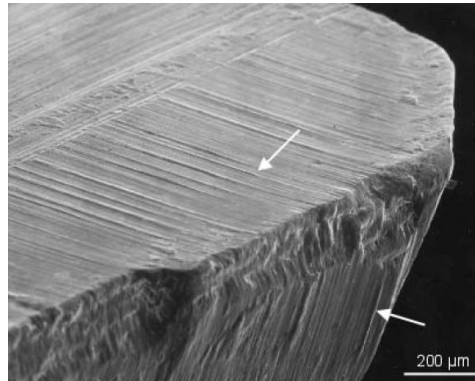


Figure 2.3. SEM micrograph showing ploughing/scratch marks on the flank and rake surfaces of a HSS cutting tool [49], with kind permission from the Society of Mechanical Engineers.

## Adhesive wear

Adhesive wear is a tearing of tool surface material by high shear forces between the chip-rake interface and the newly machined surface and the flank face, resulting in the removal of the surface layer and or small fragments in the direction of chip flow and tool (Figure 2.4(a)). Adhesive wear increases when the cutting edge reaches high temperatures or when cutting a chemically aggressive material, this may result in large scale plastic flow of surface material (Figure 2.4(b)). This form of wear can be resisted by using tool materials with high yield strength at elevated temperature or by applying a protective ceramic coating [20, 52].

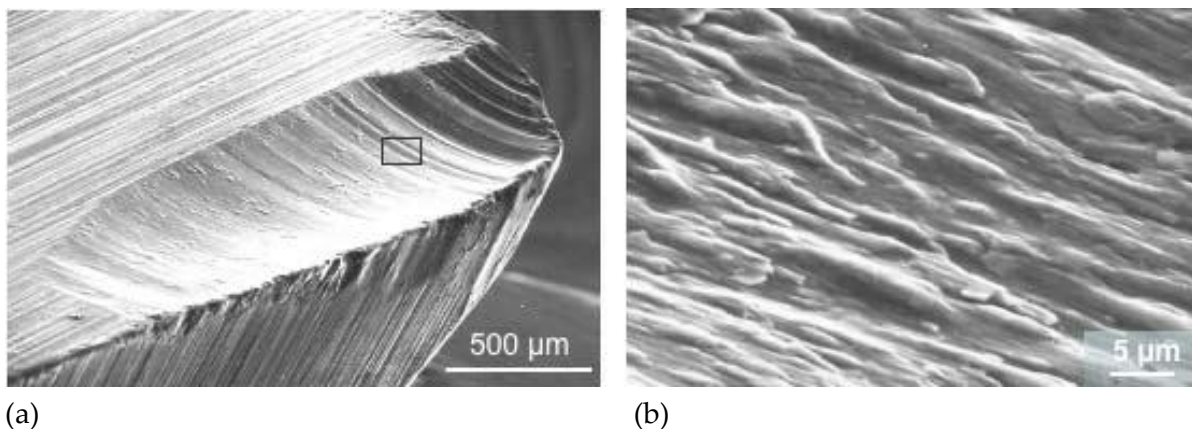


Figure 2.4 (a,b) SEM micrograph showing adhesive wear on the rake face of a HSS cutting tool. (a) low magnification of rake face, wear initially appears to be abrasive. (b) high magnification reveals that work/tool material has plastically deformed in the direction of chip flow [49], with kind permission from the Society of Mechanical Engineers.

## Plastic deformation

Severe plastic deformation may occur along the cutting edge if the tool material is loaded beyond the yield strength (Figure 2.5(a, b)). This may result in edge blunting and is exacerbated by an increase in cutting temperature [13, 49].

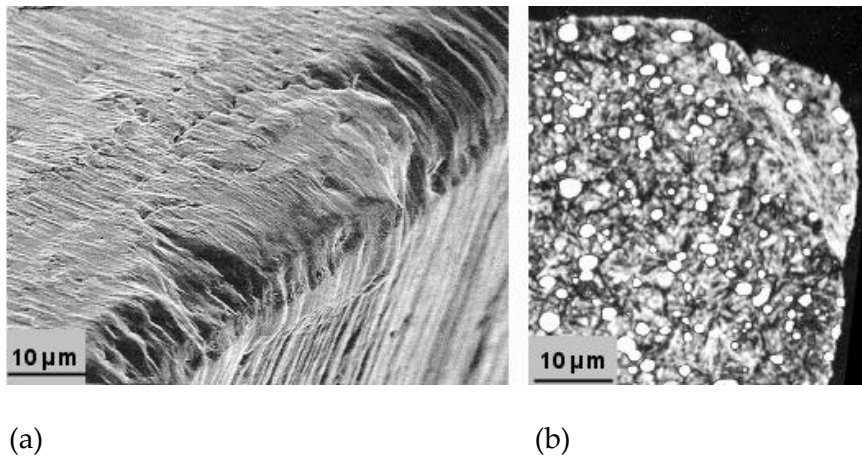


Figure 2.5(a, b). SEM micrographs showing (a) large scale plastic deformation blunting the cutting edge, (b) cross sectioned and etched showing region of deformation [49], with kind permission from the Society of Mechanical Engineers.

## Fracture and chipping

Macroscopic fracture of the cutting edge (Figure 2.6) may occur if the tool material is loaded beyond the yield strength at which point localised chippings may occur through brittle fracture. Edge chipping is most common during interrupted cutting operations such as milling and is counteracted by a high toughness material, however a high toughness material will have the hardness reduced.

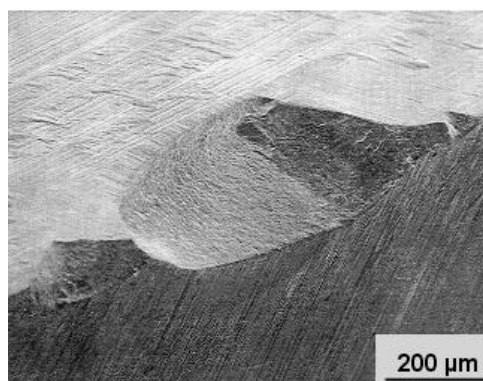


Figure 2.6. SEM micrograph showing localised chipping on the cutting edge [49], with kind permission from the Society of Mechanical Engineers.

## Crater wear

At low cutting temperatures crater wear is caused by a combination of abrasive and mild adhesive wear from the chip flow across the rake face (Figure 2.7) [13]. As the cutting temperature increases, severe adhesive wear in combination with oxidation and diffusion processes, increase the rate of tool material removal especially reactive metals like titanium [13]. PVD coatings offer protection from this type of wear as they offer a passive layer with a low chemical affinity to the workpiece.

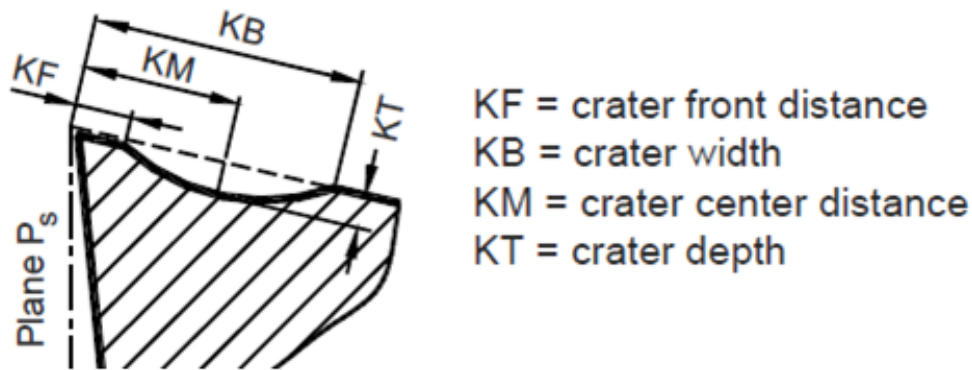


Figure 2.7. Schematic cross section of a cutting tool which shows crater wear on the rake face with corresponding definitions of how to measure the crater wear [13], with kind permission from Springer Science+Business Media.

## Built up edge

Built-up-edge (BUE) will occur during the machining of alloyed materials with two phases in their structure such as steels, a coating may diminish the size and adhesion strength of the BUE. Strain hardened workpiece material accumulates on the rake and flank faces as a series of successive layers (Figure 2.8) [14]. A BUE will eventually break away once it has grown unstable and will either travel up the rake face with the chip or be embedded in the newly machined surface reducing surface integrity.

Figure removed due to copyright reasons.

Figure 2.8. SEM micrograph showing built-up-edge on the rake face of a cutting insert [14].

### 2.4.3 Tool Wear Evolution

Cutting tools wear during use. An important characteristic of a cutting tool is the tool life. Tool Life is the length of time, length of cut or the number of components machined before the surface roughness, dimensional accuracy or some other measure important to the user is unsatisfactory [13]. A standard method used in the machining industry of quantifying the amount of wear is by measuring the amount of flank wear termed  $VB_B$ , ISO standard 3685 [38]. Figure 2.9 shows where on a Jobber drill the  $VB_B$  is measured. The maximum allowable flank wear  $VB_{B_{Max}}$ , depends on a number of factors such as the machining operation, tool size and the tolerances of the machined component set by the user. For example, rough milling allows a higher  $VB_{B_{Max}}$  as opposed to finish milling, justification for which is that sharpness of the cutting edge directly affects the surface roughness of the finished part. Once this  $VB_{B_{Max}}$  limit is reached the tool is said to have reached its useful life and can be classified as failed, at which point the tool will either be thrown away or sent to be re-sharpened.

Tool wear evolves over the lifetime of a cutting tool. The relationship between flank wear  $VB_B$  and length cut reveals three distinct phases of life (Figure 2.10(a)). Region I shows a steep gradient revealing a high initial wear rate with possible causes being damaged surface layers during the grinding process and edge rounding of the cutting edge [13]. Region II is referred to as 'steady state wear', which has a lower wear rate than region I and is usually the longest operating region. Region III also has an accelerated wear rate and is the final stage of tool life. As the tool wears, the cutting edge becomes blunt (rounded) and the contact lengths between the tool-chip-workpiece interfaces increase. This process directly increases the cutting temperature and forces at the cutting edge, leading to rapid tool failure.

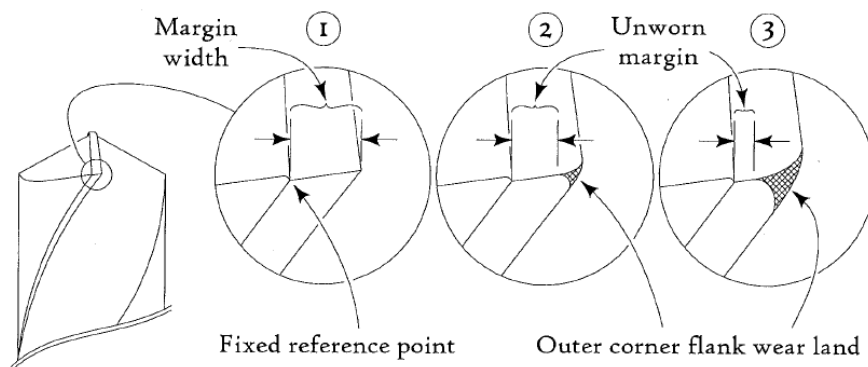


Figure 2.9. A schematic diagram of a worn Jobber drill showing the outer corner flank wear [20], With Kind permission from Sam Harris.

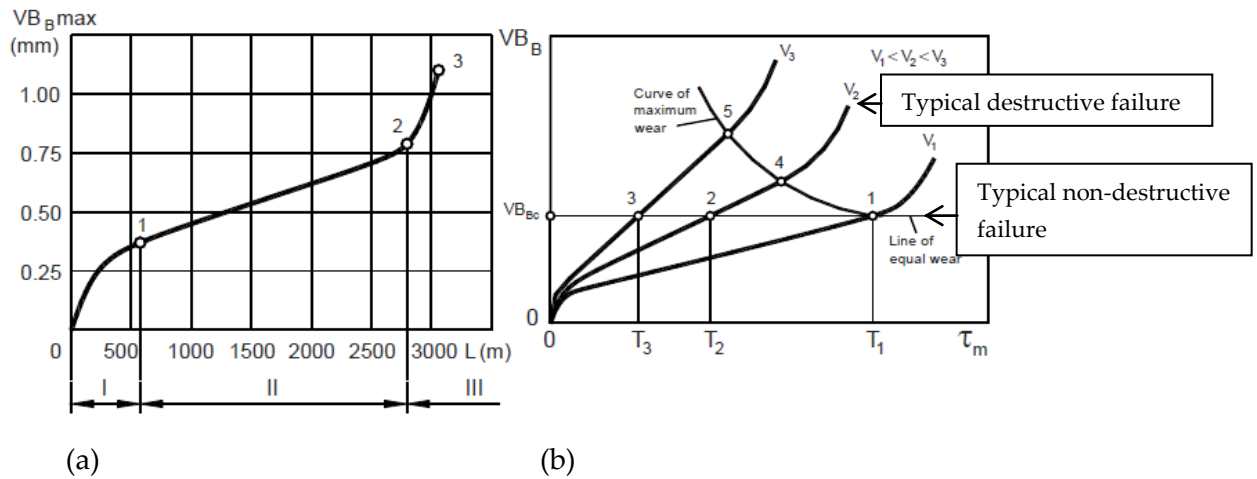


Figure 2.10 (a, b). Tool wear curves. (a) General wear curve, showing the three main stages of tool life. Stage 1 rapid initial wear, stage 2 steady state wear and stage 3 rapid final wear (b) Graph of wear versus time showing an idealised tool life evolution for 3 different cutting speeds and 9 different failure criteria. Point 1, 2, and 3 represent the time at which a cutting tool has reached a predefined wear point (non-destructive). Point 1, 4, and 5 represent the point in time where the tool has entered the third stage of life (non-destructive, prior to rapid tool wear but difficult to determine). The last three failure points coincide with the notation  $V_1 - V_3$  this is to destruction [13], with kind permission from Springer Science+Business Media.

Tool wear curves have been used to characterise the performance of cutting tools in wear studies [51]. Tool wear curves also reveal the effect of machining factors on the evolution of tool wear. One of the most significant machining parameters to effect tool life is the cutting speed, as it directly effects the rate of wear and cutting temperature and can affect the types of wear mechanisms in progress [13]. In Figure 2.10 (b), three tool wear curves are shown for three different cutting speeds,  $v_1 < v_2 < v_3$ . The tool wear curves show that the higher the cutting speed the higher the wear rate. This tool life information is important for process management as the information may give a reasonable approximation for changing and resetting tools for automated machining processes as well as an indicator that the tool needs to be resharpened.

## 2.5 Metal Cutting as a System

The metal cutting process can be viewed as a complex system with a large number of sub-systems[1]. Figure 2.11 shows the components of the gundrilling system, revealing the scope of managing this operation. These components are similar for every machining operation with specific differences depending on the machining operation, material to be cut and productivity requirements. For example tool material (Figure 2.11), instead of quality of carbide it may be quality of HSS, with sources of variance such as distribution of carbides and subsequent heat treatment. In the context of cutting tool testing it is this author's hypothesis that, only when we can manage the complex behaviours and sufficiently minimise or model the effect of sources of variance on tool life, will we be able to achieve productive use of cutting tool test data. This section will therefore discuss the research findings of complex behaviours and sources of variance in metal cutting and their effect on tool life.

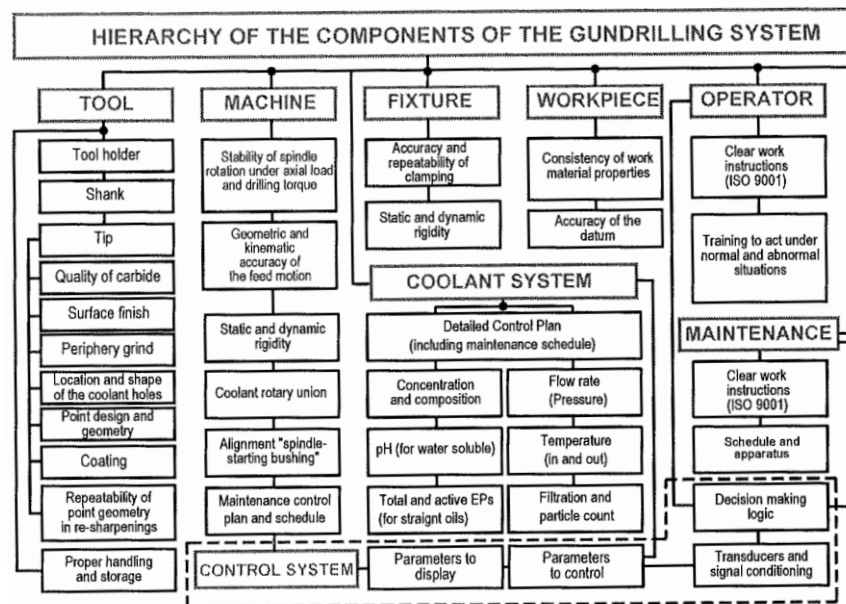


Figure 2.11. Components of the gundrilling system revealing the complexity of managing this manufacturing process[1], with kind permission from Springer Science+Business Media.

Williams, Smart and Milner [53] showed that the cutting force and thrust force (Figure 2.12 a & b) exponentially fall when turning materials such as pure iron, copper and brass over cutting speeds between 1-100m/min. However, when machining low carbon steels the cutting force is significantly lower at low cutting speeds. At low cutting speeds a built up edge (BUE) forms on the cutting edge, rake and flank faces up until a medium cutting speed of roughly 50m/min. The BUE acts like a restricted contact length cutting tool reducing the cutting forces on the rake face. As the cutting speed increases the BUE



formation stops and the cutting force increases to its maxima. Further increases in the cutting speed will then lead to an exponential decrease in cutting forces.

Figures removed due to copyright reasons.

(a)

(b)

Figure 2.12. Empirical data collected by Williams, Smart and Milner of the cutting force and thrust force in turning operations at a feed rate of 0.25mm/rev and a depth of cut of 1.25mm. (a) shows the cutting force and thrust for iron, copper and titanium. (b) shows the cutting force and thrust for iron, low carbon steel, copper and 70/30 brass [14].

Astakhov and Osman [26] investigated the complex behaviour between wear mechanisms and their effect on tool life by varying a number of cutting conditions. Their experiment characterised the change in tool life over a cutting speed range of 1-150m/min as well as turning dry, with oil and with emulsion coolant, labelled graph 1, 2 and 3 respectively (Figure 2.13). Their results show there are zones (zone 1, 2, 3 and 4) in which a cutting tool can exhibit increased and/or decreased tool life. The relationship between tool life and cutting speed was explained by the authors as to change depending on the predominate wear mechanism in progress which affects the thermal and mechanical conditions at the cutting edge. As the cutting speed increases the cutting force reduces, as also shown by Williams [53], however, the thermal gradient applied to the cutting tool increases. At these high cutting temperatures, oxidation and diffusion wear begin to play a significant role in tool wear. However, there are regions of linearity. If these regions can be identified for a particular cutting tool test, it may be possible to model the linear portion only.

Figure removed due to copyright reasons.

Figure 2.13. Tool life versus cutting speed data from turning tests. Workpiece: high alloy steel (0.2% C, 25% chromium 20% Nickel, 2% Silicon). Cutting parameters: feed rate 0.06mm/rev and a depth of cut 2.5mm [54].

Shaw [4] states that for the practical range of cutting parameters used for HSS cutting tools, the relationship between tool life and cutting speed will be generally linear on a Taylor's tool life graph (Figure 2.14). However, tool life may begin to show non-linearities if BUE formation is exhibited or if the HSS cutting tool reaches its tempering temperature and begins to soften.

Figure removed due to copyright reasons.

Figure 2.14. A general Taylor's tool life relationship for a HSS cutting tool machining steel with the log of tool life versus the log of cutting speed. This graph reveals a linear region, if the cutting speed is too low or too high then it begins to show nonlinearity by BUE formation and thermal softening respectively[4].

Another source of complex behaviour is the machine tool interaction with the cutting tool and workpiece [1]. The dynamic and static rigidity of the spindle and workpiece fixturing are sources of vibration during machining. The cutting tool is attached to the spindle via a chuck or collet; it interacts with the workpiece which is fixed to the machine bed. The acoustic vibration of the spindle has been used as a measure to determine a machining systems optimal MRR and tool life [55]. This relationship is the main reason why cutting tools made from 'super' hard materials such as WC-Co must be used in a highly rigid system, as excessive vibration may cause the cutter to chip and fracture, causing premature failure.

There are many sources of variance which effect the distribution of tool life results. The intrinsic plate hardness and batch to batch variability has already been introduced. Another significant source of variance in the workpiece is the chemical composition and carbide distribution defined by the ASM committee of 1990 [24]. They report that a non-uniform chemical composition and carbide distribution within a steel plate will increase the variance in tool life by affecting the wear rate.

The cutting tool itself has many sources of design variance. The variance in macro geometry features is a significant source of tool life variance. According to the American National Aerospace Standard (NAS) for split point drill design [16] the primary lip relief, lip height variation and chisel edge centrality (chapter 2.2 for definitions) are key features which require repeatability and uniformity in manufacture. If these features deviate from required specifications and/or are non-uniformly ground, the tool life performance in regard to dimensional accuracy and life will be significantly lowered [17]. Secondly, if the repeatability of the grinding process varies across a production run, then the tool life distribution will directly reflect this variance [18].

Another source of cutting tool design variance which can significantly affect the dispersion of tool life results is the coating thickness. Posti [41] published work characterising the effect of TiN coating thickness on tool life for planing and turning operations. The tool life results showed that for turning, a continuous cutting operation, coating thickness and tool life follows a linear relationship. Reviewing Posti's results for turning showed that an increase in coating thickness of  $1\mu\text{m}$  can increase tool life by 36%. Posti also observed that the

amount of free titanium inside the TiN coating decreases wear resistance, however TiN coatings aim to be deposited with a stoichiometric balance of titanium and nitrogen. Drill testing conducted for coating research may need tool life results to be normalised for the effect of coating thickness variation with the calculation of a holes/micron of coating value, so the tool life data is more representative of the specific coating process factor under investigation such as chemical composition, temperature or voltage.

## 2.6 Tool Life Modelling

Tool life is an important parameter, as Marksberry states [56]“it is one of the most important factors in process planning and total machining economics”. The use of the scientific method for tool life calculation began in 1880 with F. W. Taylor’s work ‘On the art of cutting metals’ and published in 1906 [29]. This work developed the well-known Taylor’s Tool Life equation (Eq. 1) determining the relationship between cutting speed and tool life.

$$C = V_c T^n \quad \text{Eq. 1}$$

Where:

C = Cutting speed for a lifetime of 1min.

$V_c$  = Cutting speed in m/min

T = Tool Life in min

n = Exponent which depends on the machining system, cutting tool design, workpiece material etc.

Since this time researchers such as Niebel, Draper and Wysk [57] have extended the equation to account for more of the cutting parameters such as, cutting speed, feed rate and depth of cut (Eq. 2) [58]. An extended Taylor’s tool life model has also been developed by Lau, Venuvinod and Rubenstein [59] to model the effect of cutting tool geometry features such as the rake and flank angles on tool life. Models may be designed for any number of factors, however, as this is an empirical based model this equation may become quite large and the number of machining trials needed to calculate the exponents becomes costly and time consuming.

$$C = V_c T^n f^a d^b \quad \text{Eq. 2}$$

Where:

f = Feed rate in mm/rev.

a = Exponent which describes the effect of feed rate in a machining system.

d = Depth of cut in mm.

b = Exponent which describes the effect of depth of cut in a machining system.

Another drawback from using an empirical model is that the results may only be representative for a particular machining system (machining operation, workpiece material, tool geometry, lubrication) which limits its wide spread use from one factory to another or one machine to another. Another important factor in the context of cutting tool testing is to determine the effect of plate hardness variability on tool life, either within a plate or batch to batch. This is a factor with a significant effect on tool life as shown by Vogel and Bergmann [12] as the researcher often has little control on the variability in steel plate. They may either reject sections of plate which are outside tolerances or preform expensive heat treatments to reduce plate hardness variability.

To develop a tool life model an experiment must be designed with particular boundary condition encompassing the region of interest for determination of the effect of machining factors on tool life. It is beneficial to incorporate more than two levels per factor to determine if the range chosen has a linear or non-linear relationship, if two levels are chosen then any nonlinearities will not be able to be determined. It is also valuable to account for the variability in tool life performance by collecting data using a number of samples.

## 2.7 Statistical Methods

To test new products and manage the level of quality of mass manufactured goods a statistical approach is a valid and powerful method. As Logothetis writes [60] "Everything varies. No two things are ever the same, no matter how similar they seem to be". This premise has driven statisticians to develop techniques to assess how similar objects are or how not similar they are, in the case of this work, cutting tool lifetime performance. Statistics are often classified as either 'parametric' or 'non-parametric' and engineers often implicitly work with parametric statistics. A parametric distribution may be defined by measures of central tendency; such as the mean, median or mode and the measures of dispersion; such as the standard deviation, variance and range. Therefore, quoting the mean and statistical deviation of data is satisfactory.

In a manufacturing environment, potentially thousands of products are produced daily; in order for a manufacturer to estimate the population statistic of a particular product, small sample sets are collected, possibly at random and parametrically characterised. Once the samples have been tested for a particular measure usually a hypothesis is tested using the data. Hypothesis testing is a method of evaluating "two mutually exclusive statements about a population"[61]. The first statement is called the null hypothesis, simply, the null hypothesis will contain a statement that "two or more things are equal, or unrelated" [62]. The other contrasting statement is called the alternative hypothesis, which states that the population statistic is different to the value of the null hypothesis or there "is a relationship between variables". A hypothesis test can only be conducted after an inferential statistical test is performed. An inferential test calculates the probability (an estimate) of what the population statistic really is. Calculating the probability that a population statistic lies within a certain range (confidence limits) is possible due to the central limit theorem [61] which states that, a sample distribution will be approximately normal if the original population (parent population) is repeatedly sampled (Figure 2.2). The more asymmetric the original population is the larger the sample size needs to be to yield a normal distribution from the sample also known as the population of means.

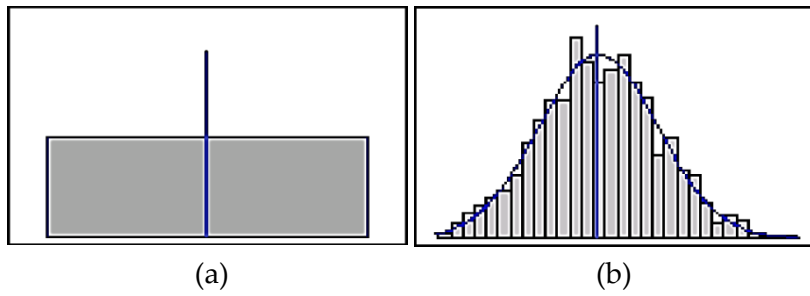


Figure 2.15. (a) Uniform distribution, (b) Normal distribution

Inferential statistics apply some probable accuracy to the estimated population statistic. A level of confidence is chosen such as 90, 95 or 99% depending on the application. The following formula Eq.3 is used to calculate confidence intervals of where the population mean statistic is likely to reside.

$$\mu = \bar{X} \pm t(df; \alpha) \frac{S}{\sqrt{n}} \quad \text{Eq. 3}$$

Where:

$\mu$  = Population mean.

$\bar{X}$  = Sample mean, arithmetic average.

$t$  = t distribution value.

$df$  = degrees of freedom.

$\alpha$  = Significance level.

$S$  = Standard deviation.

$n$  = number of samples.

$$S = \sqrt{\frac{\sum_{i=1}^n (X_i - \bar{X})^2}{n - 1}} \quad \text{Eq. 4}$$

Where:

$X_i$  = The value of sample  $i$

The confidence intervals are calculated by adding and subtracting a probability dispersion value which is calculated by knowing the 't' value which is dependent on by the degrees of freedom and the level of confidence chosen and found in the 't tables'. Degrees of freedom can be thought of as the number of observations in a sample set used to estimate a parameter (such as the mean) from which that sample is drawn.

## t-Value Versus Sample Size (n)

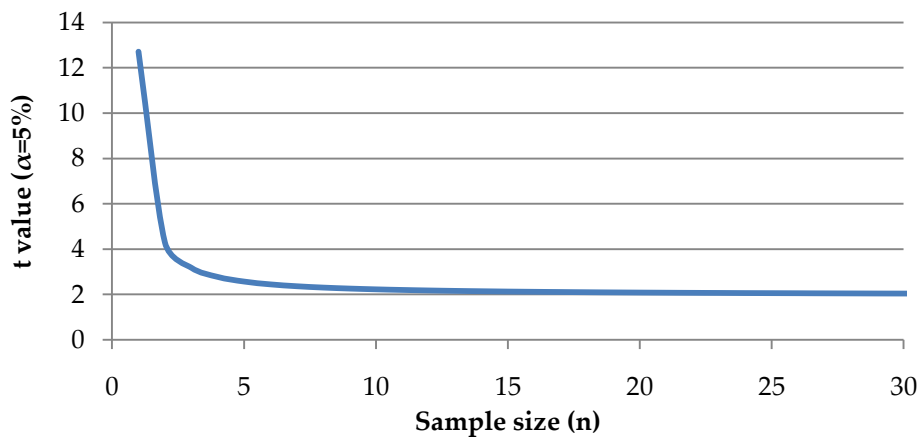


Figure 2.16. Graph of the t value for a two tailed  $\alpha$  level of 5% versus sample size. Showing that after 5 samples there is only a small decrease to the 't' value as  $n$  increases ('t' values from Devore [61]).

The 't' value is then multiplied by the standard deviation divided by the square root of the number of samples. The researcher may only change the level of confidence, the number of samples and potentially design an experiment which minimises the standard deviation. The level of confidence in a majority of engineering applications is usually 95%; however it is raised when dealing with critical mechanisms such as jet engine components. The number of samples is usually limited by the time and cost of the experiment and in the application of drill testing which is somewhat costly and time consuming the requirement to keep sample size small is significant. Some experiments are designed to block external factors which may contribute to a large standard deviation (in this case minimising sources of machining variance).

This idea will be explored within the design and subsequent drill test experiments in later chapters but the important idea here is that there is most always a pressure to keep samples sizes low and the only factor left to the researcher is to 'adjust' is the standard deviation (Eq. 4). There may be limitations on lowering the standard deviation. There may be only a limited number of factors in a particular system which can be adjusted and this may not reduce the standard deviation. In some cases the natural distribution of the sample may not be normal but fit some other distribution, for example a batch of drills with a large distribution of macro geometry features.

In R&D and production engineering, inferential statistics need to be combined with a suitably designed experiment so that a researcher may infer something about a product or process in a timely and inexpensive manner. This may be to test the significance of a new design feature or the change to a manufacturing process. To keep the experiment timely and costs low, it has been beneficial but difficult to move away from the 'change one factor at a time method' and move to a factorial experimental design developed by R. A. Fisher in the 1920's where multiple factors or treatments are studied in the one experiment. As



Logothetis says [60] “One should start the experimental process with the understanding that real life rarely allows the manipulation of only a single factor”. Factorial experimental design becomes difficult to manage if the number of factors or the available levels within that factor are high, Eq. 5.

$$n_o = l^f \quad \text{Eq. 5}$$

Where:

$n_o$  = Number of experimental groups.

$l$  = Number of levels of a particular factor.

$f$  = Factor.

Hence, if the number of factors becomes too large then a fractional factorial design is more suited. However, both experimental designs require that there is a sufficient level of reproducibility in the treatment or process for reliable information about the factors effects.

Once an appropriately designed experiment has been conducted and the results collated, it is then time to apply an appropriate statistical test that will determine whether or not a significant change has or has not occurred for the factor or factors under investigation and allow the null hypothesis to be accepted or rejected. The analyses of means and variance (ANOM & ANOVA) provides that capability [63]. Both test for a lack of homogeneity among means. However, the alternative hypotheses are different. The alternative hypothesis for ANOM is that one of the population means is different from the other means, which are equal. The alternative hypothesis for ANOVA is that the variability among population means is greater than zero.

Another statistical method which is particularly useful in analysing failure data is Weibull analysis Eq. 6. This tool is able to define a characteristic life and define a failure probability for a distribution of sample data with a level of confidence. A product, component etc. is reliable or unreliable by assessing failure data and determining a frequency of failure [60]. Reliability in a Weibull analysis is defined as when an expected lifetime is reached, when a product satisfies expectations and when a product is not impaired in terms of its function[64].

$$F(t) = 1 - e^{-\left(\frac{t}{T}\right)^b} \quad \text{Eq. 6}$$

Where:

$F(t)$  = Frequency of failure.

$t$  = Lifetime variable, distance covered, operating time, etc.

$T$  = Scale parameter, characteristic life during which a total of 63.2% of samples have failed.

$b$  = Shape parameter, slope of the fitting line in the Weibull plot.

A distinguishing feature of this analysis method is that it is able to analyse multiple distributions. The slope (shape parameter) indicates the type of distribution the failure data represents. This is due to the fact that the derivative of Eq. 6 is the Weibull density function. A Weibull graph shown in Figure 2.17 with three generalised failure plots with three different slopes (shape parameters),  $b=1$  corresponds to an exponential distribution,  $b=2$  corresponding to a Rayleigh distribution and  $b=3.2-3.6$  corresponding to a normal distribution [64].

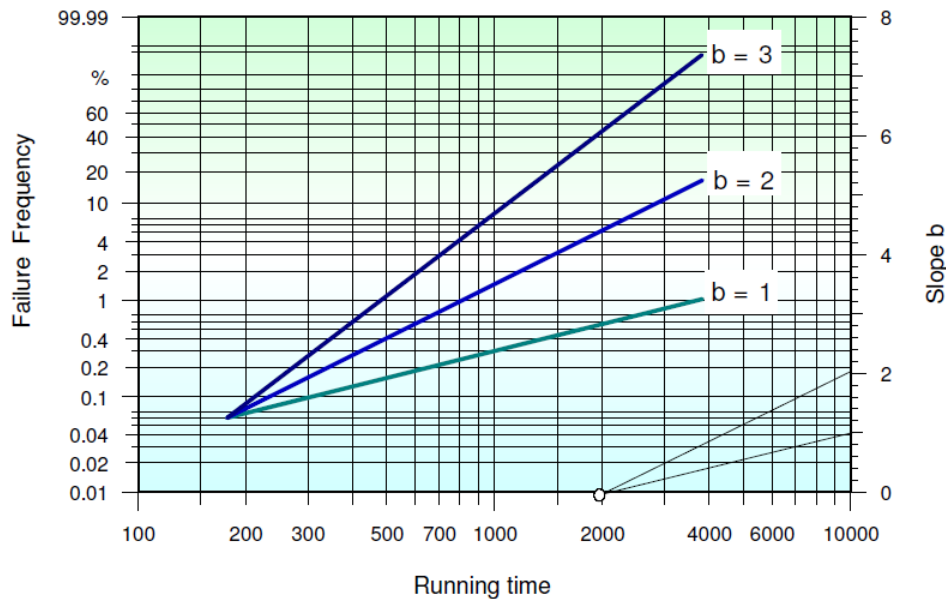


Figure 2.17. Weibull graph with three generalised failure plots with different slopes i.e. three different failure types [64], with kind permission from Curt Ronniger.

Table 2.1 Slope  $b$  (shape parameter) with corresponding failure type with possible examples[64], with kind permission from Curt Ronniger.

Slope $b$	Failure Type	Example
$b < 1$	Early-type failures (premature failures)	Due to production/assembly faults
$b = 1$	Chance-type failures (random failures) there is a constant failure rate and there is no connection to the actual life characteristic (stochastic fault),	Electronic components
$b = 1-4$	Time depending (aging effect) failures within the design period	Ball bearings $b \sim 2$ , roller bearings $b \sim 1.5$ corrosion, erosion $b \sim 3 - 4$ rubber belt $b \sim 2.5$
$b > 4$	Belated failures	Stress corrosion, brittle materials such as ceramics, certain types of erosion

This analysis method also allows the determination of mixed failure modes using the slope test and characteristic life test. These tests help researchers to potentially identify different wear/failure mechanism in progress or problems during the fabrication process. It is important to understand that the analysis method may identify that a different wear/failure mechanism has occurred to particular data points, but not exactly what they are. This would require physical examination of the failed component/sample.

Combining the aforementioned analysis methods and design of experiment leads to techniques which may offer insight into the tool life performance of drills tested using an accelerated cutting tool test [65, 66].

## 2.8 PVD Technology

The PVD (Physical Vapour Deposition) TiN coating used in this work was deposited onto jobber drills using a cathodic arc evaporation deposition system. The following chapter describes in detail the sample cleaning applied and the coating process to allow the replication of this coating.

### 2.8.1 Substrate Cleaning

All drills were cleaned, prior to coating; using multi stage water based cleaning line. An ultrasonic bath was used with alkaline detergent to remove oil and soils from tools followed by rinsing in de-ionised water and drying at approximately 110°. After the tool surface was cleaned of the majority oils and impurities they were then ready to be loaded onto a triple rotation carousel and loaded into the coating chamber.

### 2.8.2 Cathodic Arc Deposition

Tools were loaded into the cathodic arc coating chamber Figure 2.18, the base pressure was pumped down to  $1 \times 10^{-3}$  mbar which took approximately twenty five minutes, after which radiant heaters located on the chamber walls increased the substrate temperature to approximately 375°. Once this temperature was achieved the current across the filament in the ionisation chamber was ramped up from 50A to 250A and the substrate holder was set to a positive bias to commence the electron heating stage, using the Helmholtz coils to focus the electrons on the substrate to a temperature of approximately 400°. Hydrogen gas was then introduced into the chamber to remove any organic material and reduce iron oxides such as  $\text{Fe}_2\text{O}_3$  and  $\text{FeO}_2$  on the surface of the tools, this step lasted 30 minutes, a secondary reason for the time length is to equalise the bulk temperature across all tools. After this process, argon etching was used to sputter clean the tool substrate via pumping argon through the ionisation chamber which ionised the gas through collisions with electrons. The chamber pressure was then increased to  $2.4 \times 10^{-3}$  mbar, the bias on the substrate was switched to negative and ramped up to -170V for thirty minutes. After this step the process switched to the coating phase which commenced at approximately 350°C. Six titanium sources were set at an arc current of 160A and a bias voltage of 100V, nitrogen was then introduced to the chamber for ten minutes to deposit an interlayer. After the interlayer was deposited the arc current was increased to 170A and argon as well as nitrogen was admitted into the chamber at 400sccm and 800sccm respectively for forty nine minutes. The final step used an arc current of 160A without argon for ten minutes.



(a)

(b)

Figure 2.18. (a) Image of the cathodic arc deposition chamber used in this work (b) Chamber door with pair of cathodes and radiant heaters.

## 2.9 Metrology Tools

### 2.9.1 Alicona Infinite Focus Microscope

The Alicona IFM was used in this work to characterise the surface roughness of Jobber drills. As this is a novel technology this capability must be explained in order to understand what the measurement output is and how it was measured.

The infinite focus microscope (IFM) is a high resolution optical microscope designed to generate 3xD Images. The IFM is capable of capturing form and roughness in one measurement due to the focus variation technique. This technique operates by combining the small depth of field of high resolution optical lenses with a vertical scanning range. This combination of small depth of field and vertical scanning can be seen in Figure 2.19, this image shows that a three dimensional object such as the outer corner of a drill, will only have a small section in focus at a high resolution.

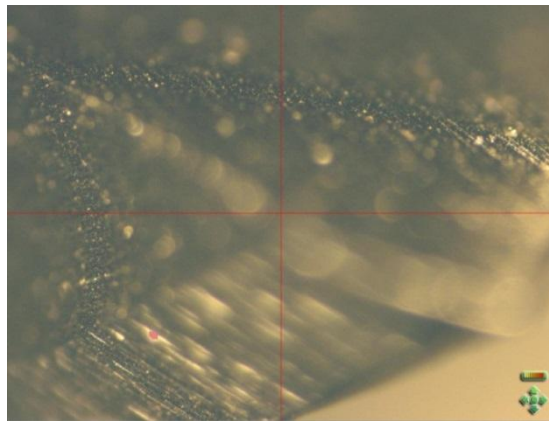


Figure 2.19. Screen shot of the outer corner through the IFM at 10x. Reveals where the drill intersects the focal plane of the lens.

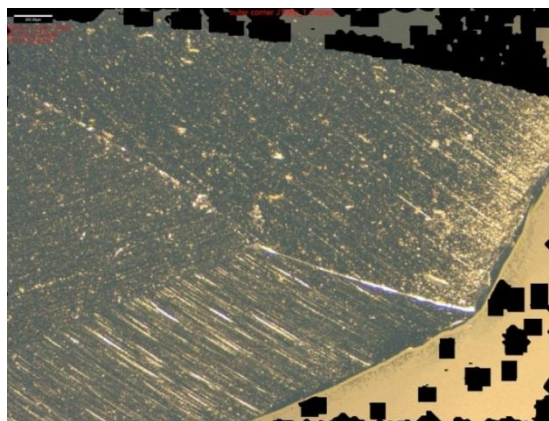


Figure 2.20. 10x image of the outer corner compiled from the 3D scan. Scale bar equals 100 $\mu$ m

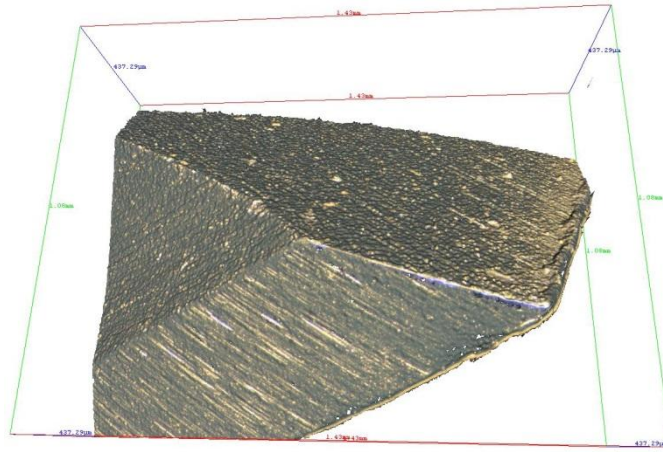


Figure 2.21. Screen shot, 3D surface representation of the outer corner, constructed from a large number of images along a vertical scan range. Dimensions of scan, length 1.08mm, width 1.43mm and height 437.29µm

The user must select a vertical scanning range which covers the area of interest; this is accomplished using a fine motorized stage which allows any section of the sample to be scanned. As the distance between the sample and objective lens is varied, images are continuously captured. The images are collected by illuminating the sample with modulated white light, which has passed through a beam splitter, at which point the light is passed through an objective lens. The resulting image is similar to conventional optical microscopy see Figure 2.20. Once the harmonized interaction between modulated illumination, vertical scanning and sensor capturing, a 3 dimensional model is constructed Figure 2.21. The 3D model is a surface representation made up of a large number of elements in space. Figure 2.22 shows that the 3D model of the drill outer corner is constructed from 3159121 triangles

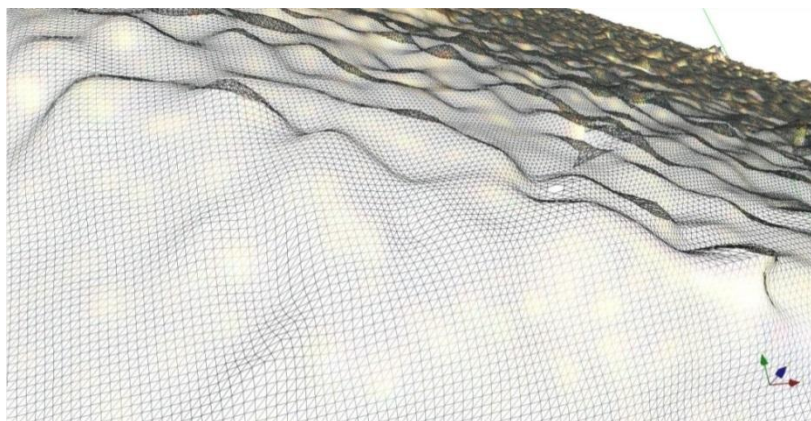


Figure 2.22. Screen shot zoomed in on the surface of the drills outer corner, the entire scan of the surface is made of 3159121 triangles.

Focus variation has been added to the latest ISO standards for classifying surface texture methods. The new ISO standards 25178 for the first time includes standardized parameters to classify area based measurements. As this new method of surface characterisation is used in this thesis, the author feels that it is required to explain the nuances of the ISO standard

surface profile measurement using a tactile probe and its incorporation into this new non-contact method of capturing a surface profile using focus variation.

ISO standard 4288 requires that for a surface profile captured using the focus variation technique to be comparable to a tactile probe measurement some information about the profile must be known, such as an estimated surface roughness range for example between  $0.1\mu\text{m}$  and  $2\mu\text{m}$ . This will dictate how long the scan length must be and what cut off wavelength must be used, in this example the scan length must be 4mm long and a cut off wavelength must be  $800\mu\text{m}$ . The cut off wavelength is the parameter that separates the waviness and roughness from the primary surface profile. Figure 2.23 shows the primary surface profile of a rake face from a TiN coated Jobber drill. The primary profile shows high frequency and low frequency waves, by applying a cut off wavelength ( $L_c$ ) of  $800\mu\text{m}$  (Figure 2.24) some of the low frequency has been separated and can be seen in Figure 2.26.

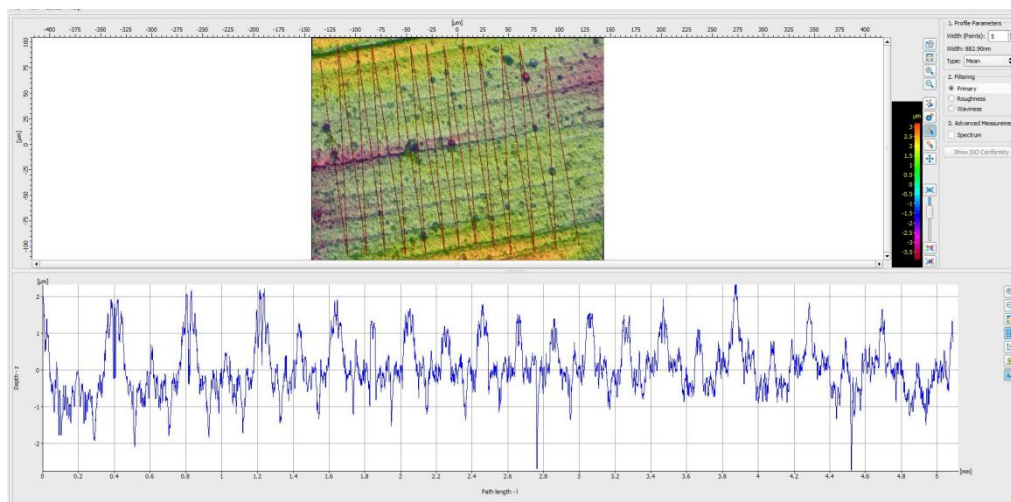


Figure 2.23. Screen shot, showing a topographical image of the scanned surface. The line across the scan is a graphical representation of the line scan, similar to the idea of a probe running across the surface. The primary surface profile can be seen at the bottom showing both high and low frequency data. The repeated pattern is due to the roughness line scan being repeatedly run across the surface.

Observing the roughness profile it can still be seen that there is waviness in the roughness profile (low frequency), therefore, the cut off wavelength must be reduced. By reducing the cut off wavelength the measurement will not conform to the ISO 4288 standard, however, this must be done to eliminate all waviness; this is stated in the Alicona procedure manual for surface profile measurements. By applying a cut off wavelength of  $L_c 80\mu\text{m}$ , all of the waviness from the primary surface profile has been separated Figure 2.25 and Figure 2.27.



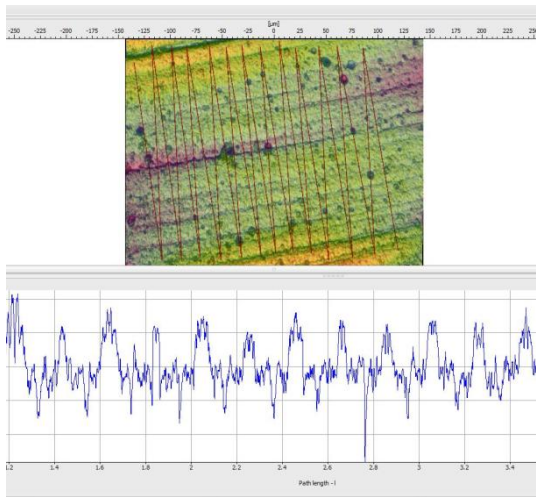


Figure 2.24. Screen shot, roughness profile Lc 800 $\mu\text{m}$ , shows partial separation of waviness features.

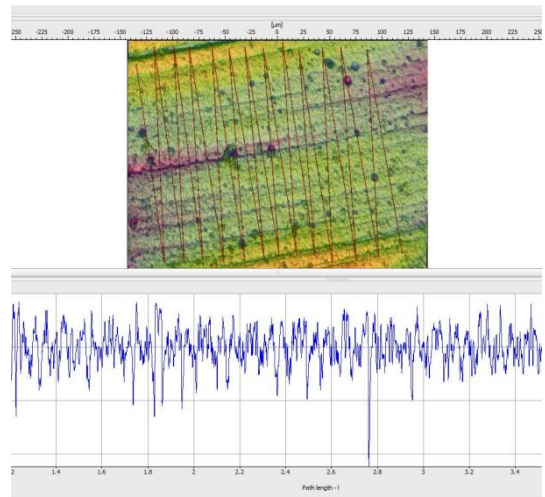


Figure 2.25. Screen shot, roughness profile at a cut off wavelength of Lc 80 $\mu\text{m}$ , shows only high frequency data with all waviness separated from primary profile.

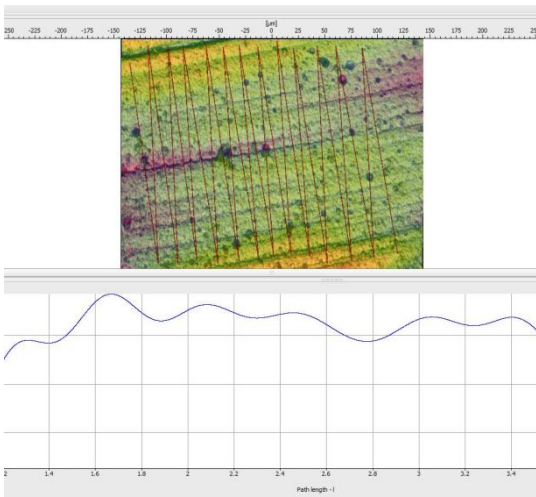


Figure 2.26. Screen shot, waviness profile at a cut off wavelength of Lc 800 $\mu\text{m}$ , shows the partial separation of the waviness from the primary profile.

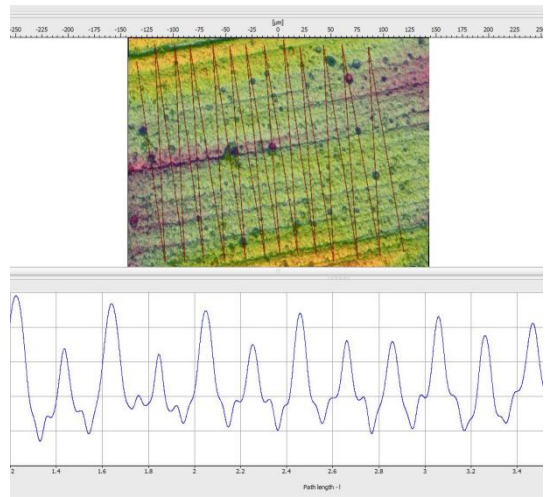


Figure 2.27. Screen shot, waviness profile at a cut off wavelength of Lc 80 $\mu\text{m}$ , shows only the low frequency data and no high frequency data 'roughness'.

## 2.9.2 Tool Maker's Microscope

Cutting tool geometries were measured using Tool maker's microscopes. The two devices used were the Mowhawk (SOP [67]) and the Euro-tech. The same operating procedure applied to both as the only differences between the devices is that the Eurotech has a digital camera and a three roller self-centring tool holder assembly, these two differences allow quicker measurements to be made as they allow a better view and control of the cutting tool. The Mowhawk tool maker's microscope is shown in Figure 2.28.



Figure 2.28. Image of the Mowhawk tool maker's microscope showing the Vee slide at a position of  $90^\circ$  relative to the objective lens.[67]

Chisel angles were measured by first placing the drill against the stop inside the vee slide and positioning the vee slide to  $0^\circ$  relative to the objective lens. The cross hairs were then lined up with one of the cutting edges as a reference point for the angle measurement seen in Figure 2.29, then the eyepiece was rotated counter clockwise to superimpose the horizontal cross hair on the chisel angle.

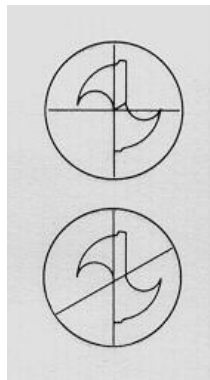


Figure 2.29. A diagram showing the measurement of the chisel angle. Firstly, positioning the vertical cross hair to line up against the cutting edge. Then to rotate horizontal cross hair to line up with the chisel.[67]

To measure the point angle the vertical cross hair was positioned up against a cutting edge. The vee slide was then rotated  $90^\circ$  as seen in Figure 2.30. At which point the eyepiece was rotated clockwise until the cross hair was superimposed on the cutting edge.

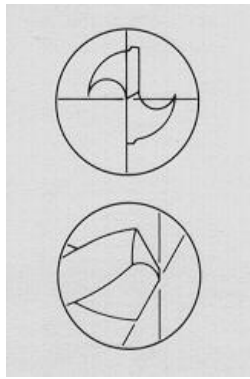


Figure 2.30. Drawing showing the two steps in measuring the point angle. Firstly showing the vertical cross hair lined up against the cutting edge, followed by the horizontal cross hair lined up against the cutting edge.[67]

To measure the lip relief angle drills were placed against the stop inside the vee slide and rotated 90° (Figure 2.31). The left hand horizontal cross hair was then lined up against the cutting edge at which point the vee slide was rotated 90°. The protractor on the eyepiece was then rotated clock wise until the horizontal cross hair lined up with the point face and margin.

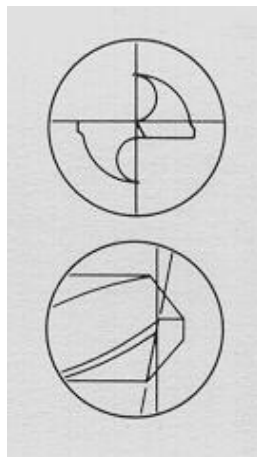


Figure 2.31. Drawing showing the two steps in measuring the lip relief angle. Firstly, the horizontal cross hair is lined up against the cutting edge, followed by the horizontal cross hair on the intersection of the point face and margin.[67]

Any helical feature, in this case the margin width, can be measured in three ways, by measuring the axial, normal and transverse width. The axial margin width is measured along the longitudinal axis of the drill. The normal margin width is measured normal to the helix angle, while the transverse margin width is measured across the margin. The transverse margin width was measured in this work by positioning the drill against the stoper in the vee slide with the vertical cross hair lined up against the cutting edge shown in Figure 2.32, the vee slide was then rotated 90° at which point the digital vernier callipers were set to zero and the vertical scale was moved to the trailing edge of the margin.

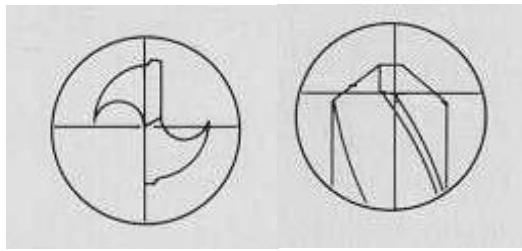


Figure 2.32. Drawing showing the two steps in measuring the margin width. Firstly, the vertical cross hair lined up against the cutting edge, followed by measuring the margin using a digital vernier calliper.[67]

To measure the web thickness a pin micrometre was used. Drills were set up in a vertical magnetic vee holder to keep them steady, at which point the micrometre was carefully wound up so the pin did not indent the drill webbing and affect the measurements. The helix angle was measured using the Euro-tech software which required the operator to position the drill as shown in Figure 2.32 at which point three points along the flute were inputted into the software to calculate the helix angle using an inverse tan relationship.

## 2.10 Summary

The choice of cutting tool testing methodology was found to depend on a number of factors for example the justification for the test, QA, benchmarking etc. as well as the type of data output required, progression of wear or failure data. Testing methodologies can be broadly categorised into two groups, non-destructive and destructive testing. Non-destructive testing the progression of wear is measured periodically for a low number of samples to a predefined wear or force limit, at which point the cutting tool may be recovered by re-grinding. Destructive testing typically uses a larger sample set but tested to failure.

The machining system was found to comprise of a number of complex behaviours with corresponding sources of variance. Table 2.2 shows a summary of the three complex behaviours and related sources of variance in machining which affects the performance and dispersion of tool life. The preliminary drill test design was developed by taking into consideration these factors (Chapter 3.1). The drill test was designed to operate in a cutting regime which could offer a repeatable, single wear/failure mode cutting tool test (robust) which minimises the effect of sources of variance on tool life variance, in order to allow conclusions to be drawn using small data sets (sensitive).

Table 2.2 A Summary of three complex behaviours and their related sources of variance within the machining system in the context of the developed test.

<b>Object</b>	<b>Complex Behaviour</b>	<b>Source of Variance</b>
Workpiece	The intrinsic ability of a material to resist cutting i.e. machinability	Chemical compositions Distribution of carbides Batch heat treatments Microstructure/Hardness Different suppliers
Cutting Tool	Drill design features interaction with workpiece (chip formation and tribology i.e. wear mechanisms): Substrate Macro Geometry Micro Geometry Surface finish Coating architecture	Distribution and volume of carbides. Deviations of macro and micro geometries. Surface roughness variation. Coating thickness variation.
CNC Machine	Machine tool interaction with cutting tool and workpiece: Coolant quality Static and dynamic rigidity(vibration) Stability of spindle	Workpiece fixturing position Coolant pH and concentration Flow rate Temperature Worn components

Empirical modelling has been used to characterise the effect of machining factors on tool life, the limitation of which is that the model will only be representative of the machining system the data was collected from. Therefore, it was used as a tool within this work to model sources of tool life variance which a researcher has limited control over, such as batch to batch workpiece hardness.

## 3 Experimental Design, Development and Application of an Accelerated Drill Test

### 3.1 Drill Test Design

The drill test methodology adopted in this work is that of an accelerated destructive test of relatively inexpensive cutting tools (Jobber drills). This work was undertaken to reduce scatter in the tool life results. It has been shown in chapter 1 that in order to accomplish this task the complex behaviour within the machining system must be managed and sources of variance minimised such as the workpiece fixturing, tool holder and coolant. Therefore, careful clamping of the test plate was needed to reduce any vibrational effects as well as deflection caused by the thrust force when drilling (Figure 3.1.). The previous drill test used by the partner organisation drilled 4D (4xDiameter) through holes. This machining strategy potentially exposes the drills cutting edges to chipping (wear mechanism), therefore blind holes were used in this drill test to eliminate this potential source of tool life variance. The developed test also limited the depth of hole drilled to 2.5xD, minimising any chip jamming effects, which has been shown by Balzers to be a source of cutting torque fluctuation and tool breakage Figure 3.2 a & b. Limiting the hole depth to 2.5xD also reduced any coolant access issues, potentially reducing the effect of thermal softening at the cutting edges which is a significant factor affecting the performance of HSS cutting tools.

The choice of cutting tool material was limited to HSS as all grades of WC Co are expensive, while HSS is relatively inexpensive. Also cost and practicality are important issues when commercial testing is carried out, therefore, the principle of the value of information gained versus the cost of obtaining that information must remain equal or greater, hence M2 HSS Jobber drills were chosen as a vehicle for cutting tool development as it is a relatively low cost material with a simple design. There are issues using HSS, it is temperature sensitive, once temperatures reach over the tempering temperature ~560 degrees Celsius the material begins to lose its hardness and at ~650 the material becomes weak and ductile [68]. This temperature limitation restricts the application of the material because it limits the cutting speed one can use. In order to overcome this limitation metal cutting fluids must be used. Additionally it is difficult to compare uncoated tools to coated tools due to the difference in tool life at the same cutting conditions as coated tools are able to last much longer and withstand higher cutting speeds [12]. In addition, once the coating has been worn from the outer corner; the tool will be under highly accelerated wear conditions and wear rapidly. Therefore, thermal softening must be avoided as the tool life results affected by this will not portray an accurate description of the sample sets intrinsic life during use by end users.

A test material is needed which accelerates tool wear and provides low tool life variance. Ideally, this material would have uniform hardness and carbide distribution which may allow a sample of cutting tools to wear uniformly. The test material also needs to be readily available and have similar properties over time (batch to batch). Therefore, D2 cold work tool steel and P20 plastic mould steel have been chosen for this study. D2 cold work tool

steel is supplied in the annealed condition which is soft ~ 200 Brinell, however this material has large chromium carbides distributed throughout its ferritic matrix therefore it has a low machinability by offering a predominately high abrasive wear rate during machining. On the other hand P20 plastic mould steel is supplied in the quenched and tempered condition with a Brinell hardness ~310. This is considerably harder than the D2 steel, however there are no hard inclusions to wear the tool which translates to potential high cutting parameters to accelerate wear. This was considered detrimental as HSS is known to be temperature sensitive, this wear mechanism has been shown to be a non-linear for a Taylor's tool life graph. A pseudo random drilling array is also employed to minimise any potential unavoidable heterogeneous characteristics in the test plate such as hardness and hard carbide inclusions, so all tools in the sample group will be exposed to the same conditions. The two test materials were examined through paralleled tool life testing and analysed using t tests, bivariate analysis and Weibull analysis then compared against the criteria set.

A drill test was designed which incorporated the findings from the appraisal of the current literature as well as discussions with partner organisation engineers. The drill test design is examined as well as the implications of the choices made for aspects such as the choice of cutting tool, workpiece material and the cutting conditions. An outline of the work in this thesis is then put forward.

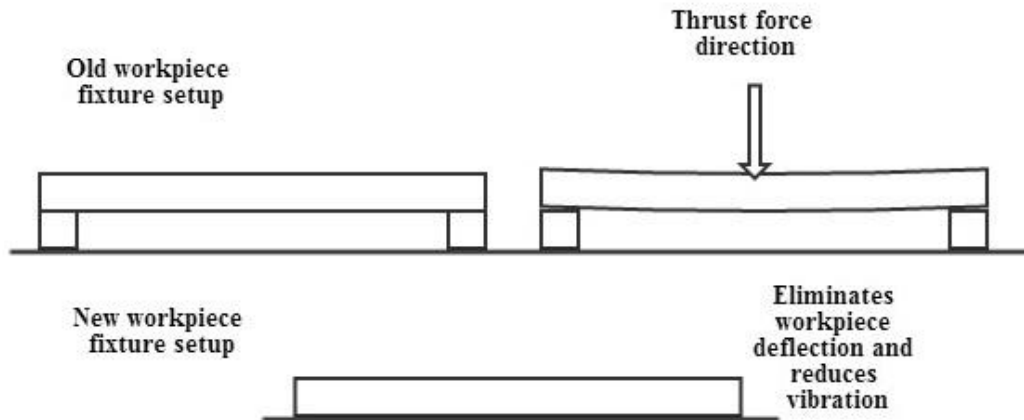


Figure 3.1. Diagram showing the change in workpiece fixturing from the old accelerated drill test employed by the partner organisation to the new workpiece fixturing employed during the preliminary drill test design phase. Clamping directly to the CNC bed will eliminate plate deflection caused by the thrust forces during drilling, as well as reduce vibration, a source of variance from the machine tool system.



Figures removed due to copyright reasons.

Figure 3.2. Spindle torque data published by Balzers comparing TiAlN PVD coating on 5D hole drilling with (a) and without (b) post polishing. Drill test: 8.5mm WC-Co drilling into graphite cast iron at cutting conditions of 70m/min 0.2mm/rev [69].

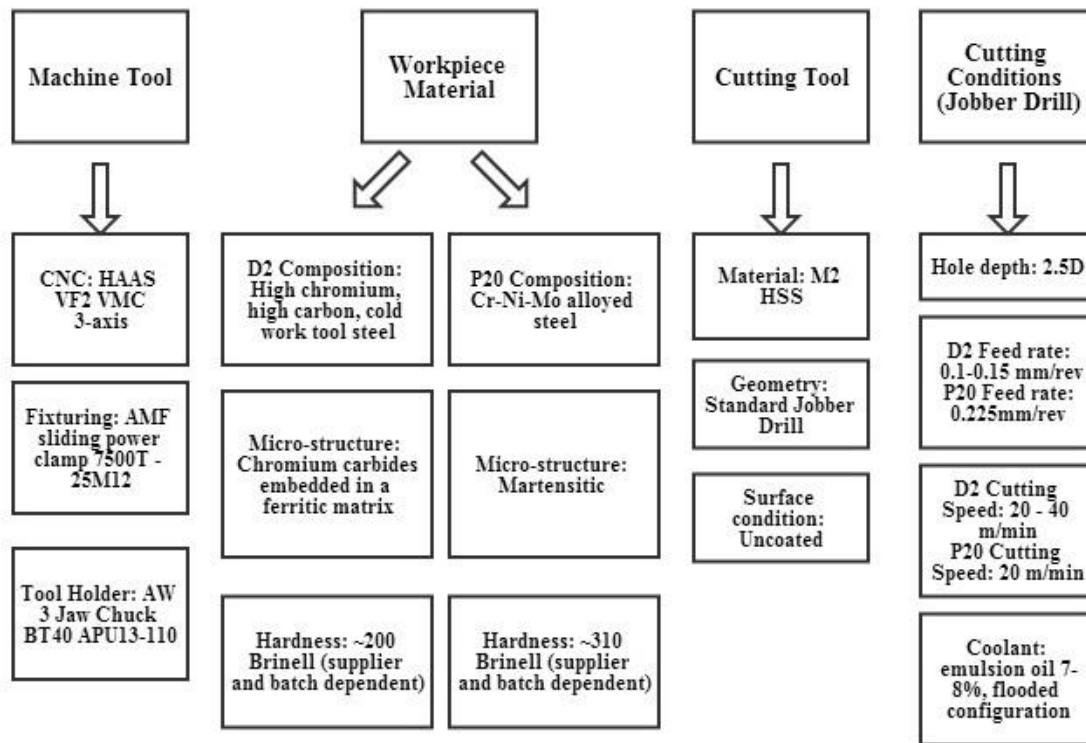


Figure 3.3 Diagram summarising the drill test design as a system.



Figure 3.4. Image showing the drill test setup in a HAAS VF2 VMC.

This thesis firstly examined the tool life and the failure modes induced by two workpiece materials D2 and P20 steel plate at accelerated cutting conditions in order to decide which material could offer an accelerated yet predominately single wear and failure mode. Sample statistics, boxplots, bivariate analysis and Weibull analysis in conjunction with the slope and characteristic life tests were used to analyse the data. The determination of mixed failure modes when testing in P20 was determined while D2 did not.

At this point the machinability of D2 was investigated by measuring the cutting forces during drilling for 9 different cutting parameters. Sources of variability in the drilling system were also characterised, such as, the hardness distribution across a steel plate (D2) using Leeb D and Vickers hardness measurements as well as the variability in macro geometry features of mass manufactured Jobber drills. The findings showed that plate hardness was heterogeneous across a plate but the variance was small. Jobber drill geometry features were found to have a large variance but the majority were within tolerances.

The developed drill test was then evaluated for its sensitivity to small changes in tool life using a surface engineering case study, pre and post polishing of TiN coated Jobber drills. A full factorial experiment was designed to evaluate the effect of pre and post drag polishing on tool life at two different cutting speeds. Statistical tests such as ANOVA and Mood's median were used to distinguish whether population changes had occurred to tool life and surface roughness measures using small samples. The results of which showed that although both pre and post polishing significantly affected surface roughness measures the only treatment which significantly effected tool life was pre polishing, this result was reproduced at both cutting speeds using ANOVA, however the Mood's median test suggests that the sample size may need to be 6 or greater with the current drill test design (current standard deviation).

Batch to batch plate hardness was observed. Therefore the effect of batch to batch plate hardness on tool life for uncoated Jobber drills was empirically modelled by extending the Taylor's tool life formula. The range of plate hardness this work covered was based on the variability in the supplied D2 steel from one supplier (Schmolz and Bickenbach) and was limited by the steel plates left. The cutting conditions characterised were of the range for uncoated M2 HSS Jobber drills.

An overall discussion is presented which incorporates the implications of all research findings in the context of the design, characterisation and application of the developed accelerated drill test. The thesis ends by highlighting the significant conclusions and future work.

## **3.2 A Statistical Analysis Comparing Tool Life and Failure Modes from Accelerated Drill Tests in P20 and D2 Steel Plate**

### **3.2.1 Introduction**

It has been shown (chapter 1 & 2.5) that the complex behaviour exhibited by the workpiece material needs to be managed in the context of cutting tool testing. The crystal phase [23] thermal conductivity and carbide distribution [24] for example, will influence a materials ability to resist cutting i.e. machinability. This intrinsic resistance to cutting can be observed by measuring the cutting forces, rate of tool wear or life (time or no. of holes) at failure during machining.

The cutting tool chosen for this particular study was the Sutton Tools 2.9mm uncoated R40 stub drill with a 130° split point angle and parabolic flute shape. This drill geometry was used (instead of the simpler Jobber drill design), because it offered a real manufacturing case study the partner organisation had, which was to determine the effect of two drill body hardness's on tool life. The work allowed the evaluation of the preliminary drill test design using the existing workpiece material used by the partner organisation P20 compared against D2.

The objective of this experiment was to determine the tool life distribution and the number of wear/failure modes present when drilling under accelerated conditions into P20 and D2 steel plate via statistical methods.

In order to design and develop a robust yet sensitive drill test which operates rapidly, it has been identified that a test material is needed which provides low tool life variance by offering a single/repeatable failure mode under accelerated tool wear conditions. The solution may be provided by drilling a material with low machinability and/or accelerating the cutting conditions and limiting the number of wear/failure modes in operation. Ideally, this material would have uniform hardness and microstructure and if applicable, carbide distribution. These properties may allow a sample of cutting tools to wear uniformly and fail by one mode repeatedly. Typically, wear-out processes follow a normal distribution compared to fatigue failure [15]; notwithstanding, depending on the type and number of wear and failure modes in operation, the distribution may be non-normal.

D2 cold work tool steel and P20 plastic mould steel have been chosen for this study. D2 steel is supplied in the annealed condition which is soft ~ 200 Brinell, however this material has large chromium carbides distributed throughout its ferritic matrix therefore it has a low machinability by offering a predominately high abrasive wear rate during machining [24]. On the other hand P20 plastic mould steel (partner organisations current testing material) is supplied in the quenched and tempered condition with a Brinell hardness ~310. This is considerably harder than the D2 steel; however there are no hard inclusions (carbides) to

wear the tool. Therefore, P20 may need a high cutting speed and/or feed in order to attain failure within an economic test duration.

### 3.2.2 Experimental Procedure

This work generated optical micrographs and measured the surface hardness of two different workpiece materials D2 cold work tool steel and P20 plastic mould steel. The body hardness was also measured on all R40 drills, followed by accelerated drill testing to failure in the two aforementioned materials.

#### 3.2.2.1 Workpiece Material D2 and P20

The supplier of the D2 steel, Schmolz and Bickenbach, supply an equivalent D2 plate material within the AISI tolerances [70], trade name Cryodur. They report a hardness value of approximately 200 Brinell and a nominal chemical composition shown in Table 3.1 [71]. From this point on in the work this material will be referred to as D2, unless specified. The supplier of the P20 steel, Bohler Uddeholm, supply an equivalent P20 steel within AISI standards [70] trade name M200. They report a plate hardness within the range of 290-330 Brinell hardness [72] and a nominal chemical composition shown in Table 3.2.

The hardness was measured across the surface using Leeb D hardness tester. A microstructural analysis of the two materials was completed. A top, bottom and side piece was cut off from the test plate, first by using a KASTO mechanical hacksaw at a low feed rate with cutting oil, followed by a Struers Labotom cut off wheel using emulsion coolant. A slow feed rate was used not to excessively heat the workpiece. The samples were then mounted in conductive phenolic resin in a Presi Mecapress. After which, the samples were polished in a Struers RotoPol using the MD-Piano disk with water for plane grinding then the MD-Allegro and MD-Largo with a 9 $\mu$ m diamond suspension for fine grinding, followed by a polishing step using the MD-Plus with a 3 $\mu$ m diamond suspension. Lastly the MD-Nap with 1 $\mu$ m diamond suspension was used for a final polishing step. Once samples were ground and polished a chemical etching treatment of 4% Nitric acid 96% ethanol was accomplished with 25 seconds for D2 and 15 seconds for P20.

Table 3.1. Nominal workpiece composition for D2 cold work tool steel supplied by Schmolz and Bickenbach [71].

Chemical composition (wt%)							
	C	Si	Mn	Cr	Mo	V	Fe
D2	1.55	0.3	0.35	12.0	0.75	0.9	Balance

Table 3.2. Nominal workpiece composition for P20 plastic mould steel supplied by Bohler Uddeholm [72].

Chemical composition (wt%)							
	C	Si	Mn	Cr	Ni	Mo	Fe
P20	0.37	0.3	1.4	2.0	1.0	0.2	Balance

### 3.2.2.2 *Drilling Conditions in D2 and P20 Steel*

Using tool life as the machinability criterion [73] preliminary testing was completed to find accelerated cutting conditions which would give between 100 and 200 holes tool life, this method of determining cutting conditions has also been used by Posti [41] and shown to be a reliable method of cutting condition determination . The chosen accelerated conditions was a cutting speed of 23m/min, feed rate of 0.08mm/rev for D2 while 35m/min and a feed of 0.14mm/rev was used for P20. A drill depth of 7.25mm or 2.5xD was used to minimise any chip packing and coolant flow issues. Testing was conducted in a HAAS-VF2 CNC machine (Vertical Machining Centre) VMC. The lubricant used was Houghton Hocut960 with concentration of approximately 7-8% in a flooded configuration.

### 3.2.2.3 *R40 Drill Hardness*

The body hardness for the 2.9mm R40 drills used in this study was measured using a Vickers Limited hardness tester with a 30kg load. Drills were first secured to a V-block clamp designed for multiple drill measuring, followed by a small flat ground into the body of the drill. Three indents were made per drill and the results averaged.



Figure 3.5. Image of the R40 stub drills held in a multiple vee clamp with the Vickers indenter above.

### 3.2.2.4 *Statistical Analysis methods*

Tool life data was analysed using the boxplot [74] and sample statistics to compare the measures of central tendency and dispersion of tool life between sample groups. Bivariate analysis [61] was used in order to determine if there existed a correlation between drill body hardness and tool life and whether body hardness could be responsible for tool life scatter. Weibull analysis using the median rank was used in order to apply the  $b$  slope and characteristic life tests for mixed failure distributions. The median rank was used compared

to the mean rank, as it has been shown to represent a sample group central tendency more accurately for sample sizes lower than 49[64].

### **3.2.3 Results**

#### **3.2.3.1 *P20 and D2 microstructure and hardness***

Optical micrographs of the microstructure for D2 cold work tool steel in the annealed condition and P20 plastic mould steel in the quenched and tempered condition are shown in Figure 3.6. Inspecting Figure 3.6 a, c and e confirms that the microstructure of D2 plate used has a ferritic matrix with large chromium carbides as the chromium carbides did not etch while the ferrite grain boundaries are slightly exposed. Chromium carbide grain size was measured to be between 5 and 30 $\mu\text{m}$  wide. Additionally, there appears to be slight banding of the chromium carbides across the side sample (Figure 3.6 e). Figure 3.6 b, d and f, reveals that P20 has a fine martensitic microstructure, as evidenced by the acicular grain structure, with a small number of inclusions sparingly distributed across the samples between 5-10 $\mu\text{m}$  wide. Plate hardness measurements shown in Table 3.3 reveals that P20 has a mean hardness of 559 HLD (~280 Brinell) and D2 a mean hardness of 470 HLD (~193 Brinell), with both plates having a small dispersion of hardness measurements.

Table 3.3. Sample statistics of measured hardness data for D2 and P20 test plate.

Variable	N	Mean	St Dev	Min	Q1	Median	Q3	Max
D2 Plate HLD	28	470	3.9	460	467	471	473	476
P20 Plate HLD	28	559	5.2	549	555	560	564	573

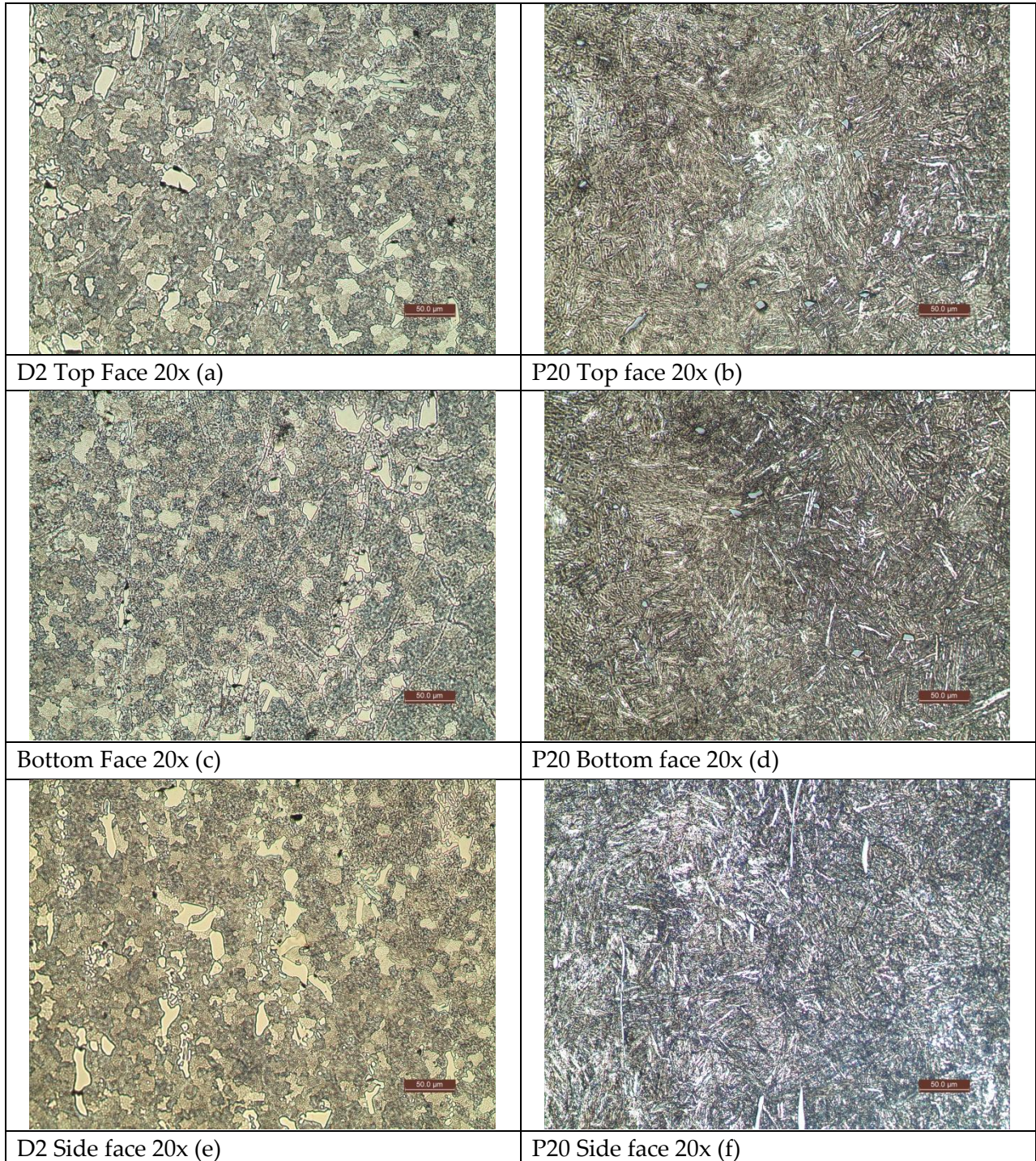


Figure 3.6 (a,b,c,d,e,f). SEM micrographs with a 50μm scale bar showing top, bottom and side face of D2 and P20 steel plate used in drill testing. Samples etched with Nital 4%

### 3.2.3.2 R40 Drill Hardness

The drill hardness results show that the low hardened R40 drills have a mean Vickers hardness normally distributed around 760HV<sub>30</sub>, while the high hardened drills have a mean Vickers hardness normally distributed around 864HV<sub>30</sub>. Both drill samples have a small standard deviation of 10HV<sub>30</sub> and 7HV<sub>30</sub> respectively. From this point on in the work the low and high hardened drills will be referred to as 760HV<sub>30</sub> 860HV<sub>30</sub>.

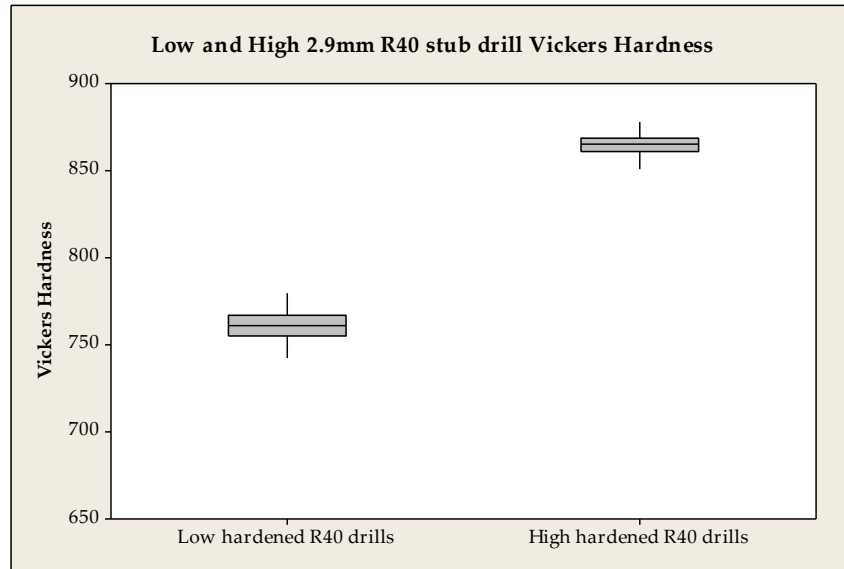


Figure 3.7. Boxplot of drill body hardness measurements made from the average of three Vickers hardness readings on the body of each low and high hardened R40 drill.

Table 3.4. Sample statistics for low and high hardened R40 drills made from the average of three Vickers hardness readings on the body.

Description	N	Mean	St Dev	Min	Q1	Median	Q3	Max
Low hardened drills	20	760.3	10	742	755	761	767	780
High hardened drills	20	864.5	7	851	861	865	869	878

### 3.2.3.3 Tool life results

Individual tool life results for the R40 drills tested in P20 and D2 test plate are shown in Figure 3.8, sample statistics of the tool life are shown in Table 3.5, in addition the mean tool lives with their corresponding 95% confidence intervals are shown in

Table 3.6. These results show that from the 760HV<sub>30</sub> drills tested in P20 and D2 the mean results are similar, 158.7 and 133.0 holes respectively, however, the results show that the drills tested in D2 have a higher median value, 99.0 and 137.0 respectively. Comparing the mean and median value of the drills tested in P20 and D2 the tool life distribution for the R40 drills tested in P20 are skewed while the tool life distribution for D2 is normal. The tool life from drills tested in P20 have a higher standard deviation than the drills tested in D2, 122.4 and 46.7 respectively. The confidence intervals for the mean tool life show that the P20



results with the lower and upper confidence interval being 71.2 – 246.2 respectively and for D2 the confidence intervals are 100.5 to 167.3.

The 860HV<sub>30</sub> R40 drills tested in P20 and D2 have significantly different means of 247.9 and 183.9 respectively, however, the median results reveal the same relationship as the 760HV R40 drills with the median being higher for the D2 tool life of 160.5 to 14.0 2.5xD holes respectively. Table 3.5 indicated that the tool life is highly skewed for the 860HV drills tested in P20 and only slightly skewed for the 860HV drills tested in D2. The standard deviation is extremely high for the 860HV drills tested in P20 compared to the D2 results, with values of 386.5 and 90.0 respectively.

Table 3.6 shows a large range between the lower and upper confidence intervals for 860HV R40 drills tested in P20 -28.5 to 524.3 indicating that calculating the confidence intervals for the population mean is not practical for this data set, as it is not a normal distribution. The 860HV<sub>30</sub> drills from the same population tested in D2 have a confidence interval range of 119.2 – 248.3 for the population mean.

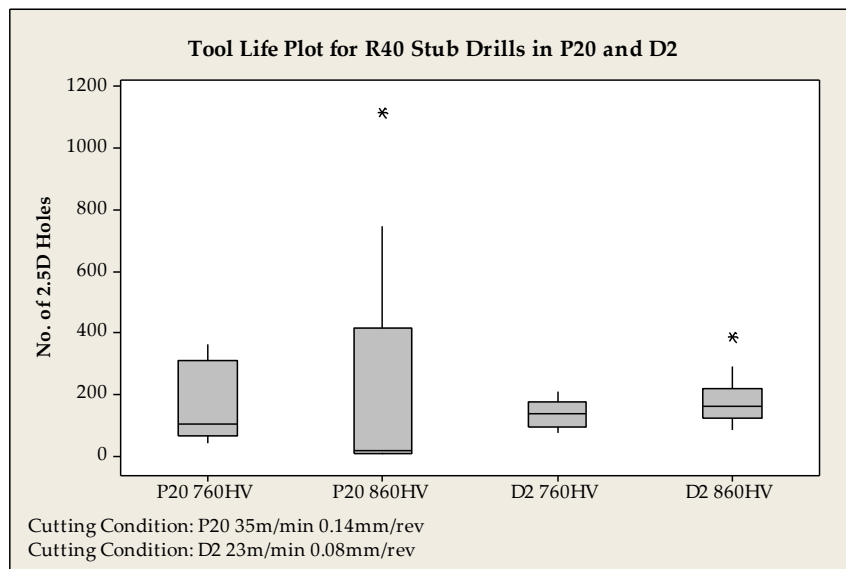


Figure 3.8. Individual value plot for 750 and 850HV<sub>30</sub> R40 2.9mm bright stub drills tested in P20 and D2 steel showing a smaller range of results testing in D2.

Table 3.5. Sample statistics for tool life results represented as the number of 2.5xD holes for R40 760HV<sub>30</sub> and 860HV<sub>30</sub> drills tested in P20 and D2 workpiece.

Description	N	St Dev	Min	Q1	Median	Q3	Max
P20 760HV <sub>30</sub>	10	122.4	39.0	61.2	99.0	306.7	363.0
P20 860HV <sub>30</sub>	10	386.5	4.0	6.7	14.0	414.0	1114.0
D2 760HV <sub>30</sub>	10	46.7	70.0	93.0	137.0	171.0	208.0
D2 860HV <sub>30</sub>	10	90.0	83.0	120.5	160.5	215.7	383.0

Table 3.6. Mean tool life of 760HV<sub>30</sub> and 860HV<sub>30</sub> R40 drills tested in P20 and D2 with corresponding lower and upper confidence intervals for the mean number of 2.5xD holes.

Description	N	Mean	Mean 95% CI Lower	Mean 95% CI Upper
P20 760HV <sub>30</sub>	10	158.7	71.2	246.2
P20 860HV <sub>30</sub>	10	247.9	-28.5	524.3
D2 760HV <sub>30</sub>	10	133.0	100.5	167.3
D2 860HV <sub>30</sub>	10	183.9	119.5	248.3

Referring to Figure 3.9, the results show that the 760HV<sub>30</sub> R40 drills tested in P20 had six drills performing below the average tool life, with two of the six drills having hardness above the mean and four below. The remaining four drills performed above the mean tool life with two drills above and below the mean hardness. The 860HV<sub>30</sub> R40 drills tested in P20 had six drills with tool lives far below the mean tool life, with five drills below the mean hardness and one above. While the remaining four drills had tool lives above the mean tool life and above the mean hardness.

The results from Figure 3.10 shows that the 760HV<sub>30</sub> R40 drills tested in D2 have six drills which performed below the mean tool life with two drills having hardness's above the mean and four below. Four of the 760HV<sub>30</sub> drills performed above the mean life with two above the mean hardness and two below. The 860HV<sub>30</sub> R40 drills tested in D2 had six drills with tool lives below the mean, with five drills below the mean hardness and one above. Furthermore the remaining four drills performed above the mean life with three having body hardness's below the mean and one above

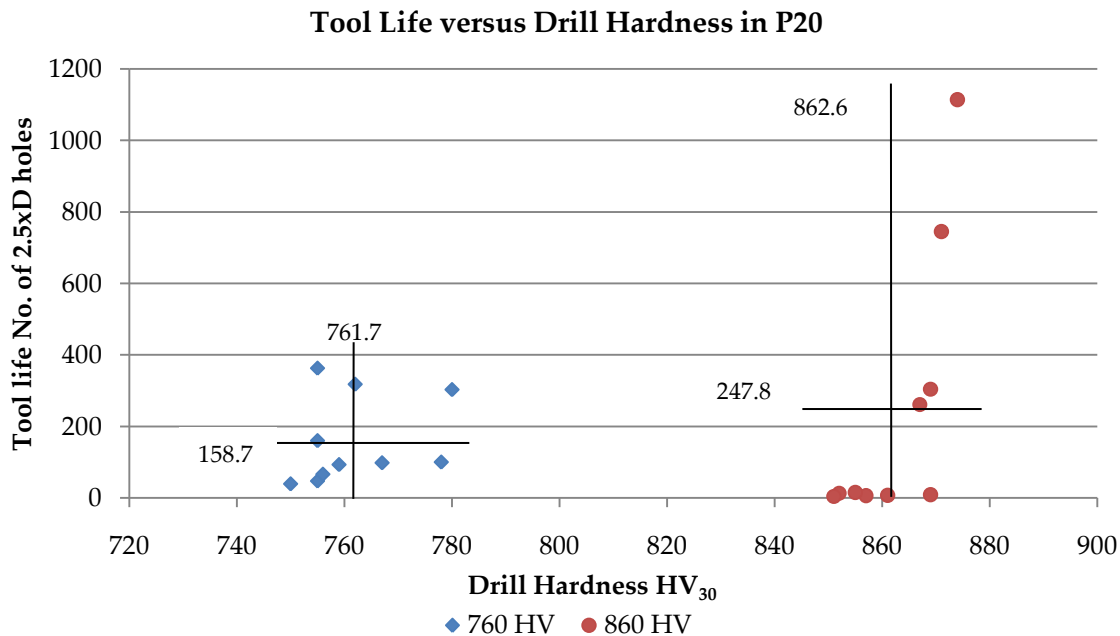


Figure 3.9. Tool life results versus corresponding drill hardness measurements for samples drilled in P20 test. Vertical and horizontal lines refer to the means of the tool life and drill body hardness.

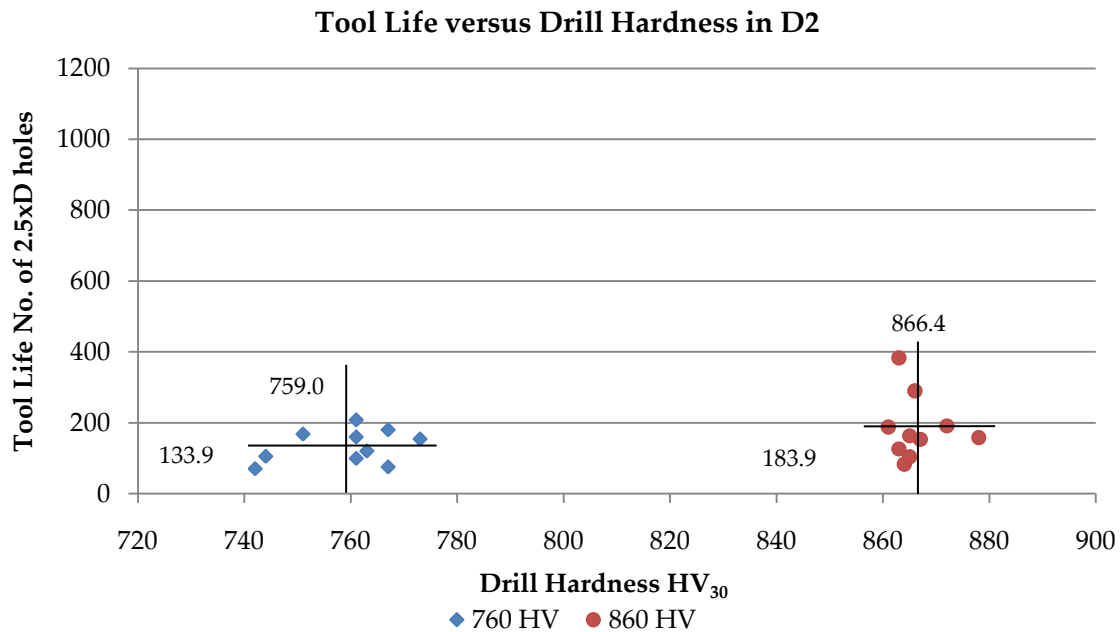


Figure 3.10. Tool life results versus corresponding drill hardness measurements for samples drilled in D2. Vertical and horizontal lines refer to the means of the tool life and drill body hardness.

### 3.2.3.4 Weibull Failure Mode Analysis

Weibull analysis was applied to the failure data collected from accelerated drill tests, (chapter 2.7 Eq. 6). Samples 760HV<sub>30</sub> and 860HV<sub>30</sub> drills tested in P20 appear to have mixed failure modes in operation as two different slopes are observed in both groups (Figure 3.11). The shape factor (*b*) for the 760HV<sub>30</sub> drills is 1.33 indicating a wear out failure mode within the design period (Table 3.7). The shape factor for the 860HV<sub>30</sub> drills is 0.45, this shape parameter is below 1, indicating that early life failures have predominately occurred due to the low gradient and therefore the spread of results. In the context of cutting tools

In order to test the hypothesis of mixed failure modes, the failure transition point was estimated in both 760 and 860HV<sub>30</sub> drills tested in P20. Using the rule of maximising the linear correlation coefficients the data sets were split into two subsets labelled 760HV<sub>30a</sub> and 760HV<sub>30b</sub>, the same was applied to 860HV<sub>30</sub> failure data. Applying the *b* slope test with a 95% confidence limit (Eq. 7) resulted in the hypothesis of mixed failure modes being confirmed. The flatter slope of both subsections lied below the lower confidence bound and or the steeper slope lied above the upper confidence bound Table 3.8. The subsections have been shown to be statistically different groups with different failure modes. The 760HV<sub>30a</sub> data has a shape factor of 1.84, still indicating failure within the design period. The 760HV<sub>30b</sub> data has a shape factor of 3.66 (Table 3.8) which is also failure within the design period, however, this value indicates a normal distribution unlike the 760HV<sub>30a</sub> which is a

skewed distribution. The 860HV<sub>30a</sub> subsection has a shape factor of 1.76 which is a failure within the design period with a skewed distribution Table 3.8. The 860HV<sub>30b</sub> has a slope of 0.57 indicating early life or premature failure.

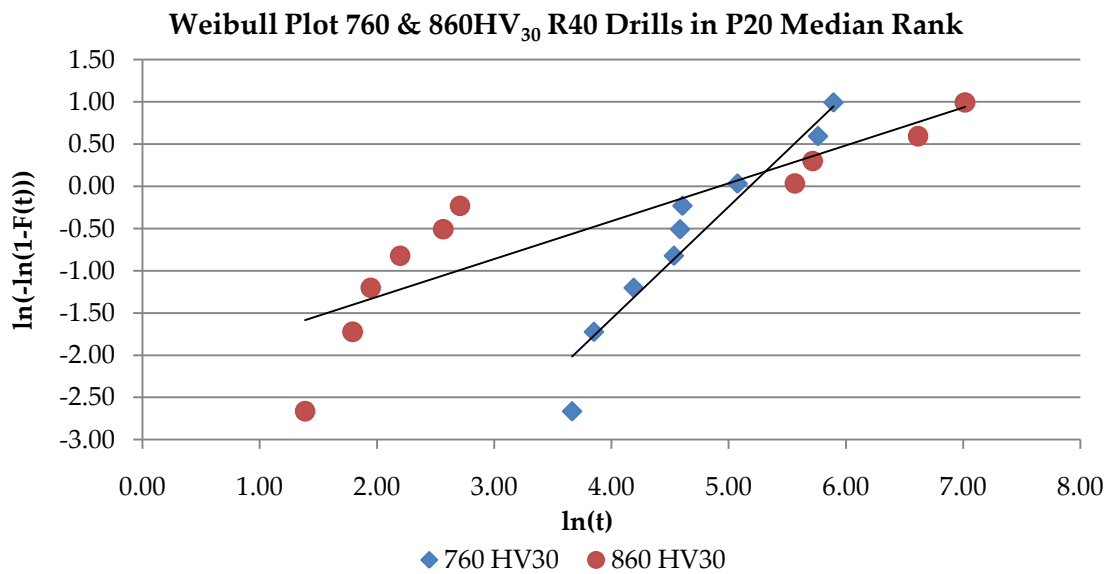


Figure 3.11. Weibull plot of the life time data using median rank for 760 and 860HV<sub>30</sub> R40 2.9mm bright stub drills tested in P20 steel plate.

Table 3.7. Weibull factors using median rank, shape factor b, Characteristic life T and linear correlation coefficient R<sup>2</sup> for 760 & 860HV<sub>30</sub> drills failure data.

Median rank			
Description	b slope	T characteristic life	R <sup>2</sup>
P20 760HV <sub>30</sub>	1.33	177.84	0.91
P20 860HV <sub>30</sub>	0.45	136.64	0.78

Slope test for mixed failure distribution

$$b \left( 1 \pm u_{1-\frac{\alpha}{2}} \frac{0.78}{\sqrt{n}} \right) \quad \text{Eq. 7}$$

Where:

$u_{1-\frac{\alpha}{2}}$  = Confidence limit for both sides (1.96 for 95% confidence limit)

b = Shape parameter, slope of the fitting line in the Weibull plot.

n = Number of samples.

Characteristic life test for mixed failure distribution

$$T \pm u_{1-\frac{\alpha}{2}} \frac{1.052 T}{b\sqrt{n}} \quad \text{Eq. 8}$$

Where:

$u_{1-}$  = Confidence limit for both sides (1.96 for 95% confidence limit)

n = Number of samples.

T = Scale parameter, characteristic life during which a total of 63.2% of samples have failed.

b = Shape parameter, slope of the line of best fit from the Weibull plot.

The lower and upper 95% confidence bounds are calculated using the data from Table 3.7.

Slope test for 760HV<sub>30</sub> drills in P20.

$$1.33(1 \pm 1.96 \frac{0.78}{\sqrt{10}}) \quad \text{Eq. 9}$$

$$b_{lower} = 0.69 \quad b_{upper} = 1.97$$

Slope test for 860HV<sub>30</sub> drills in P20.

$$0.45(1 \pm 1.96 \frac{0.78}{\sqrt{10}}) \quad \text{Eq. 10}$$

$$b_{lower} = 0.23 \quad b_{upper} = 0.66$$

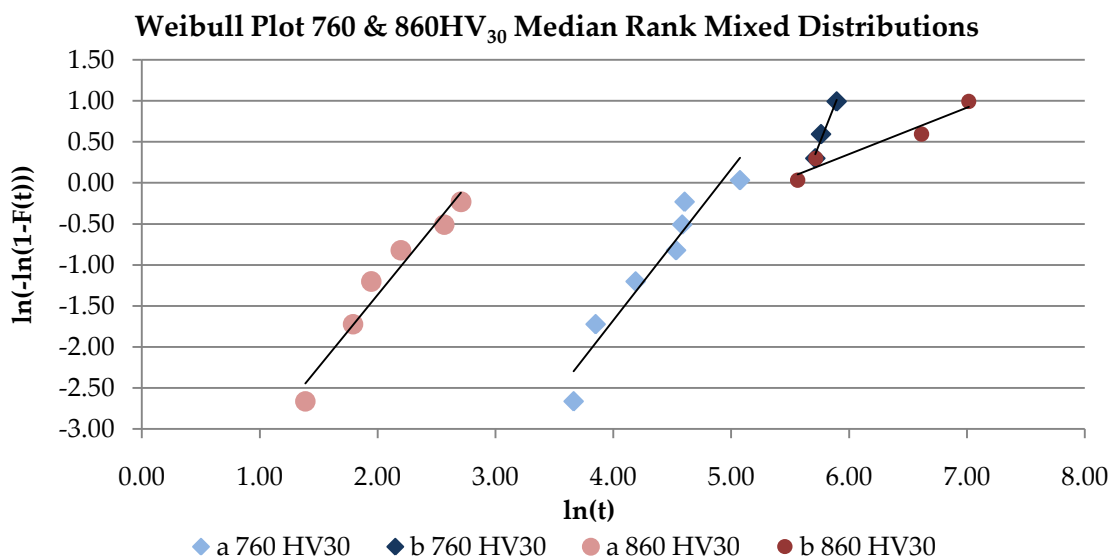


Figure 3.12. Mixed Weibull plot of the life time data using median rank for 760 and 860HV<sub>30</sub> R40 2.9mm bright stub drills tested in P20 steel plate.

Table 3.8. Separated Weibull factors using median rank. Shape factor  $b$ , Characteristic life  $T$  and linear correlation coefficient  $R^2$ . Within bounds meaning that the distributions do not have mixed failures.

Median rank				
Description	b slope		T characteristic life (no. of 2.5xD holes)	$R^2$
P20 750 HV <sub>30</sub> a	1.84	Within Bounds	135.4	0.92
P20 750 HV <sub>30</sub> b	3.66	Out of Bounds	275.5	0.97
P20 850 HV <sub>30</sub> a	1.76	Out of Bounds	16.0	0.95
P20 850 HV <sub>30</sub> b	0.57	Within Bounds	218.1	0.94

The Weibull graph (Figure 3.13) of the 760HV<sub>30</sub> and 860HV<sub>30</sub> R40 drills tested in D2 also showed possible mixed failure modes. The 760HV<sub>30</sub> drills had a shape factor of 2.91 with a characteristic life of 151 holes (Table 3.9), indicating that these drills failed within the design period. The 860 HV<sub>30</sub> drills have a shape factor of 1.36 and a characteristic life of 135 holes (Table 3.9) also indicating failure within design period. The 760HV<sub>30</sub> group appears to have similar slopes but offset in time, while the 860HV<sub>30</sub> group appears to have different slopes (Figure 3.13). Therefore the slope (Eq. 11) and characteristic life (Eq. 12) test was conducted on these data sets. The 760HV<sub>30</sub> and 860HV<sub>30</sub> groups were split into subsets by using the rule of maximising the linear correlation coefficients. The characteristic life test revealed that the 760HV<sub>30</sub> groups 'a' and 'b' are not offset in time; however the slopes are significantly different with subset 'b' lying above the upper slope limit. The 760HV<sub>a</sub> and b subsets have a shape factor 3.96 and characteristic tool lives of 136 and 158 holes. The results showed that the 860HV<sub>30a</sub> and 860HV<sub>30b</sub> passed the slope test indicating that all drills in this sample failed uniformly.

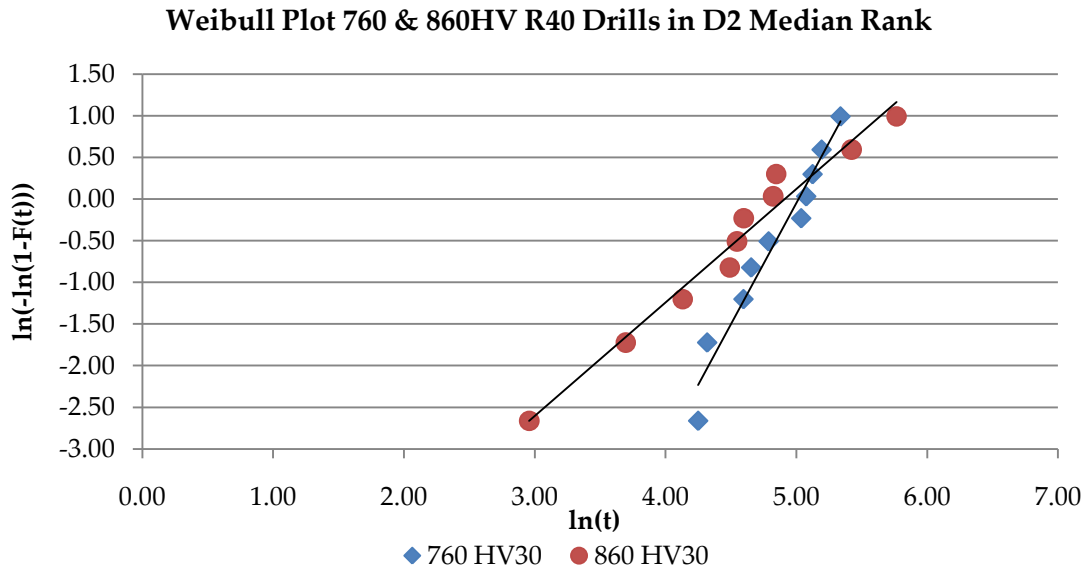


Figure 3.13. Weibull plot of the life time date using median rank for 760 and 860HV<sub>30</sub> R40 2.9mm bright stub drills tested in D2 steel plate.

Table 3.9. Weibull factors using median rank, shape factor b, Characteristic life T and linear correlation coefficient R<sup>2</sup> for 760 & 860HV<sub>30</sub> drills failure data.

Median rank			
Description	b slope	T characteristic life (no. of 2.5xD holes)	R <sup>2</sup>
D2 750HV <sub>30</sub>	2.91	150.9	0.97
D2 850HV <sub>30</sub>	1.36	135.8	0.97

Slope test for 760HV<sub>30</sub> drills in D2 with median ranking.

$$2.91(1 \pm 1.96 \frac{0.78}{\sqrt{10}}) \quad \text{Eq. 11}$$

$$b_{lower} = 1.51 \quad b_{upper} = 3.87$$

Characteristic life test for 760HV<sub>30</sub> drills in D2 with median ranking.

$$150 \pm 1.96 \frac{1.052 \times 150}{2.91 \times \sqrt{10}} \quad \text{Eq. 12}$$

$$T_{lower} = 116.5 \quad T_{upper} = 183.7$$

Slope test for 860HV<sub>30</sub> drills in D2 with median ranking.

$$1.36(1 \pm 1.96 \frac{0.78}{\sqrt{10}}) \quad \text{Eq. 13}$$

$$b_{lower} = .71 \quad b_{upper} = 2.01$$

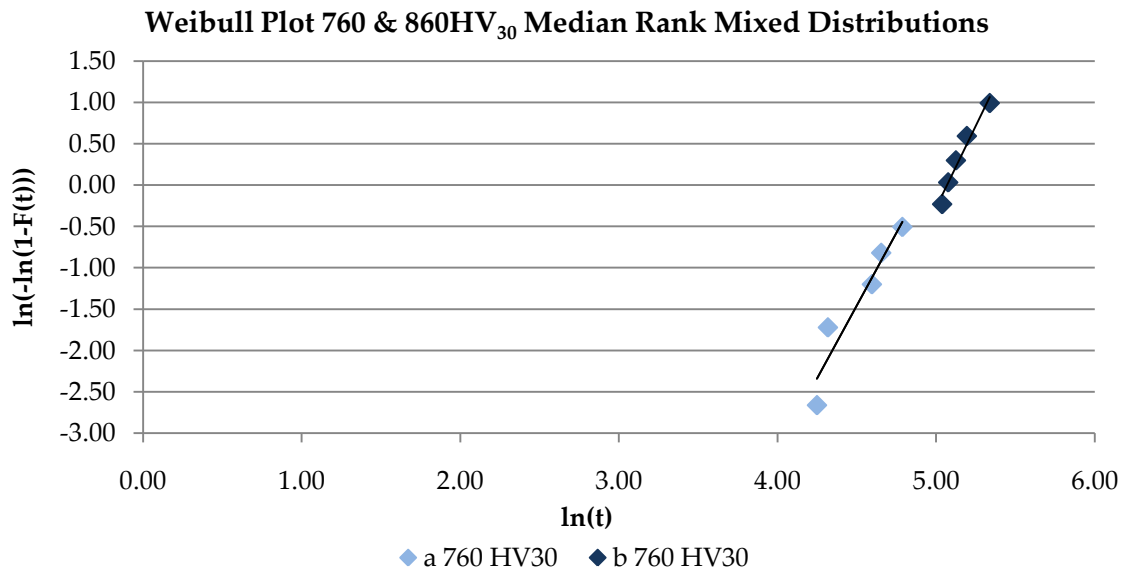


Figure 3.14. Mixed Weibull plot of the life time date using median rank for 760 and 860HV<sub>30</sub> R40 2.9mm bright stub drills tested in D2 steel plate.

Table 3.10. Separated Weibull factors using median rank. Shape factor b, Characteristic life T and linear correlation coefficient R<sup>2</sup>. Within bounds meaning that the distributions do not have mixed failures.

Median rank					
Description	b slope		T characteristic life (no. of 2.5xD holes)		R <sup>2</sup>
D2 760HV <sub>30</sub> a	3.52	Within Bounds	136.1	Within Bounds	0.91
D2 760HV <sub>30</sub> b	3.96	Out of Bounds	158.9	Within Bounds	0.96
D2 860HV <sub>30</sub> a	1.28	Within Bounds	155.2	Not Tested	0.99
D2 860HV <sub>30</sub> b	0.96	Within Bounds	114.1	Not Tested	0.94

### 3.2.4 Discussion

This experiment was designed to identify which of the two test materials could offer a single wear and failure mode during a test and accelerate tool wear in order to minimise time spent testing, so as to provide low tool life variance induced by the complex behaviour of the material and the wear mechanisms interacting with a HSS drill. It has been identified that wear-out processes follow a normal distribution compared to fatigue failure [15]. Therefore this indicator was considered during the analysis of tool life data. The materials microstructure was also examined, as a material with a uniform hardness and microstructure and if applicable, carbide distribution may offer low tool life variance by having all samples interacting with notionally the same material over a test.

A microstructural examination of D2 and P20 steel showed that the D2 equivalent steel plate on a microscopic scale is an inhomogeneous material. The D2 plate consisted of large



chromium carbides embedded in a ferritic matrix, with weak banding of carbides. This is consistent with the microstructural analysis of annealed D2 reported by Roberts [75]. However, the D2 steels inhomogeneity is uniformly distributed. Coupled with the fact that the scale of the drill features used such as the cutting edge lengths (~1.2mm) is an order of magnitude larger than any localised non-uniformity (carbide size 5-30 $\mu$ m), in the context of drill testing the material may be considered uniform. Therefore, a sample of drills will be interacting with notionally the same microstructure. Variation of the surface plate hardness was measured in D2, with a mean hardness of 470HLD and a standard deviation of 3.9HLD; however, this is still a low dispersion of hardness. Therefore, D2 steel in the application of drill testing can be described as a homogeneous material with uniform properties.

The P20 plate examined was found to be homogeneous with a martensitic micro structure and a small amount of inclusions distributed sparingly throughout. The P20 plate was considerably harder than the D2 plate with a mean hardness of 559HLD. The standard deviation was also slightly higher with a value of 5.2HLD; however this is a low dispersion of hardness measurements. Therefore, P20 steel may also be considered, in the application of drill testing, to be a homogeneous material with a uniform hardness and microstructure suitable for testing. However, these results are only applicable to a small region of the plate where the sample was taken. A sample from the centre and edge of the plate may reveal a difference in the microstructure across the plate, as the cooling rate is an extremely important factor in grain size [76].

The sample statistics and box plots of the tool life data from drilling in D2 and P20 reveal that a lower tool life standard deviation was attained when testing in D2 rather than P20. Additionally the drills tested in D2 had normal distributions of tool life, this indicates a wear-out process [15].

The Weibull slope and characteristic life test for mixed failure distributions revealed that both sample groups had at least two different failure types when tested in P20, while only the 760HV<sub>30</sub> R40 drills tested in D2 had mixed failures due to the *b* slope test. The mixed failures while testing in P20 is one reason for the significantly larger standard deviations calculated, while the mixed failure in the 760HV<sub>30</sub> drills tested in D2 did not influence the standard deviation as much. The bivariate graphs revealed that the cause of the failures was potentially not due to the variance in the body hardness of the R40 drills as the standard deviation for both 760HV<sub>30</sub> and 860HV<sub>30</sub> samples are small, 10HV<sub>30</sub> and 7HV<sub>30</sub> respectively and drills with similar hardness performed well when tested in D2. Additionally, the drill's hardness is still significantly harder than the workpiece materials.

The early life failures may be due to microstructural defects within the HSS, such as fractured ledeburite carbides which have fractured during the drawing process which may weaken the cutting edges. Another possible reason could be the macro geometry features out of tolerance, such as the primary lip relief [16]. If the primary lip relief of the six drills which failed early was not high enough then their interaction with the workpiece at the

accelerated feed rate used would result in severe friction conditions on the flank face, however, this is impossible to be done post-test. It may be acceptable for the inspection of the primary lip relief pre-test, in order to eliminate this factor as a potential cause, as this feature is relatively simple and quick to measure compared to point centrality or lip height variation. However, the D2 material was more difficult to machine due to the chromium carbides and did not require high cutting speed or feed rate in comparison to P20 to accelerate wear and therefore would not require any pre-test inspection of macro geometries. Note that the abrasive wear encountered while machining annealed D2 is difficult to identify. The 2 body abrasion model as described by Misra and Finnie [77] where the hard particles are embedded or rigidly attached in or to the second body and are able to cut deeply into the first body may explain this type of abrasive wear encountered while machining D2. However, Leed [78] states that while machining annealed D2 the cutting edge is able to “plough through the soft [ferritic] matrix and literally push the hard carbides aside” which is more in favour of a closed three body abrasion model as defined by Misra and Finnie [77] where the hard particles are free to move between two closely mating surfaces. A source of complexity in defining the abrasive wear holistically arises from the questions, are the chromium carbides truly fixed, free to move or somewhere in between? How do the carbides interact with the cutting tool as the chip flows across the rake and the flank moves across the freshly machined surface?

The analysis of tool life performance of the 760HV<sub>30</sub> and 860HV<sub>30</sub> R40 drills revealed that the 860HV<sub>30</sub> high hardened drills had the highest mean tool life performance when tested in P20 and D2 steel. The median tool life results only show this relationship for drills tested in D2, as the 860HV<sub>30</sub> drills resulted in a large standard deviation in tool life and a large number of early life failures (60% of drills) which significantly skewed the distribution to the lower end. However, when comparing the 760HV<sub>30</sub> and 860HV<sub>30</sub> R40 drills tested in D2 there is no significant difference between the mean of the samples at a confidence limit of 95%, as the confidence limits cross over. This conclusion could not be drawn from the drills tested in P20. It can be argued that if no significant conclusion can be drawn from a test, therefor no new information has been gathered yet a cost has been paid. This places D2 as the preferable test material in the context of developing a robust, sensitive and timely drill test.

### **3.2.5 Conclusions**

As expected, D2 cold work tool steel was found to have an inhomogeneous microstructure, however, it was confirmed that it is evenly distributed across the sample examined with weak banding of the chromium carbides. Conversely, P20 plastic mould steel was found to have a homogenous microstructure with inclusions found sparingly distributed. Surface hardness measurements were within a small range for both materials. Localised heterogeneous characteristics such as carbide banding in D2 and inclusions in P20 were found to not be in the same order of magnitude as the length of cutting edges for the 2.9mm diameter drill used. Notwithstanding, in the context of drill testing, the inhomogeneous

material (D2) did not lead to an increase in tool life variance, while the homogenous material (P20) did.

Tool life data analysed revealed skewed tool life distributions when testing in P20 and Weibull tests for mixed failures distributions suggests that multiple failure modes operated during accelerated drill testing in P20. This resulted in a large standard deviation which did not allow a statistically significant comparison to be made between the 760HV<sub>30</sub> and 860HV<sub>30</sub> drills. In stark contrast, no mixed failures were found from 860HV<sub>30</sub> drills tested in D2 but a mixed failure distribution was found within the 760HV<sub>30</sub> drills tested. However, this did not significantly increase the standard deviation in tool life and therefore the conclusion that there is no difference in the population mean for the two hardness drills could be made. The D2 material potentially offered an accelerated wear rate through predominately abrasive wear, however, the actual wear mechanism was not determined. The tool life criteria used to determine accelerated cutting conditions (100-200 holes) for P20 was potentially too high for drills which may have had their primary lip relief too low. This work suggests the importance of the acceleration of the abrasive wear mechanism for low tool life variance in testing of HSS drills and not high mechanical or thermochemical wear mechanisms with P20.

The findings from this experiment indicate that D2 steel is the preferable test material over P20 steel, as it has shown to offer a repeatable failure mode with a low standard deviation of tool life, potentially via a predominately abrasive wear mode. D2 has also shown to accelerate wear without significantly increasing the cutting parameters in comparison to P20, offering an economic test duration. Therefore this material was exclusively used during the subsequent accelerated drill tests.

### **3.3 Examining Sources of Tool Life Variability and Torque and Thrust Response to Cutting Parameters in Drilling of D2 Steel**

#### **3.3.1 Introduction**

A premise of this thesis is that if sources of tool life variance are eliminated and/or reduced and the complex behaviours of the machining system can be managed for a single and repeatability wear/failure mode, then small differences between samples (which themselves are small) may be distinguished by reducing scatter in the tool life results. It is known that sources of variance within the machining system effect the distribution of tool life results. It was shown in the previous experiment (chapter 3.2) that two physically different sample sets of the same drill design tested in P20 were not able to be tested for a population change/difference as the standard deviation in tool life was large and the distribution non-normal and bi-modal. However, this did not occur with the same samples tested in D2, as the standard deviation was small compared to the sample size and the distributions were close to normal which allowed a statistical test to show that there was no significant difference in tool life between the two samples. It was postulated that D2 drilled in the specific cutting regime was able to offer a single and repeatable failure mode as shown by the low standard deviation.

A source of tool life variance previously identified in chapter 1.3 is the macro geometry features. Key features which have significant effects on the central tendency and dispersion of tool life results are the primary lip relief, lip height variation and chisel edge centrality [16]. Therefore, the variability in macro geometry features of the 6.35mm uncoated Jobber drills was determined using tool maker's microscopes, as this drill has been chosen by the partner organisation to be used exclusively in cutting tool design experimentation. Therefore an estimate of the dispersion of the population is justified.

Another source of tool life variance examined within this chapter is the plate hardness. The effect on tool life dispersion has been shown to be significant in the study by Vogel and Bergmann [12]. They determined the effect of plate hardness on the tool life for Jobber drills tested to screech failure in 42CrMo4V steel. They showed that between 28-36 HRC an exponential fall in the number of holes drilled (tool life) occurs. Therefore, tool life is sensitive to plate hardness, hence, the plate hardness was measured using a Leeb D portable hardness device and a Vickers 30Kg hardness machine, in order to map the spatial hardness distribution in the test plate. The hardness distribution was a factor investigated in the previous experiment however, the distribution of hardness across the plate was not determined, additionally an evaluation of the accuracy of the portable hardness method needed to be conducted as this method will be used in future tests due to the size of the steel plate.

It has been shown by Williams, Smart and Milner in their turning experiments of low carbon steel (Figure 2.12) that a minimum in cutting force occurs between 30-35m/min as the cutting speed is increased from 0-50m/min due to BUE formation. Additionally, according to Dolodarenko and Ham [79] “In actual drilling operations, built-up-edge is observed in all but a few exceptional cases” as HSS drills are typically operating in the BUE formation region (Figure 2.12). Balzers have also shown that the cutting torque will increase the deeper a hole is drilled due to chip removal issues (Figure 3.2) [69]. With all the complex interactions and large number of factors which influences the cutting forces, can a specific cutting force be prescribed to a drill? Hence, the machinability of D2 was investigated through the evolution of torque and thrust over the life of a drill at a set of nine cutting parameters using the M2 uncoated 6.35mm Jobber in order to determine whether a specific cutting force can be prescribed as well as to determine if 2.5xD hole depths offer no chip removal issues.

### 3.3.2 Experimental Procedure

The macro geometry features of 52 randomly selected 6.35mm uncoated Jobber drills from a batch of 500 was measured. The surface hardness measurements of a plate of D2 cold work tool steel. Lastly, the torque and thrust was progressively measured during drilling into the aforementioned D2 plate for nine different cutting conditions using nine of the 52 drills randomly sampled.

#### 3.3.2.1 Jobber Drill Geometry

The drill used in this study was the Sutton Tools 6.35mm uncoated M2 HSS Jobber. The drill macro design was measured using two tool makers’ microscopes, the first model MohawkTools Co. 560 Tool Analyzer consisting of the standard 90° pivot vee stage with objective lens, the second, a Euro-tech tool makers microscope fitted with a digital camera. Both measurement devices follow the same procedures (chapter 2.9.2) in order to measure cutting tool features, it is the same measurement tool after all. The Jobber drill design specification is shown in Table 3.11. Jobber drills used in the work were selected at random from a batch of 500 drills in total were measured to gauge the macro geometry variance.

Table 3.11. Design specifications measured for the 6.35mm jobber drill.

Design specification 6.35mm diameter jobber drill	Value	Standard
Chisel angle (°)	120-125	Sutton Tools standard
Point angle (°)	118 ± 5	ASME B94.11M-1993
Web thickness (mm)	0.95-1.00	DIN 1414 Twist Drills
Mean transverse margin width (mm)	0.315–0.63	DIN 1414 Twist Drills
Lip relief angle(°)	14 ± 2	Sutton Tools standard

Mean helical angle (°)	30-35	DIN 1414 Twist Drills
Point centrality (µm)	102 MAX	ASME B94.11M-1993
Relative lip height (µm)	76 MAX	ASME B94.11M-1993

### 3.3.2.2 Workpiece Material & Hardness

The D2 steel used in this work was supplied by Bohler Uddeholm. The D2 plate steel is supplied in the annealed condition with a hardness approximately 210 Brinell and a composition given in Table 3.12. The plate hardness was measured using a hand held Leeb D tester (HLD) and a Vickers Limited hardness tester with a 30kg load (HV<sub>30</sub>). The measurements were made across the top surface of a 40cm x 36cm D2 plate in an 8x8 grid. Four measurements were made per grid and averaged.

Table 3.12. Nominal workpiece composition for D2 cold work tool steel supplied by Bohler Uddeholm [80].

Chemical composition (wt%)							
	C	Si	Mn	Cr	Mo	V	Fe
D2	1.55	0.25	0.35	11.8	0.8	0.95	Balance

### 3.3.2.3 Accelerated Cutting Conditions

Nine accelerated cutting parameters (cutting speed and feed rate) were selected in a 2 factor 3 level array. The lowest cutting parameter (30m/min and 0.1mm/rev with emulsion coolant) was the lowest recommended accelerated conditions from discussion with Sutton Tools engineers [81]. The feed rate of 0.1mm/rev is the recommended for general purpose, however the cutting speed is double that advised for tool steels. The other eight cutting parameters were determined by increasing the lowest cutting speed by intervals of 5m/min and the feed rate by 0.025mm/rev see (Table 3.13). Nine jobber drills were selected from the 52 drills test each of the cutting condition over their entire life measuring torque and thrust. The drill test was carried out in a VMC HAAS-VF2SS CNC machine. The lubricant used was a Houghton Hocut960 with concentration of approximately 7-8% in a flooded configuration.

Table 3.13. Showing experimental design of accelerated cutting conditions for study.

Drill No.	Feed rate (mm/rev)	Cutting Speed (m/min)
28	0.100	30
38	0.100	35
35	0.100	40
40	0.125	30
37	0.125	35
34	0.125	40
36	0.150	30
32	0.150	35

### 3.3.2.4 Torque and Thrust Measurements

Prior to the trial a strip of D2 material from the test plate was cut and machined to provide a small test piece (180mm x 40mm) which could be mounted to the dynamometer (Figure 3.15). Torque and thrust measurements were recorded starting at hole 1 and every hole after till the 20<sup>th</sup> hole, at which point the torque and thrust measurement were recorded after every 20<sup>th</sup> hole till failure. Measurements were recorded using a Kistler 9272 dynamometer, via Kistler charge amplifiers (5011B) and an Iotech Daqbook 2000. The larger D2 test piece was mounted in a rigid workpiece clamp, this test piece was used to drill holes between torque and thrust measurements.

A torque and thrust measurement was then collected at recommended cutting conditions from the Machining Data Handbook [82] (Figure 3.16). The cutting conditions were 30m/min at a feed rate of 0.1mm/rev at 2.5xD hole depth in a flooded coolant configuration. The results show a steady torque and thrust trace with little noise and no chip packing. As a result of this test it was decided to characterise the torque and thrust with cutting conditions boundaries of a 50% increase in feed rate and 33% increase in cutting speed. All torque and thrust measurements were averaged across the section where the outer cutting edges are engaged refer to the red boundary conditions in Figure 3.16.



Figure 3.15. Image showing the drilling setup in the HAAS VF2SS for torque and thrust measurements, left shows the Kistler dynamometer with a D2 test piece, followed by on the right a larger D2 test piece mounted in a rigid workpiece holder.

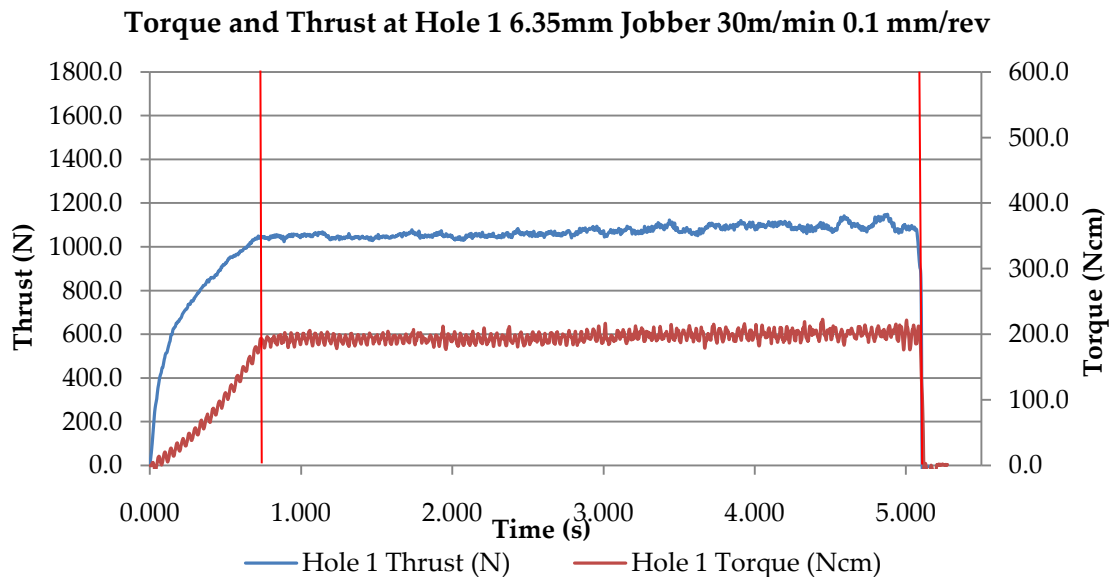


Figure 3.16. A torque and thrust versus time graph showing an initial increase in drilling torque and thrust which levels off and becomes constant once the peripheral cutting edges are engaged. Small fluctuations in forces increase with hole depth.

### 3.3.3 Results

#### 3.3.3.1 Jobber Drill Geometry

The drill geometries which were measured are shown in Table 3.11, with a total of fifty two drills measured in this study. The 6.35mm jobber twist drill designed by Sutton Tools is made up from a combination of standards, ASME B94.11M-1993, DIN 1414-1977 and Sutton Tools own standards. Comparing the measured features in Figures 3.10-3.13 to the design specification, the results show that there are a number of drills that fall outside the tolerance. The measured chisel angles show that 67.3% were outside of the tolerance limit, as can be seen in Figure 3.17. The point angles measured all fall within tolerance with a small standard deviation Table 3.14. The web thickness results show that 57.7% lie outside the tolerance limit. The mean margin width results show that the majority of drills fell within tolerance with a small standard deviation (Table 3.15); 7.7% fell outside the tolerance limit. Lip relief angles measured also fell within tolerance see Figure 3.19 with a tight distribution (Table 3.16) with only 7.7% lying outside. The mean helical angle for all fifty two drills had a very tight distribution with a mean and standard deviation of 31.69 and 0.40 respectively (Table 3.16), with all drills within tolerance. The point centrality had 19.2% over the maximum tolerance see Figure 3.20 and the relative lip height showing 7.7% over the maximum, with both drill features having large standard deviations (Table 3.17).



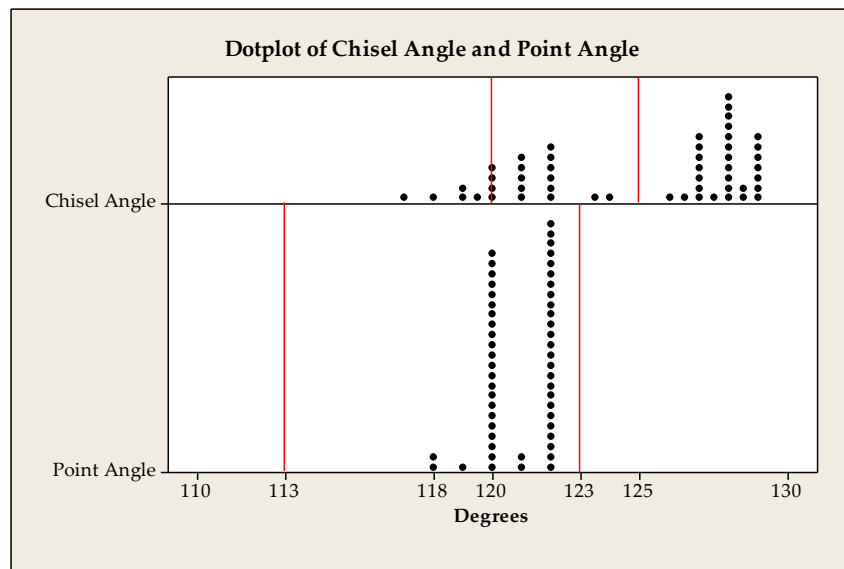


Figure 3.17. Dot plot showing the distribution of chisel angle and point angle measurements from fifty two Jobber drills.

Table 3.14. Table showing sample statistics of chisel angle and point angle measurements.

Variable	N	Mean	St Dev	Min	Q1	Median	Q3	Max
Chisel angle (°)	52	124.8	3.8	117.0	121.0	127.0	128.0	129.1
Point Angle (°)	52	120.9	1.2	118.0	120.0	121.0	122.0	122.0

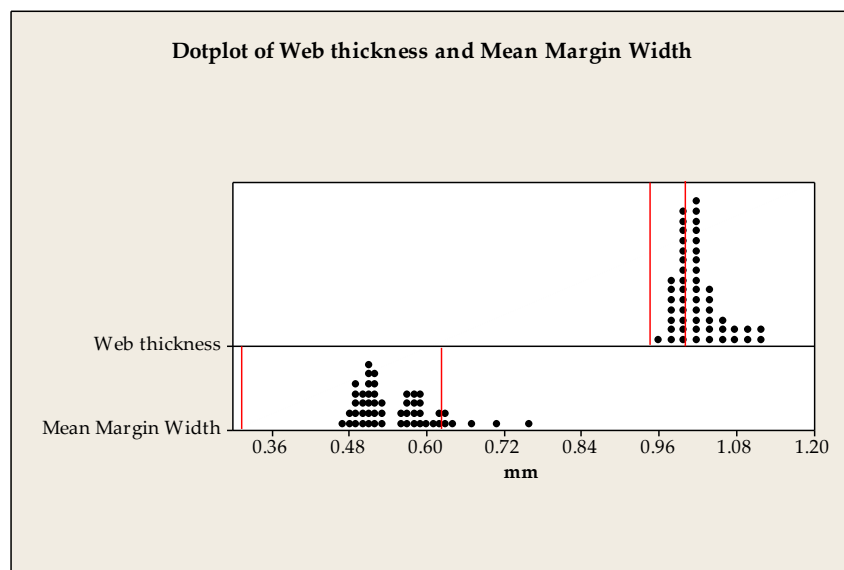


Figure 3.18. Dot plot showing the distribution of web thickness and mean margin width from fifty two uncoated Jobber drills

Table 3.15. Table showing sample statistics of web thickness and mean margin width.

Variable	N	Mean	St Dev	Min	Q1	Median	Q3	Max
Web thickness (mm)	52	1.02	0.04	0.96	0.99	1.01	1.04	1.11
Mean margin width (mm)	52	0.552	0.061	0.467	0.507	0.532	0.587	0.758

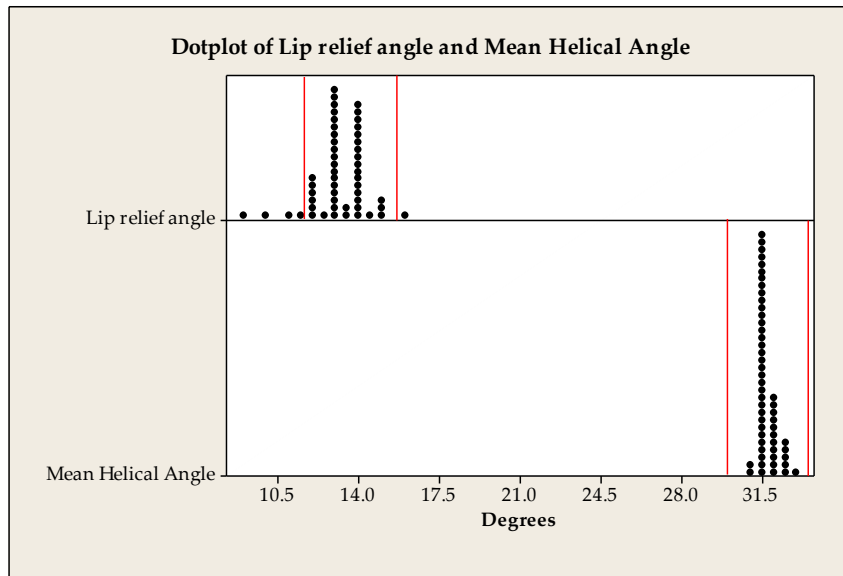


Figure 3.19. Dot plot showing the distribution of lip relief angle and mean helical angle from fifty two uncoated Jobber drills.

Table 3.16. Table showing sample statistics for lip relief angle and mean helical angle.

Variable	N	Mean	St Dev	Min	Q1	Median	Q3	Max
Lip relief angle (°)	52	13.2	1.2	9.0	13.0	13.0	14.0	16.0
Mean helical angle (°)	52	31.7	0.4	30.9	31.4	31.5	31.9	32.9

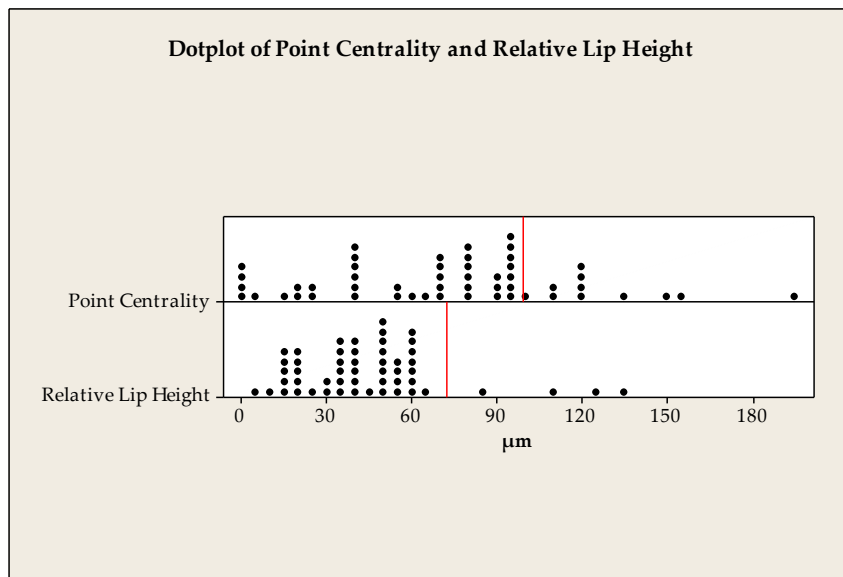


Figure 3.20. Dot plot showing the distribution of point centrality and relative lip height from fifty two uncoated Jobber drills.

Table 3.17. Table showing sample statistics for point centrality and relative lip height.

Variable	N	Mean	St Dev	Min	Q1	Median	Q3	Max
Point centrality (µm)	52	72.8	43.2	0.0	40.5	81.0	94.5	195.0
Relative lip height (µm)	52	44.6	26.1	7.0	27.2	40.5	56.7	133.0

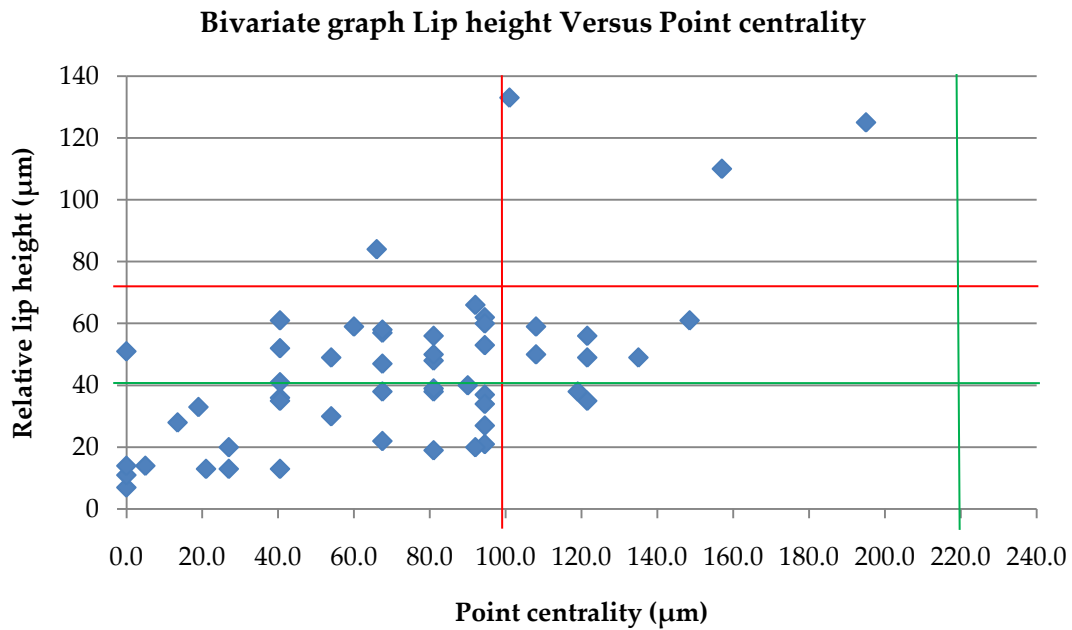


Figure 3.21. Bivariate graph of relative lip height versus point centrality. The red lines indicate the maximum tolerance for ASME B94.11M-1993 and the green lines indicate the maximum tolerance for AS/NZS 2438.1:1994.

The bivariate graph (Figure 3.21) shows that there is little correlation between the relative lip height and the point centrality, which means that the two design features are not dependent on one another in the grinding process. The results also highlight that using the ASME standard 23% of the drills measured are outside tolerance while using the AS/NZ standard which is based on the German DIN 1414 standard 46.1% of drills are outside tolerance.

### 3.3.3.2 Workpiece Material

Sample statistics for the D2 steel plate measured using Leeb D and Vickers (30Kg) instruments are shown in Table 3.3. The sample statistics for both instruments show a low standard deviation in the hardness results, 3.7 HLD and 1.8 HV<sub>30</sub>. A small deviation in results is also shown by the range, 430-445HLD and 204-214HV<sub>30</sub>. Referring to the Leeb and Vickers contour plots Figure 3.22 & Figure 3.23 respectively, reveals small differences between the measurement methods. The Leeb contour plot shows lower hardness values near around the edges of the plate, while the Vickers plot shows a few regions near the edge where the hardness is higher but only slightly (2.5 HV<sub>30</sub>). Both plots show that there a localised regions of higher and lower hardness values with respect to each other, however, the difference are low.

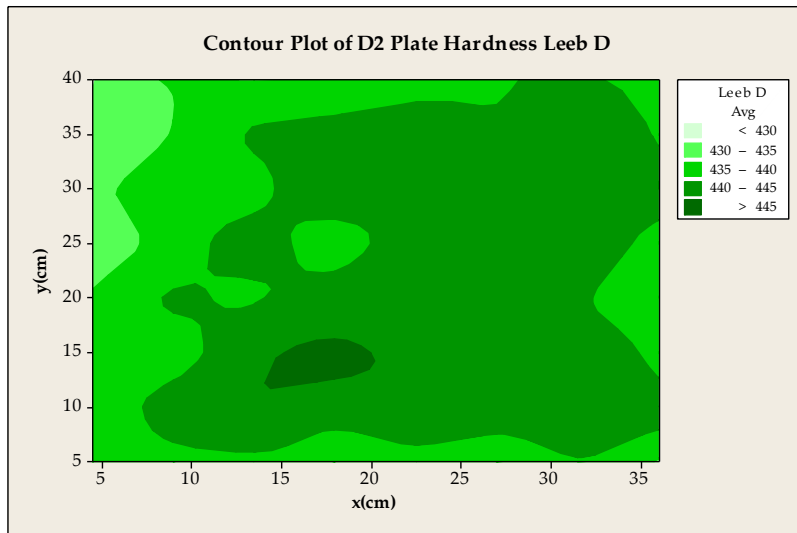


Figure 3.22. A contour plot showing the surface hardness distribution measured via a Leeb D hardness tester of a 40cm by 36cm D2 test plate.

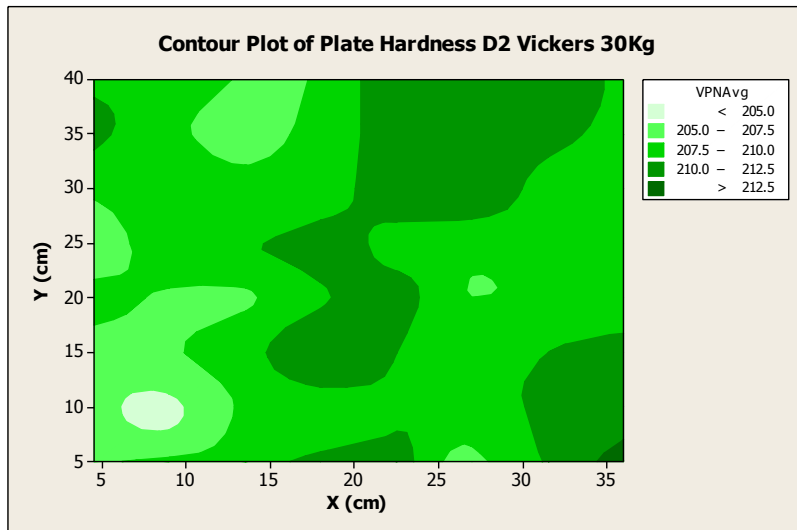


Figure 3.23. A contour plot showing the surface hardness distribution measured via a Vickers indenter with 30kg load of a 40cm by 36cm D2 test plate.

Table 3.18. Table showing sample statistics for a D2 plate with a Leeb D hardness measurement device and a Vickers indents under 30kg load.

Description	N	Mean	StDev	Min	Q1	Median	Q3	Max
Leeb D	64	439	3.7	430	436	440	442	445
Vickers 30Kg	64	209	1.8	204	208	209	211	214

### 3.3.3.3 Torque and Thrust Results

The torque and thrust data plotted in Figure 3.24 & Figure 3.25 show that for all cutting conditions, besides the thrust at 40m/min 0.15mm/rev, the forces follow mimic the general 3

stage wear progression shape (see chapter 2.4.3). The results first show a short initial rapid increase in torque and thrust, followed by stage 2, a period of steady state forces with a small increase and lastly stage 3 a rapid increase in forces acting on the tool and usually the indication of tool failure. For six of the cutting conditions cutting speeds 30 and 35m/min for all feed rates there was not enough plate to continue characterising this pattern however, all 40m/min at three different feed rates showed this pattern and it may be expected that if testing continued the same would be observed. The nine cutting conditions were largely grouped by their feed rates. In Figure 3.24 initially only small changes in torque for the 30, 35 and 40 m/min cutting speeds in ascending order can be seen however, after entering stage 2 of the classical 3 stage wear pattern the changes in torque become larger. This is not observed in the thrust shown in Figure 3.25, thrust has a larger change across all cutting conditions early in drilling, showing that the thrust force is more sensitive to the initial rapid wear stage.

Examining the torque measurements at hole 1 Figure 3.26 the cutting speed did not significantly change the torque measured for 0.1mm/rev, conversely for 0.125mm/rev increasing the cutting speed from 30m/min to 35 and 40 the torque measured was considerably lower. At a feed rate of 0.15mm/rev the torque remained constant up until 40m/min. The thrust results in Figure 3.27 reveal a different pattern, as the feed rate increases from 0.1mm/rev to 0.15mm/rev a minima occurs at 35m/min. The results for torque at the point of steady state see Figure 3.28 show no significant change across the cutting conditions besides a slight drop when increasing the cutting speed from 30m/min to 35 and 40m/min for the feed rate of 0.125mm/rev. The thrust values at the point of steady state seen in Figure 3.29 are constant across all feed rates between the speeds of 30 and 35m/min, however, by increasing the cutting speed to 40m/min all torque results increase. Torque measurements at hole 20 show that there is a small decrease from 30m/min to 35 and 40m/min for 0.125 and 0.15mm/rev seen in Figure 3.30 while a small increase for 0.1mm/rev. The thrust results Figure 3.31 show no correlation to the torque, the 0.1mm/rev feed rate shows a steady increase in thrust while at 0.125mm/rev there is a slight minima at 35m/min and at 0.15mm/rev the thrust remains constant between 30 and 35m/min with a significant increase at 40m/min.

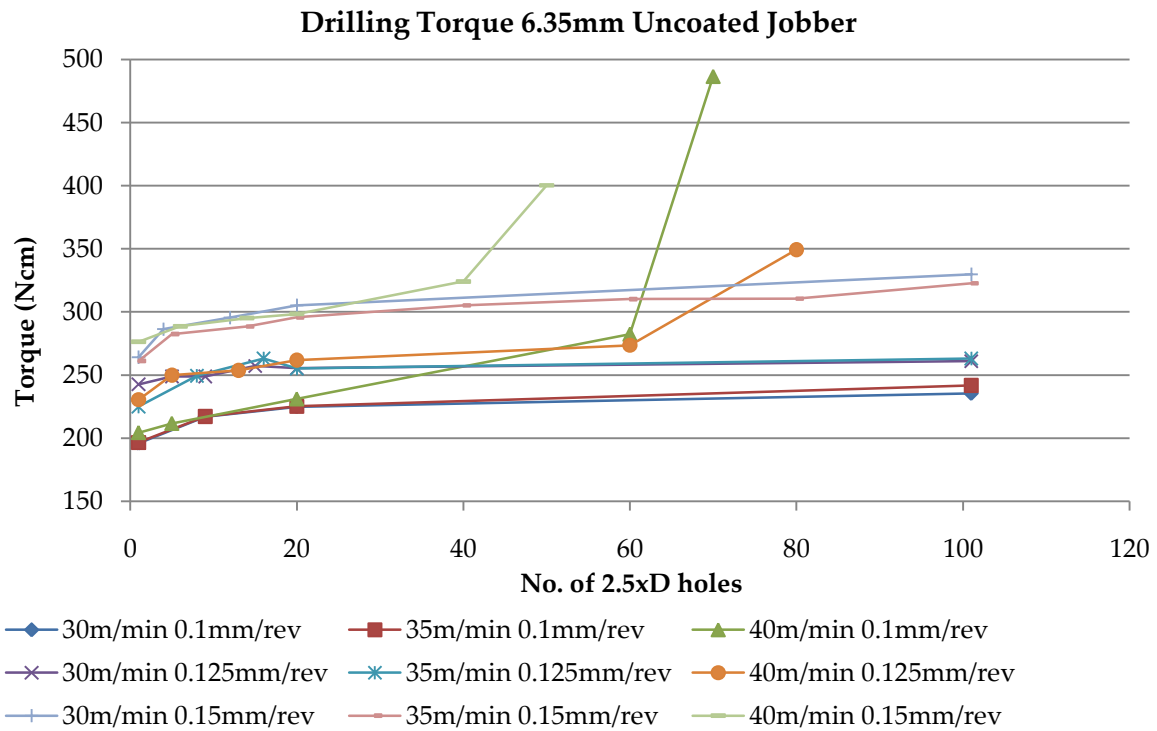


Figure 3.24. The average drilling torque results through the life of the drill for the nine accelerated cutting conditions selected.

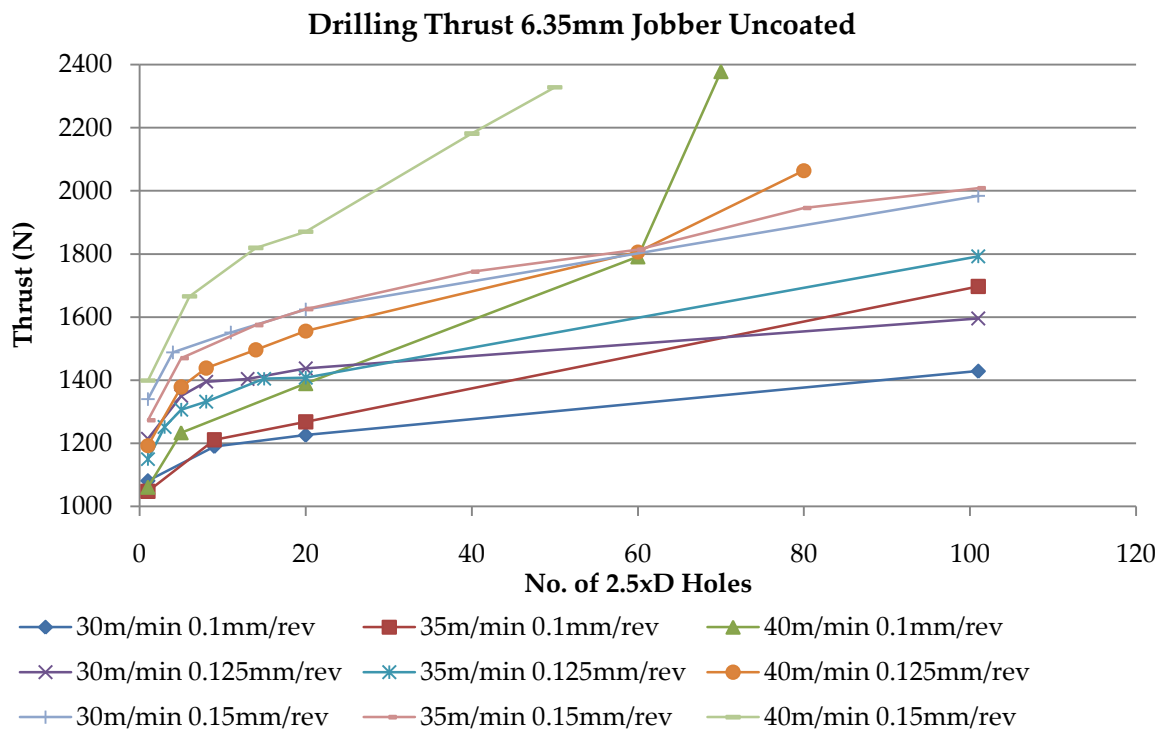


Figure 3.25. The average drilling thrust results through the life of the drill for the nine accelerated cutting conditions selected.

Torque versus Cutting Speed at Hole 1

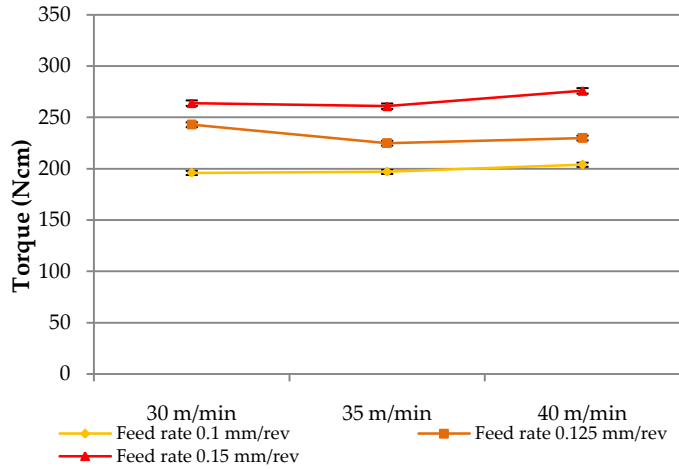


Figure 3.26. Average drilling torque measured at the 1<sup>st</sup> hole.

Torque versus Cutting Speed at Point of Steady State Drilling

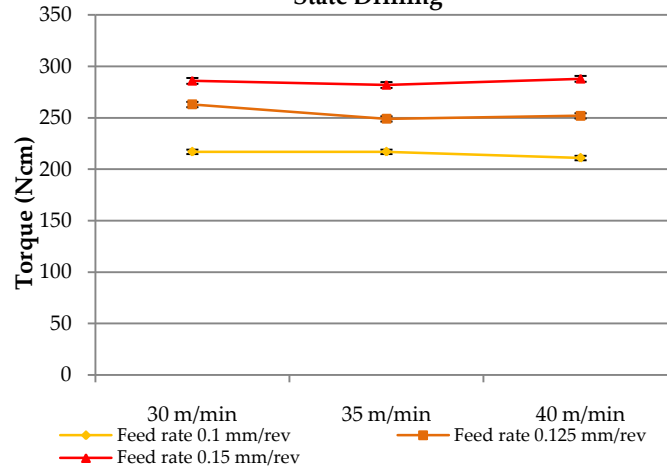


Figure 3.28. Average drilling torque operating in the steady state life region.

Torque versus Cutting Speed at Hole 20

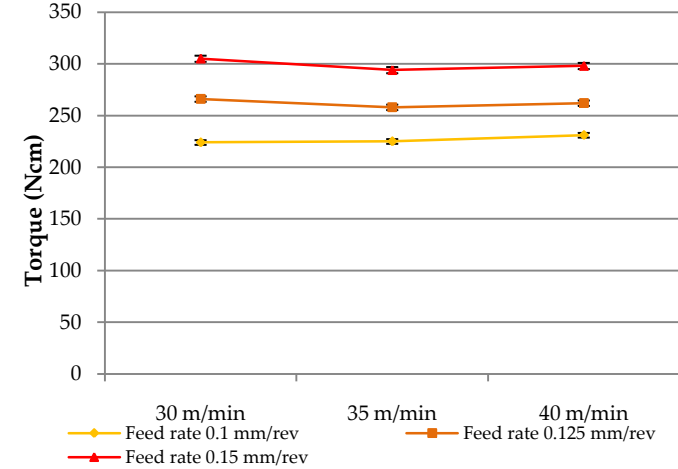


Figure 3.30. Average drilling torque measured at the 20<sup>th</sup> hole.

Thrust versus Cutting Speed at Hole 1

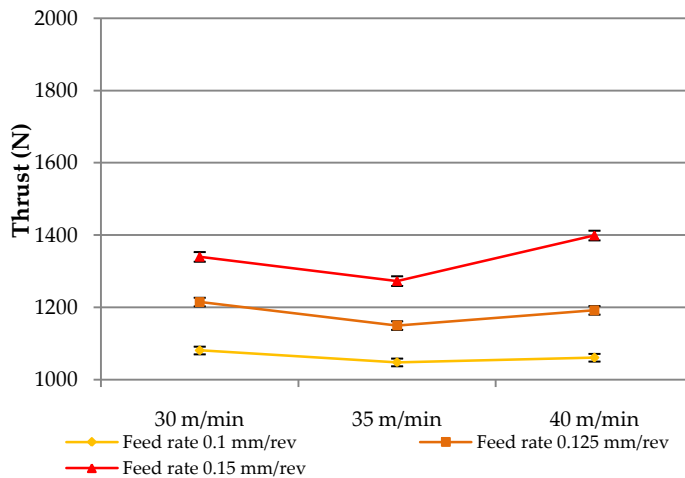


Figure 3.27. Average drilling thrust measured at the 1<sup>st</sup> hole.

Thrust versus Cutting Speed at Point of Steady State Drilling

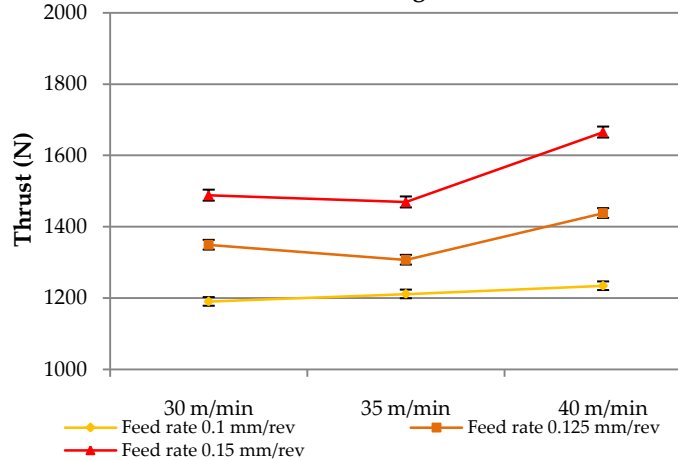


Figure 3.29. Average drilling thrust operating in the steady state life region.

Thrust versus Cutting Speed at Hole 20

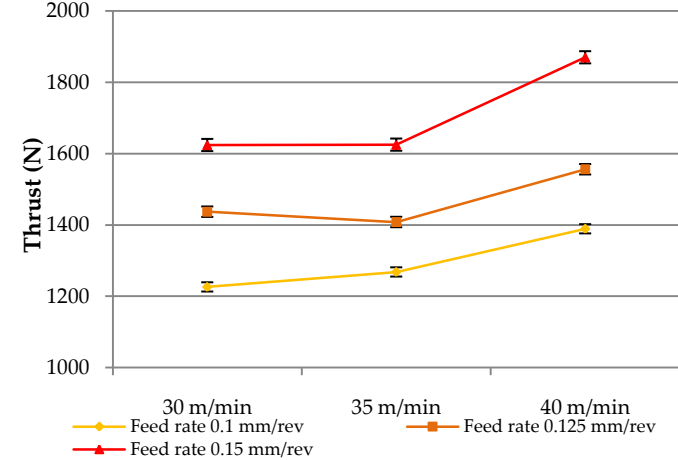


Figure 3.31. Average drilling thrust measured at the 20<sup>th</sup> hole.

### 3.3.4 Discussion

The dot plots and sample statistics of the macro geometry features revealed that there is considerable variability in a few macro design features of mass manufactured uncoated M2 HSS 6.35mm Jobber drills. Jobber drills have wide tolerances due to the fact that they are a standard drill used for low to moderate machinability applications, therefore the tolerances are not required to be tight, however, these tolerances are still required to be met, especially in features such as the primary lip relief, lip height variation and point centrality, as reported by NAS [16]. Large variability in Jobber drill macro design features from a number of cutting tool manufacturers has been reported by Armarego and Kang [18, 83]. Similar results were found in this study.

Certain geometry specification standards had larger tolerances than others. According to the ASME B94.11M-1993 standards[84] 95% of drills measured from a sample batch should conform to the tolerance limits. Out of the three features which are set by the ASME standard only the point angle conforms, with the point centrality and relative lip height features having 92.3% falling within tolerance, combining these two features 26% of drills fell outside of tolerance. When comparing these results to the Australian/New Zealand Jobber drill standard [42] all of the Jobber drills point centralities fall within tolerance as the limit is 220 $\mu$ m for 6.35mm diameter drills. For the relative lip height the limit is 45 $\mu$ m which would make 46.1% of the Jobber drills measured fall outside of tolerance. This highlights that different standards will affect the number of drills which should be rejected.

In the case of the relative lip height and the point centrality, once the relative lip height begins to increase the forces on the two cutting lips begin to be unbalanced as one cutting lip is cutting more than the other. When the previous statement occurs, one cutting edge and outer corner will wear at a higher rate than the other and will result in a lower tool life because one cutting edge will fail before the other [17]. The relative lip height and point centrality also has a significant role in the dimensional accuracy of the drilled hole with its ability to drill concentric holes diminished as the relative lip height and point centrality moving away from uniformity [17].

Armarego and Kang [18, 83] both reference Galloway's work which highlighted that deviations in drill point features will affect tool life scatter. Galloway [19] reported that for the point angle a 50% difference in drill life was observed when drilling En 10 steel between the angles of 80-90 degrees. Additionally, a 65% difference in drill life can be obtained when the primary relief angle varies between 4-12 degrees. It is reasonable to assume that drills within a sample will be randomly distributed; therefore it does not matter that a number of those drills will be outside of tolerance. This leads to the question, how small do sample sizes need be to distinguish population changes?



The surface hardness results of the D2 plate measured using a hand held Leeb D tester and a Vickers Limited hardness tester with a 30kg load shows that there is a small hardness distribution across the plate. Both measurement techniques show a small standard deviation of 3.7 HLD and 1.8 HV<sub>30</sub>. The contour plots reveal the hardness spatial distribution using both measurement methods. When comparing the contour plots the spatial hardness distribution is not considerably different. The contour plot using the Leeb D measurements reveals that the majority of the plate is between 440-445 HLD with the edges having the softest regions 430.0-439 HLD. The contour plot generated using the Vickers hardness measurements consisted of the majority of the plate being within 207.5-210HV<sub>30</sub> with regions of hard (210-212.5HV<sub>30</sub>) and soft (205-207.5) which do not show up in the Leeb D contour plot. The Leeb D testing method works by calculating the kinetic energy loss of a WC-Co ball bearing as it is vertically dropped and indents onto a workpiece. The ball plastically deforms the workpiece material, at which point the elastically accumulated energy then rebounds the ball at a particular rebound velocity [85], the energy loss is dependent on the plastic and elastic characteristics of the test material. While the Vickers hardness test measures the ability of a material, which is in a particular state, to resist deformation by indenting a 136 degree pyramidal diamond under a specific load, 30Kg in this case. As the variations in plate hardness are small, this is likely to be due to localised difference in plate hardness as the exact same position on the plate was not measured as these hardness measurement device leave an indent on the surface. Both measurement devices are able to discriminate small differences in plate surface hardness, however, to be able to use the Vickers Limited hardness tester the 40cm by 36cm D2 plate had to be cut into four pieces. This will not be able to be accomplished in future drill tests as to save time and money the plate will be used in the as received size. Therefore the Leeb D tester will be used in subsequent experiments.

A solution to the small hardness distribution found is to use a pseudo random drilling array. This has been employed in the drill test design through the CNC program so as to distribute heterogeneous hardness effects on all cutting tools within a sample, as well as any potential chromium carbide spatial non-uniformity. According to the American Society for Metal (ASM) [24] a non-uniform carbide distribution will affect the tool life distribution significantly, as these particles play a major role in the abrasive wear characteristic of this material. Future work may be to determine the carbide distribution within a large section of D2 plate steel. Dynamometer results confirmed that when drilling to 2.5xD hole depths using 6.35mm Jobber drills the cutting torque and thrust are contestant when the outer corners are engaged in the material, therefore there are no chip removal issues, confirming the choice of a 2.5D hole depth. This results has also confirmed that chip removal will not be source of tool life failure, as shown by Balzers [69], which would increase the scatter in tool life results.

Examining the evolution of torque and thrust of the nine drills each driven at nine different cutting speeds reveals that the cutting torque during the steady state region changes little over the life of a drill until the drill enters the third stage of rapid wear. In stark contrast the

cutting thrust during steady state region increases at a larger rate as shown by the increased gradient. Examining the absolute value trends of the nine cutting conditions at hole 1, steady state transition point and hole 20, for cutting speeds between 30-40m/min, there is little to no difference in torque for hole 1, steady state transition and hole 20, only the feed rate was a significant factor in increasing the value of the cutting torque. The comparison of the cutting thrust shows a minima at 35m/min for all three feed rates at hole one. By the steady state transition point thrust begins to increase linearly for 0.1mm/rev feed rate but still exhibits the minima at 35m/min for 0.125mm/min and 0.15mm/min. By hole 20, the cutting thrust is significantly larger at 40m/min at all three feed rates, while the 35m/min minimum thrust is maintained at 0.125mm/min. From these results it may be said that the cutting torque would be a suitable measure to describe the performance of a drill. The resultant cutting force may be calculated from the torque and thrust, however where would be a suitable point on a drill to calculate the resultant cutting force if, the rake angle on a standard Jobber drill changes from a low negative rake angle to a high positive angle from the chisel region to along the cutting edge, as well as the cutting velocity increasing from near zero at the centre to its maximum at the periphery outer corner [19, 86]. A solution to these issues has been provided by Abele et al [87] and Chen et al [88] who used the solution of breaking the cutting edge and chisel into small elements to calculate individual resultant forces. Notwithstanding in regard to this work a specific torque may be used to describe a drills performance however further work would need to be conducted to test this hypothesis.

### **3.3.5 Conclusions**

There exists variability in the macro design features in the uncoated M2 HSS 6.35mm Jobber drills examined and depending on which standards are used and on which design feature, certain drills will fall in and out of tolerance as others have found. However, the small number of drills found to be outside of tolerance would be randomly distributed among samples; therefore in the case of drill testing using sample groups it would still be justified to use them. Future work would need to be conducted to establish the smallest size needed so differences between samples could still be distinguished. The surface hardness distribution for D2 plate steel has been characterised by using two different methods and found to be small. The accelerated drill test has employed a pseudo random drilling array, to expose any heterogeneous characteristics of the test material to all samples. An investigation into the cutting torque and thrust for the Jobber drills used shows that 2.5xD hole depths is suitable, as chip removal problems do not arise at these depths. The torque and thrust results revealed that the torque may be a suitable measure for designating a specific force to a drill, however, this would require further work as the thrust would be ignored in this type of analysis.

## 3.4 Applying the Drill Test to a Surface Engineering Case Study

### 3.4.1 Introduction

A significant area of engineering which has evolved considerably over the past few decades is in the application of surface engineering, particularly to cutting tools. The surfaces of the cutting tool i.e. the faces which are in contact with the chip and workpiece can considerably affect the tool life [89], productivity [90] and the surface finish of a machined component [91]. This is especially evident in difficult to machine applications and where high surface finish of the machined part is demanded [92]. The severe contact conditions between the workpiece-cutting tool-chip system [49, 50, 54] can initiate a number of wear mechanisms and rates (chapter 2.4.2). Two surface treatments which increase tool life, productivity and the surface finish are the pre and post polish of a coated cutting tool which the coating has been deposited using the cathodic arc evaporation deposition technology.

Bradbury *et al* [93, 94] have shown that surface preparation, specifically via micro-blasting, improves tool life and productivity, and they point out that similar results can be achieved via drag polishing and wet-blasting methods. This improvement was attributed to removal of subsurface damage caused by the grinding process, a smoother surface finish and improved coating adhesion. Posti *et al* [41] have shown through turning experiments, (a continuous machining operation, drilling is semi-continuous) that an increase in coating thickness of  $1\mu\text{m}$  can increase tool life by 36%. In order to continually improve and develop better cutting tools through surface engineering, for the above mentioned benefits, the drill test must be able to resolve these differences in the tool life data and not be affected by sources of machining variance using small sample sizes.

Therefore, this experiment was designed to gauge the sensitivity of the drill test, (designed in chapter 3.1 and refined in chapter 3.2), in distinguishing if differences in tool life, produced by applying a pre and post drag polishing treatment to TiN coated Jobber drills, can be resolved. This work examined the effect of cutting tool surface roughness, coating thickness variation, cutting speed and sample size on determining real difference in tool life data. Measurements collected were analysed using sample statistics, box plots bi-variant analysis, ANOVA (parametric) and Mood's median test (non-parametric).

### 3.4.2 Experimental Procedure

A two factor, two level full factorial design has implemented making a total of four sample groups. 12 drills per sample (Table 3.19) were produced. The effect of cutting speed was investigated in this experiment so as to verify that the cutting speed would not be detrimental to distinguishing differences when testing for tool life changes for surface treated Jobber drills. It is not the aim of this experiment to determine linearity between tool life and cutting speed and as this is an accelerated drill test both cutting speeds need to be high, therefore, testing at 35m/min and 45m/min was justified. Sample size has been identified as crucial in determining experimental outcomes (section 3.3.4). However, when the experiment was carried out at 35m/min 1 drill from each sample was tested at too low a hole depth. This resulted in different sample sizes for the 35m/min and 45m/min tests. Notwithstanding this, the experimental variability was so low as not to be a problem. This highlights the importance of low variance. In the case low variance (scatter) in the tool life results allowed significant conclusions to be made, regardless of the small sample size.

The surface engineering case study consisted of the pre and post drag polishing of TiN coated Jobber drills. Jobber drills were coated with a TiN coating using a commercial PVD coating machine (Balzers INNOVA cathodic arc evaporation see chapter 2.8). The pre and post polishing was applied using an OTEC drag polishing machine. Prior to the pre and post drag polishing treatments all drills were de-burred using an automated walnut blasting machine for 12 seconds. ANOVA was applied to determine whether population changes had occurred to tool life and surface roughness measures. When distinguishing the effect of a factor, in this case pre and post polish and using post polish as an example, the effect of pre polish has been averaged out by comparing a group that consists of the two levels of pre polish with one level of post polishing against the other group that also consists of the two levels of pre polish, with the other level of post polishing. This is the basis of experimental design, it is finding the effect of a factor when all the other factors vary [60].

Mood's median test was applied to the tool life data as it is able to deal with skewed distributions better than ANOVA. The surface roughness was characterised using the Alicona IFM and the coating thickness variation was determined using the combination of SEM and XRF measurements. The effect of coating thickness variation on tool life was also analysed using ANOVA and Mood's median test. A bivariate analysis [61] was conducted to determine if a correlation between coating thickness and tool life existed in this particular case so as to justify correcting the tool life data for coating thickness variation by calculating a life/micron of coating value

### 3.4.2.1 Drag Polishing

The tools are held point down in a 3-axis spindle tool holder and rotated within a container which houses a mixture of fine grain silicon carbide (SiC) and walnut shells (Figure 3.32). The rotation to the drills causes the fine abrasive media to course over the surface under pressure [95]. This treatment is a material removal process; therefore the rate of material removal is defined by the revolutions per minute and the length of time. All drag polishing parameters were chosen through discussions with industry sponsor engineers who have characterised process parameters for a wide range of substrates and cutting tool geometries. Drills requiring a pre polish were set to rotate at 40rpm for 8 minutes. After which all 48 drills were coated in a cathodic arc PVD system in the same run. Drills designated for post PVD coating polishing were set to rotate at 30rpm for 3 minutes, a complete sample preparation sequence can be seen in Table 3.19.

Table 3.19. Production treatments applied to the four sample groups in a two factor two level full factorial experimental design.

Group 3.1	Nut Blasted	Pre Polish	Coated TiN Balzers A3	Post Polish
Group 3.2	Nut Blasted	Pre Polish	Coated TiN Balzers A3	-
Group 3.3	Nut Blasted	-	Coated TiN Balzers A3	Post Polish
Group 3.4	Nut Blasted	-	Coated TiN Balzers A3	-

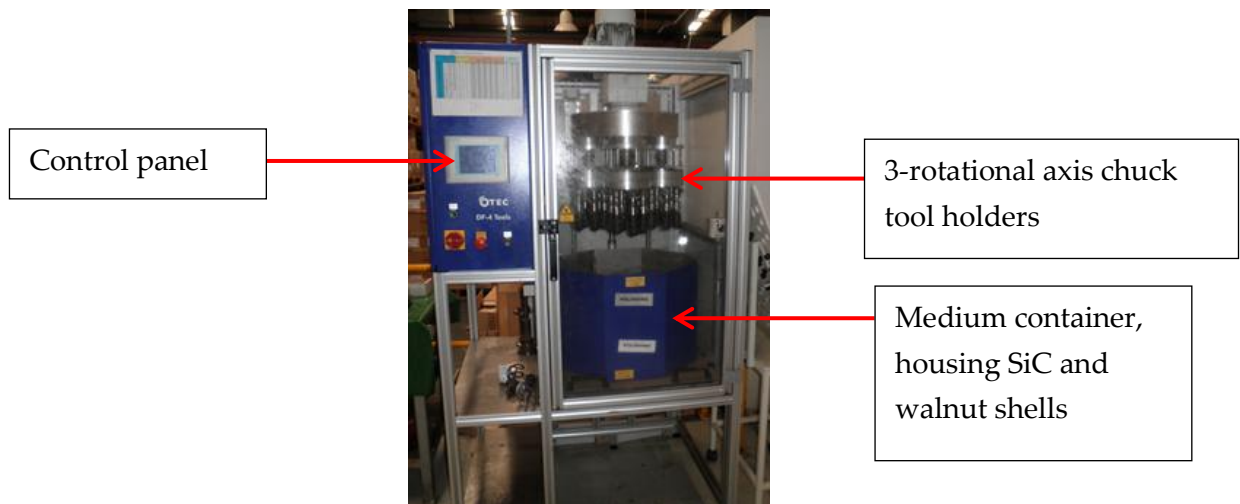


Figure 3.32. Image of the OTEC drag polishing machine. Depicting The 3 axis of rotation tool holder above the polishing medium container.

### 3.4.2.2 Surface Roughness Analysis

A quantitative and qualitative analysis of the surface was completed using the Alicona IFM (Infinite Focus Microscope). Two regions were characterised (Figure 3.33), the rake face on the outer corner of the drill and the flute 3 diameters away from the chisel point. The surface roughness was predicted to be within  $0.1\mu\text{m}$ - $2\mu\text{m}$ , therefore according to ISO 4288 the  $L_c$  (cut off wavelength) should be equal to  $800\mu\text{m}$ ; however, it was found that for scans made  $3\times D$  up the flute, a  $L_c$  of  $800\mu\text{m}$  was not suitable to remove all the waviness from the primary profile. Therefore a cut off wavelength of  $80\mu\text{m}$  was selected. Refer to the literature review chapter 2.9.1, put simply if the cut off wavelength did not remove the waviness from the primary profile the surface roughness measures being analysed such as  $R_a$  would be higher than they should be as not all the high amplitude waviness from the primary profile would be filtered out. In addition a high resolution scan was selected, with a vertical resolution of  $20\text{nm}$  and a lateral resolution of  $1\mu\text{m}$  using a  $50\times$  objective lens.

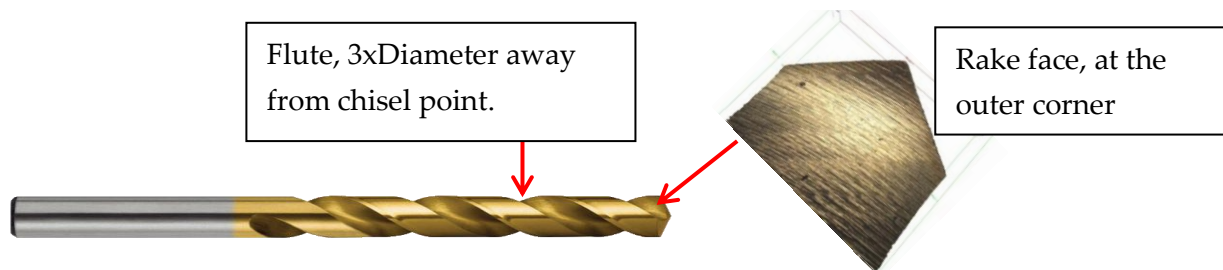


Figure 3.33. Image showing where on the rake face and the flute the surface was measured using the Alicona IFM.

The  $R_a$  value (the average height of the profile) is the most widely accepted measure of surface roughness and is reported in the majority of measurement standards literature but it is not the only measure to characterise a surface. The Alicona IFM software allows many roughness measures to be calculated from the roughness profile generated. The surface measures listed in Table 3.20 were chosen simply because they reveal different information about a surface, for example  $R_t$ ,  $R_z$  and  $R_v$  will give some indication that the pre drag polishing has reduced the larger/deeper grinding marks from the drill surface. While  $R_p$  will be an indicator whether post polishing has removed or reduced the height of macro particles.

Table 3.20. List of surface roughness measures used in this study.

$R_a$	Average height of roughness profile
$R_t$	Maximum peak to valley height of roughness profile
$R_z$	Mean peak to valley height of roughness profile
$R_p$	Maximum peak height of roughness profile
$R_v$	Maximum valley height of roughness profile

### 3.4.2.3 Coating Thickness Measurements

A comparative analysis was first conducted to verify which detector type would be most accurate in measuring the TiN coating. The two detectors in this study were a proportional counter and a silicon PIN detector. Eight drills were measured using both detectors and compared against SEM measurements. The samples measured using the SEM would also be used as calibration pieces for the device for future measurements. According to the results of the comparative test (Appendix E) the Fischerscope XDL[96] (proportional counter) showed better correlation with SEM measurements, and improved slightly after calibration, therefore it was chosen to measure the remaining samples. All drills had the coating thickness calculated by making three fifty second scans on the margin face in middle of the drill (Figure 3.34).

Coated drills measured via the SEM (Phillips XL30) were prepared by first making a transverse cross section by means of a Struers Labotom cut off wheel using water. A slow feed rate was used so not to damage the samples. The samples were then mounted in conductive phenolic resin in a Presi Mecapress. After which, they were polished in a Struers RotoPol using the MD-Piano disk with water for plane grinding then the MD-Allegro and MD-Largo with a 9 $\mu$ m diamond suspension for fine grinding, followed by a polishing step using the MD-Plus with a 3 $\mu$ m diamond suspension and lastly the MD-Nap with 1 $\mu$ m diamond suspension for a final polishing step. Samples were then thoroughly cleaned in ethanol then placed in inside the vacuum chamber of a Phillips XL30 scanning electron microscope, the on board software was used to measure the coating thickness.

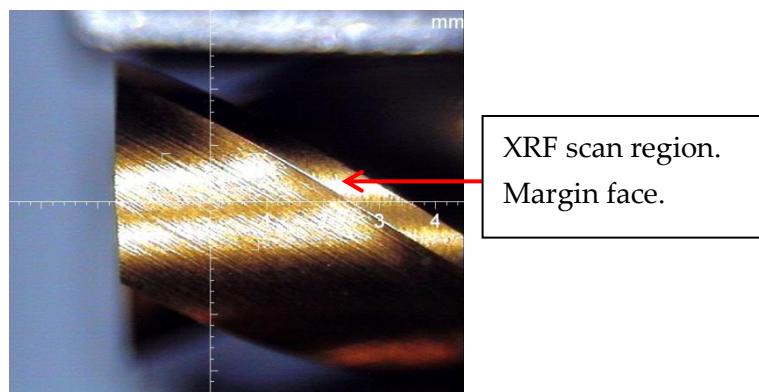


Figure 3.34. Image showing a TiN Jobber drill inside the XRF machine, pointing to where the scans were acquired.

### 3.4.2.4 Drill Test

Drills from the four sample groups were tested in a HAAS-VF2 VMC CNC and followed the experimental design shown in Table 3.21. Two different cutting speeds were chosen, both accelerated for drilling D2 steel with coated Jobber drills the first was low (35m/min) and the second was high (45m/min). Coolant used was the Houghton Hocut 960 at 7-8% in a flooded configuration.

Table 3.21. Drill test setup with corresponding cutting speeds pre and post drag polishing treatments with the number of drills tested.

Cutting conditions	Group No.	No. of drills
35m/min 0.125mm/rev	3.1	5
	3.2	5
	3.3	5
	3.4	5
45m/min 0.125mm/rev	3.1	6
	3.2	6
	3.3	6
	3.4	6



### 3.4.3 Results

#### 3.4.3.1 Coating Thickness

The coating thicknesses measurements (Figure 3.35) show a small range. Referring to Table 3.22 the mean coating thicknesses for all groups lay between  $2.57\mu\text{m}$  and  $2.78\mu\text{m}$  with group 3.1 and 3.2 having the largest standard deviations of  $278\text{nm}$  and  $146\text{nm}$  respectively while group 3.3 and 3.4 having the lowest standard deviation of  $77\text{nm}$  and  $91\text{nm}$  respectively.

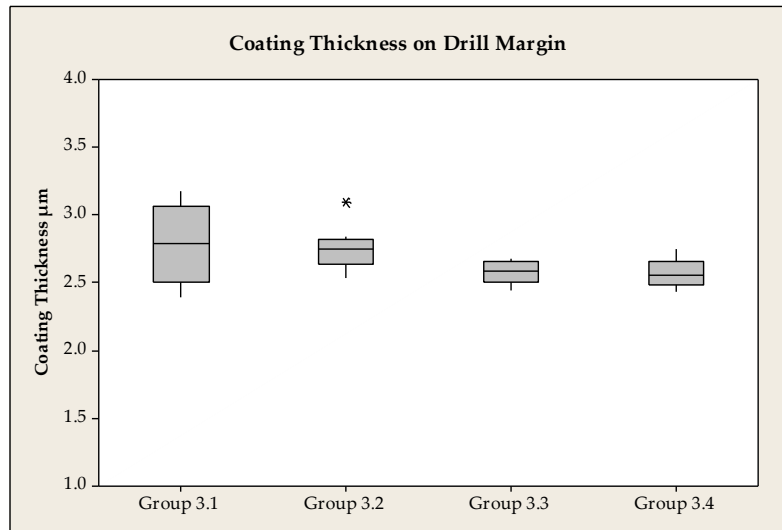


Figure 3.35. Boxplot showing coating thickness of all four sample groups made using a Fischerscope proportional counter XRF device.

Table 3.22. Sample statistics for coating thickness measurements made via XRF using the calibrated XDL for the four sample groups, all values are in units of  $\mu\text{m}$ .

Group	N	Mean	StDev	Min	Q1	Median	Q3	Max
3.1	12	2.78	0.27	2.39	2.51	2.79	3.07	3.17
3.2	12	2.75	0.14	2.53	2.64	2.75	2.82	3.10
3.3	12	2.58	0.07	2.44	2.51	2.59	2.66	2.68
3.4	12	2.57	0.09	2.43	2.49	2.56	2.65	2.74

#### 3.4.3.2 Surface Analysis

Pre polished samples (Figure 3.36 (a) and (b)), appear to have the large grinding marks slightly diminished while the number of light grinding marks are reduced. Post polishing appears to remove macro particles on the rake surface (Figure 3.36(a) and (c)) and leave the large and small minor grinding marks unaltered. Macro particles (droplets) are a consequence of using cathodic arc evaporation deposition. Put simply, due to the high power density of the arc, small droplets are produced as well as ionised metal vapour when the cathode is struck, these macro particles land on the forming thin film during deposition. Macro sockets are therefore the result of a macro particle being removed. Pseudo colour

information was applied to the micrograph (Figure 3.36) to help in distinguishing between macro particles and sockets, note: black dots seen in Figure 3.36 (b) and (d) which did not receive a post polish, should not be confused with a macro socket, they are macro particles with a height larger than the height scale which was kept the same for all scans for comparative analysis. The number of macro sockets were manually counted (Table 3.23). These results indicate that post drag polishing removes a significant amount of macro particles that leave macro sockets behind or partially broken particles.

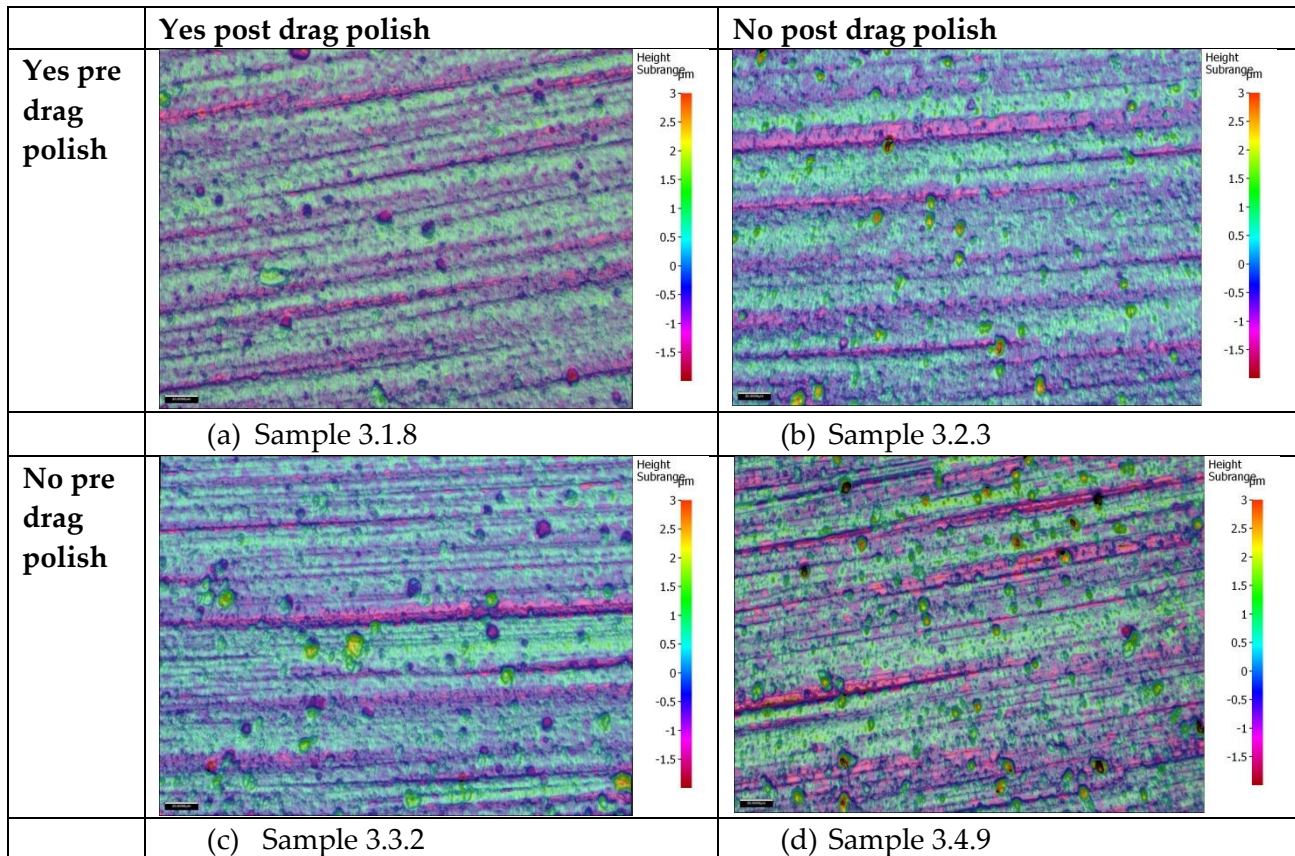


Figure 3.36 (a, b, c, d). Alicona IFM 50x optical micrographs with pseudo colour topographical information. All scans were taken at the rake face adjacent from the outer corner cutting edge, scan sizes are 286 $\mu\text{m}$  by 217 $\mu\text{m}$  with the black scale bar equal to 20 $\mu\text{m}$ . All curvature has been removed.

Table 3.23. shows the number of macro sockets manually counted from pseudo colour optical micrographs from Figure 3.36.

Sample No.	Pre Polish	Post Polish	Approximate no. of Macro Sockets
3.1.8	Yes	Yes	26
3.2.3	Yes	No	1
3.3.2	No	Yes	35
3.4.9	No	No	2

Examining the micrographs of the IFM scans taken 3xD up the flute (Figure 3.37), it appears that drag polishing has made no affect on the surface topography either pre or post treatment. Pre polishing appears to have not reduced the grinding marks and post polishing has not removed and macro particles.

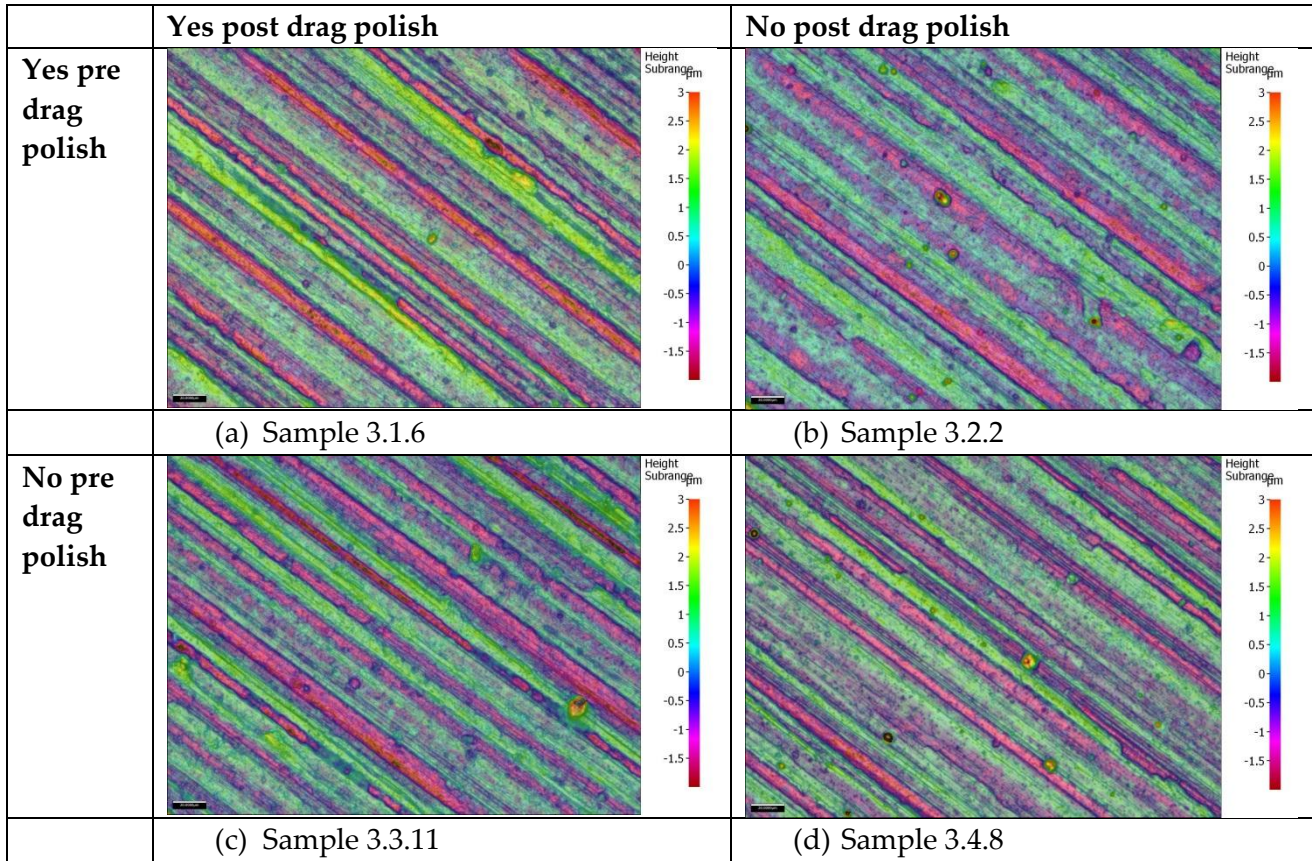


Figure 3.37 (a, b, c, d). Alicona IFM 50x optical micrographs with pseudo colour topographical information. Images taken 3xD up the flute from chisel point, scan sizes are 286 $\mu$ m by 217 $\mu$ m with the black scale bar equal to 20 $\mu$ m. All curvature has been removed.

The average height of the roughness profile ( $R_a$ ) shows that there is a decrease in the mean values due to pre and post polishing, from 687nm to 631nm and 687nm to 626nm respectively; however these decreases are not significantly different at a 95% confidence limit. The P values calculated are 9.5% and 7.3% for pre polish and post polish respectively. Alternatively, if the significance is lowered to 90% the  $R_a$  mean values would be significantly different, but only for the main effects. There would still be no significant interaction from the two treatments on  $R_a$ , as only an additive effect has been demonstrated.

Table 3.24. Summary of results to ANOVA tests applied to surface roughness data. Whether the result was statistically significant or not

<b>Response: Tested using ANOVA at 95% confidence</b>	<b>Pre Polish 3.1 &amp; 3.2 V 3.3 &amp; 3.4</b>	<b>Post Polish 3.1 &amp; 3.3 V 3.2 &amp; 3.4</b>	<b>Interaction</b>
Ra Rake face outer corner	No	No	No
Rt Rake face outer corner	Yes	Yes	Yes
Rz Rake face outer corner	Yes	Yes	No
Rp Rake face outer corner	No	Yes	Yes
Rv Rake face outer corner	Yes	Yes	No
Ra 3xD up Flute	No	No	No
Rt 3xD up Flute	No	No	No
Rz 3xD up Flute	No	No	No
Rp 3xD up Flute	No	Yes	No
Rv 3xD up Flute	No	No	No

The surface roughness measure  $R_t$  (maximum peak to valley height) supports the observations made from the micrographs, that drag polishing reduces the heights of low and high grinding marks. The results show that pre polishing lowered the  $R_t$  value from  $7.87\mu\text{m}$  to  $5.86\mu\text{m}$  and post polishing lowered the value from  $7.87\mu\text{m}$  to  $5.08\mu\text{m}$  with the group receiving both treatments changing the  $R_t$  value from  $7.87$  to  $4.97\mu\text{m}$ . The results are statistically significant at a confidence level of 95%. The P-values calculated were 0.03% and 0.00% for pre and post respectively, while the P-value for an interaction 0.08%.

The surface roughness measure  $R_z$  (mean peak to valley height) results show that the mean value dropped from  $5.87\mu\text{m}$  to  $4.58\mu\text{m}$  due to pre polishing also the mean lowered from  $5.87\mu\text{m}$  to  $4.37\mu\text{m}$  as a result from the post polishing. The results are statistically significant at a confidence level of 95% with P-Values calculated to be 0.00% for pre and post. The  $R_z$  value only having the main effects of pre and post polishing statistically significant with no interaction effect with the P-value calculated to be 9.5%, this result shows however, that at 90% there would be an interaction.

The surface roughness measure  $R_p$  (maximum peak height) had a drop in the mean value from  $4.37\mu\text{m}$  to  $3.36\mu\text{m}$  due to pre polishing and reduced the mean value down from  $4.37\mu\text{m}$  to  $2.39\mu\text{m}$  due to post polishing. The group receiving both treatments had a change in the mean  $R_p$  from  $4.37\mu\text{m}$  to  $2.63\mu\text{m}$ . The results from an ANOVA show that the changes are statistically significant for post polish only at a confidence level of 95% with P-Values calculated to be 15.9% and 0.00% for pre and post. The  $R_p$  value had an interaction effect between pre and post polishing which is statistically significant with a P-value calculated to be 2.7%. This suggests that on its own pre polishing is not enough to change the maximum peak height but the interaction with a post polish is.

The last surface roughness measure to be examined at the rake face is the  $R_v$  (the maximum valley height), the results show that pre polishing reduced the mean value from  $3.23\mu\text{m}$  to

2.49 $\mu\text{m}$  and post polishing lowered the mean from 3.23 $\mu\text{m}$  to 2.64 $\mu\text{m}$ . The group receiving both treatments had the mean value drop from 3.23 $\mu\text{m}$  to 2.34 $\mu\text{m}$ . The maximum valley height had a statistically significant decrease in the mean value for pre and post polish at a confidence level of 95% with P-Values calculated to be 0.01% and 0.15% for pre and post respectively. The  $R_v$  value had no interaction effect between pre and post polishing which is statistically significant at 95% with a P-value calculated to be 13.6%.

The only surface measure to have a statistical significant change 3 diameter up the flute was  $R_p$  (maximum peak height). Pre polishing reduced the  $R_p$  value from 3.60 $\mu\text{m}$  to 3.52 $\mu\text{m}$  and post polishing reduced the mean  $R_p$  from 3.60 $\mu\text{m}$  to 3.08 $\mu\text{m}$  with an additive effect of 3.60 $\mu\text{m}$  to 2.46 $\mu\text{m}$ . The P-Values calculated for the main effects of pre and post polishing are 74.2% and 2.30% respectively. The  $R_v$  value had no interaction effect between pre and post polishing which is statistically significant at 95% with a P-value calculated to be 94.8%. This result indicates that for drills drag polishing is not an effective treatment, this may be due to the lack of movement of the SiC particles against the surface inside the flute.

### 3.4.3.3 *Tool Life Results*

Referring to Figure 3.38 (bivariate graph), individual tool life results are graphed against their corresponding coating thickness. All sample groups cluster, the drills having received a pre polish having longer tool lives. The correlation coefficients (Table 3.25) reveal that there is no relationship between tool life and coatings thickness for the drills tested at 35m/min. Figure 3.39 reveals the individual holes per micron of coating for the drills tested at 35m/min using a box plot. The results also show that drills which had received a pre drag polish prior to coating out performed drills with no pre polishing, referring to

Table 3.26 the mean holes per micron of coating values for drills receiving a pre polish were 45.96 and 47.66 compared to 40.22 and 40.99 which did not. Drills which were post polished had slightly lower mean holes per micron values compared to their pre polished counterparts and higher standard deviations 8.11 and 5.39 to 3.82 and 3.40. Applying ANOVA (parametric test) to the raw tool life data and the corrected data for coating thickness, the results revealed that the pre polishing was the only significant factor, at 95%, which increased the tool life population mean. Mood's median test (non-parametric) was applied to both tool life data sets and the results revealed that at 35m/min pre polish did not have a significant effect on the increase on tool life with 95% confidence (Table 3.28). Tests calculated a P-value of 7.4% (see appendix 3.4).

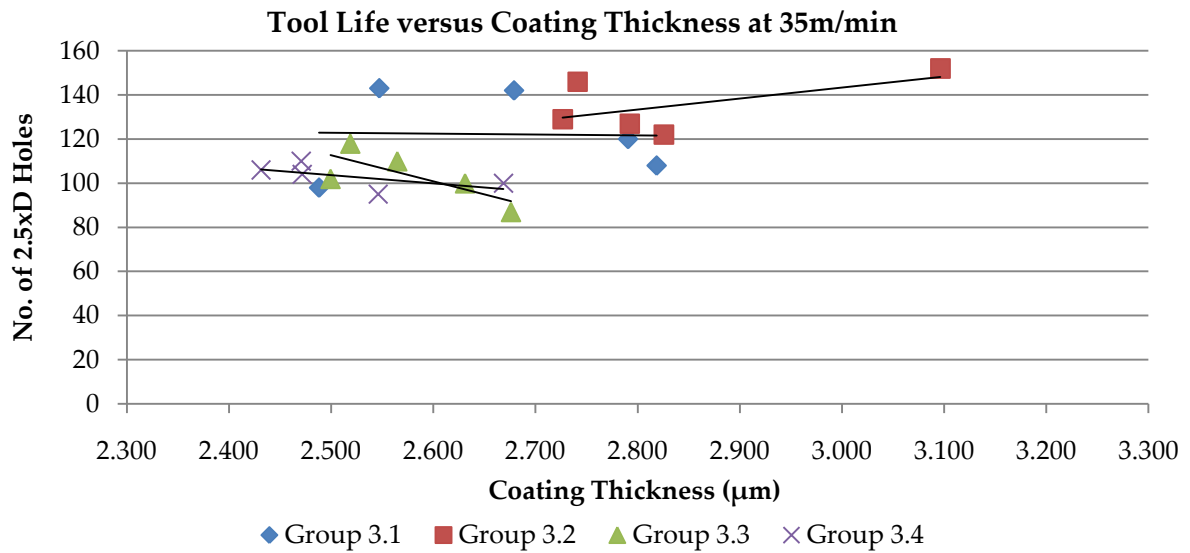


Figure 3.38. Bivariate graph comparing the tool life results tested at 35m/min 0.125mm/rev against coating thickness measurements made via XRF. Group numbers refer to polishing treatments see Table 3.13.

Table 3.25 Correlation coefficients for bivariate analysis between tool life and coating thickness. Drills tested at 35m/min

Group No. Tested at 35m/min	Correlation coefficient R <sup>2</sup>
3.1	0.0009
3.2	0.3324
3.3	0.5759
3.4	0.3695

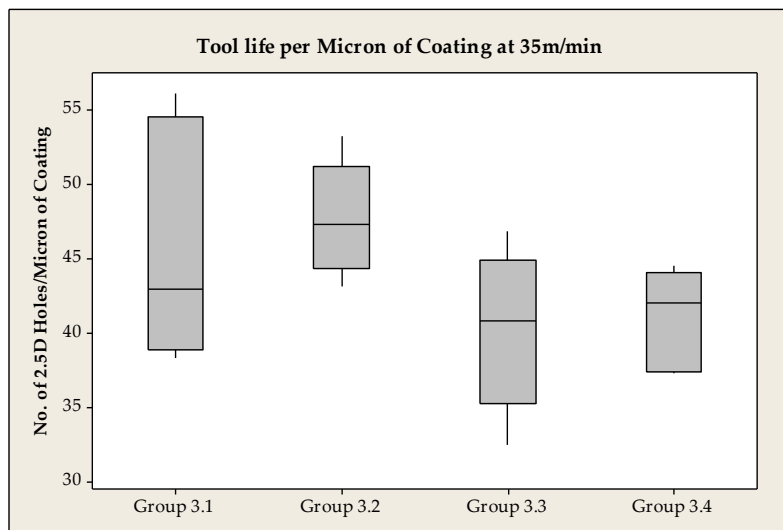


Figure 3.39. Boxplot of holes per micron of coating, drills tested at 35m/min 0.125mm/rev.

Table 3.26. Sample statistics for holes per micron of coating, tested at 35m/min 0.125mm/rev.

Cutting Conditions 35m/min 0.125mm/rev								
Group No.	Sample size	Mean	St Dev	Min	Q1	Median	Q3	Max
3.1	5	45.9	8.1	38.0	38.8	43.0	54.5	56.1
3.2	5	47.7	3.8	43.2	44.3	47.3	51.2	53.3
3.3	5	40.2	5.4	32.5	35.3	40.8	44.9	46.9
3.4	5	40.9	3.4	37.3	37.4	42.1	44.1	44.5

Table 3.27. Summary of results to ANOVA tests applied to tool life data. Whether the result was statistically significant or not.

<b>Response: Tested using ANOVA at 95% confidence</b>	<b>Pre Polish</b>	<b>Post Polish</b>	<b>Interaction</b>
Tool Life No. of 2.5xD Holes at (35m/min)	Yes	No	No
Tool Life No. of 2.5xD Holes at (45m/min)	Yes	No	No
Tool Life No. of 2.5xD Holes/Micron of Coating at (35m/min)	Yes	No	No
Tool Life No. of 2.5xD Holes/Micron of Coating at (45m/min)	Yes	No	No

Table 3.28. Summary of results to Mood median test applied to tool life data. Whether the result was statistically significant or not.

<b>Response Tested using Mood Median Test 95% Confidence</b>	<b>Pre Polish</b>	<b>Post Polish</b>
Tool Life No. of 2.5xD Holes at (35m/min)	No	No
Tool Life No. of 2.5xD Holes at (45m/min)	Yes	No
Tool Life No. of 2.5xD Holes/Micron (35m/min)	No	No
Tool Life No. of 2.5xD Holes/Micron (45m/min)	Yes	No

Examining the tool life versus coating thickness results from the drills tested at 45m/min (Figure 3.40), there is less clustering between groups than the drills tested at 35m/min. Drills with similar coating thicknesses have considerably different tool lives and drills with thick coatings having the same tool life as those with almost half a micron difference in coating thickness. However, according to the correlation coefficients (Table 3.29) there is a correlation between tool life and coating thickness for sample groups 3.1 and 3.4. The individual holes per micron of coating data shown in Figure 3.41 & the sample statistics in Table 3.30 show that drills which received a pre drag polish had higher mean holes per micron values of 17.91 and 19.93 to 14.58 and 15.54. Applying ANOVA with a 95% confidence limit table 3.27 showed that pre drag polishing was the only statistical significant treatment for increasing tool life. Mood's median test applied to both data sets (No. of 2.5xD holes and holes/micron), show that at 45m/min pre polish did have a significant effect on the

increase on tool life with 95% confidence. Both tests calculated a P-value of 1.4% indicating a strong significance of the increase in the mean tool life with a confidence of 98.6%.

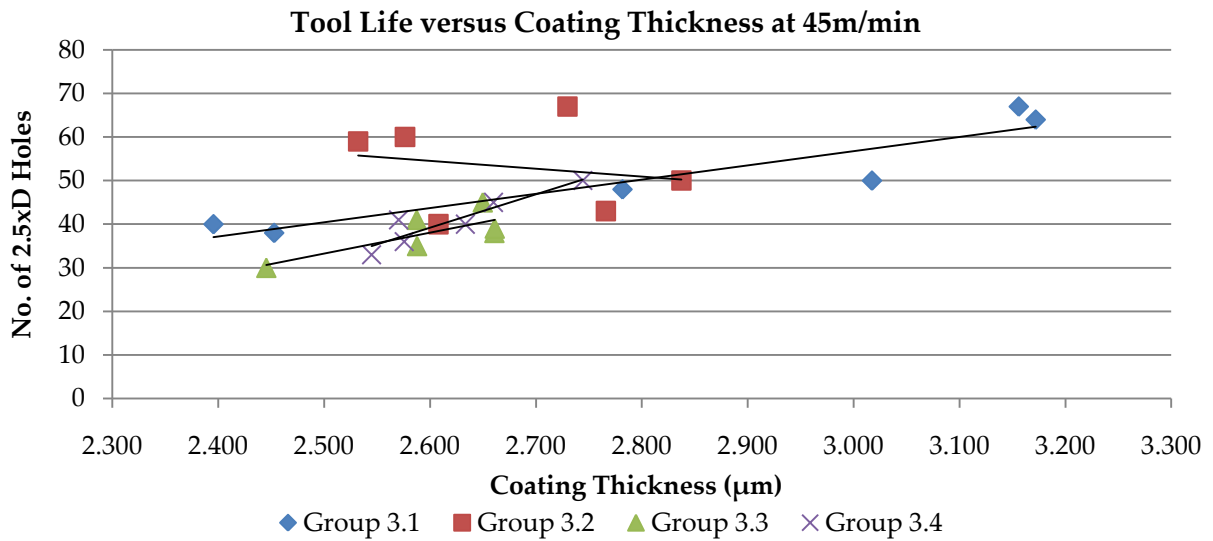


Figure 3.40. Bivariate graph comparing the tool life results tested at 45m/min 0.125mm/rev against coating thickness measurements made via XRF.

Table 3.29 Correlation coefficients for bivariate analysis between tool life and coating thickness. Drills tested at 45m/min

Group No. Tested at 45m/min	Correlation coefficient R
3.1	0.8687
3.2	0.0424
3.3	0.6013
3.4	0.8565

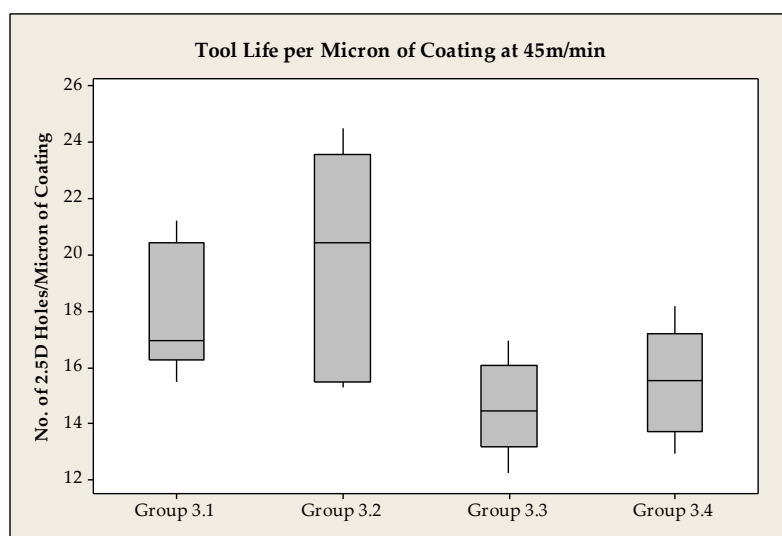


Figure 3.41. Boxplot of tool life per micron of coating results for pre and post drag polished drills tested at 45m/min 0.125mm/rev.



Table 3.30. Sample statistics for tool life results per micron of coating, tested at 45m/min 0.125mm/rev.

Cutting Conditions 45m/min 0.125mm/rev								
Group No.	Sample size	Mean	St Dev	Min	Q1	Median	Q3	Max
3.1	6	17.9	2.3	15.5	16.3	17	20.4	21.2
3.2	6	19.9	4.2	15.3	15.5	20.5	23.6	24.5
3.3	6	14.6	1.7	12.3	13.2	14.8	16.1	16.9
3.4	6	15.5	1.9	12.9	13.7	15.6	17.2	18.2

### 3.4.4 Discussion

The Optical micrographs revealed qualitatively that pre coating drag polishing reduced the appearance of light and heavy grinding marks at the rake face adjacent to the cutting edge on the 6.35mm TiN coated Jobber drills. Post coating drag polishing was found to remove or break off a majority of the macro particles on the surface which left macro sockets or fractured macro particles, the major and minor grinding marks were unaffected by post polishing (as expected). Neither pre nor post drag polishing was found to change the appearance of the flute surface 3xD up the drill. These qualitative results are supported by the quantitative analysis of the surface measures collected except in regard to 3xD up the flute. ANOVA was applied to these surface measures with a 95% confidence limit and found that pre and post polishing significantly affected the  $R_t$ ,  $R_z$ ,  $R_p$  and  $R_v$  measures at the rake face adjacent to the outer corner cutting edge. Unexpectedly, the  $R_a$  was only significant at 90% confidence which may suggest that in the application of characterising drill surfaces it is not an appropriate measure as it clearly was not sensitive enough to distinguish the changes to the surfaces. The  $R_p$  surface measure had the only significant change 3xD up the flute due to post polish. This result strongly suggests that  $R_p$  is the correct surface measure in which to characterise a change in macro particle removal as the macro particles clearly stand proud out of the surface 1.5-2 $\mu$ m above the highest grinding marks.

The lack of any real effect by pre coating drag polishing 3xD up the flute may be due to a lack of movement and pressure of the SiC particles against the surface. However, the change in the  $R_p$  surface measure strongly suggests that post drag polishing was sufficient in removing high spots in the coating due to macro particles. An area on the drill where surface roughness plays a role in machining which was not characterised in this study is the margin. This is a face where friction is encountered between the cutting tool and the wall of the hole, as the margins support the radial direction of the drill [1]. Due to the mechanism of the drag polishing process it would be highly likely that this surface was also affected and contributed to the increase in tool life. The surface measures used in this study did resolve the effects of pre a post polishing; however, the analysis may have been enhanced and simplified if  $S_a$  (average height of area) and  $S_z$  (maximum height of area) were used, as these

new ISO measures which are available to devices which use the method of focus variation calculate values by using the entire scanned area and are not effected by repeatability issues that may arise if the line scan is not placed on the exact same region every time.

The bi-variant analysis showed no correlation between coating thickness and tool life for all but two sample groups tested at 45m/min. Notwithstanding, in order to test the findings of the bi-variant analysis the raw tool life data was corrected for coating thickness. Tool life results were divided against coating thickness for each drill so a no. of holes per micron of coating value was obtained. The analysis of both data sets using ANOVA at 95% confidence showed the same results, that pre polishing was the only significant factor to increase tool life. This result strongly suggests that for this case, where the coating thickness variation was small, the coating thickness variation did not play a significant role in increasing the scatter of tool life results or in the determination of a significant change in mean tool life due to the drag polishing treatments. Comparing the findings in this study to Posti's [41] work, where a difference of 1 $\mu$ m increased the tool life by 36%, the small variation in coating thickness is what allowed this source of variance to not adversely affect the scatter in tool life results. The smallest standard deviation was found to be 90nm while the largest was 270nm. Only when the range is examined does the coating thickness variation approach 1 $\mu$ m. Of the 48 drills in this study the thinnest coating was measured to be 2.39 $\mu$ m and the thickest 3.17 $\mu$ m, a difference of 0.78 $\mu$ m. This highlights the importance of sample size as Posti only examined one cutting tool per coating thickness when determining the effect of coating thickness on tool life, while in this study the few drills which deviated from the mean were randomly distributed among all sample groups. Future work in regard to the effect of coating thickness on tool life should examine the coating thickness on the point of the drill and the rake face. As these faces are in contact with the hole wall and chips respectively. Also due to the geometry of the drill and the type of tool packing on the carousel used to deposit the TiN coating there is a possibility that the coating thicknesses may vary between the two regions due to line of sight issues of the ions during the coating process.

The analysis of the tool life results using ANOVA applied to the two factor two level experiment tested at 35m/min and 45m/min reveals that pre polishing is the only significant polishing treatment to increase tool life for holes drilled at 2.5xD. Comparing these tool life results to the extensive work completed by Bradbury *et al* [94] and Bouzakis [97] who reported the tool life improvement due to a reduction of surface roughness pre coating and a hardness increase of the protective coating post coating due to a micro-blasting treatment, the improvement to the mean tool life can be ascribed to the decrease in surface roughness, as has been shown in this work but also to the increased adhesion strength a coating acquires due to the reduced roughness. Bradbury [93] also reports that surface treatments, such as drag polishing, removes oxide scale and subsurface damage caused during the grinding process, this further increase the adhesion strength of a protective coating.

There was evidence that drag polishing significantly affected the  $R_p$  surface roughness 3xD up the flute, however the effect on tool life was not resolved in the current drill test regime. Balzers[69] have published data showing that coated drills, using the cathodic arc process, which have received post polishing have better chip removal properties due to the decrease in flute surface roughness. However, chip removal becomes a problem and a potential source of tool life variance when drilling deeper holes than were drilled in this test. However, as the drill test developed within this work was designed to eliminate this source of tool life variance it poses a limitation on what design features may be tested. Therefore, it is justified that certain machining parameters will need to change in order to test a specific design feature. In this example, to test post coating polishing treatments applied in the flute, hole depths of 5xD or greater would need to be used, however, 5xD may be the limit for standard Jobber drills as parabolic flute shapes are usually used when designing drills for deep holes.

The results of the tool life analysis using ANOVA and the Mood's median test differed. Mood's median test showed that at 45m/min pre polishing is significant but not at 35m/min. In this case the smaller sample size of 5 drills used in the 35m/min test compared to the sample size of 6 used in the 45m/min test increased the standard deviation enough so the significance of the result was not at the set 95%. However, the significance of the mean tool life increase was 92.6%, this result should not be interpreted as non-significant as the sample size is small and the significance still quite large, as Rupert Miller [98] from Stanford University writes "It cannot be denied that many journal editors and investigators use  $P \leq 0.05$  as a yardstick for the publishability of a result. This is unfortunate because not only  $P$  but also the sample size and the magnitude of a physically important difference determine the quality of an experimental finding". Therefore, this work suggests that for the particular drill test regime a sample size of 5 is adequate but a sample size of 6 is better. This result correlates well with the t-distribution versus sample size graph (Figure 2.16), that once a sample size is larger than 5-10 the t-value decreases minimally.

### 3.4.5 Conclusions

This work revealed that pre and post drag polishing is effective at reducing the surface roughness of HSS 6.35mm TiN coated Jobber drills at the rake face adjacent to the cutting edge but not 3xD up the flute. Pre drag polishing was the only significant factor in this experiment to increase the mean tool life. The analysis of the coating thickness revealed a small thickness variation among all drills. However, this small variation showed no significant effect on the scatter of tool life results. The two cutting speeds chosen did not affect the significance of the reduction in surface roughness on mean tool life. The current drill test design has limitations as the effect of flute polishing may likely not be able to be resolved in a test which only drills to 2.5xD holes depths. Therefore flexibility in the test regime must be introduced so as to allow the drill test to be more amenable to the needs of

the researcher. The minimum sample size to use for the application of product engineering testing using this drill test and to be 95% confident that the factor under experimentation is indeed the cause of the tool life improvement is 6.

## **3.5 Modelling the Effect of Batch to Batch Plate Hardness on Tool Life for Uncoated Jobber Drills using Empirical Methods**

### **3.5.1 Introduction**

Workpiece hardness invariably effects tool life, no matter the machining operation or the cutting conditions used. This relationship has been shown by Vogel and Bergmann [12] who studied the effect of plate hardness in the application of drill testing and showed that the number of holes drilled decreased exponentially for 42CrMo4 steel as the hardness increased, however, they did not provide a solution to deal with the problem. In cutting tool testing, a researcher has limited control of the workpiece hardness unless heat treatment is applied, (which is costly and time consuming) or sections of plate outside a specific tolerance are rejected.

Workpiece hardness variation can be categorised into four types; the first is the hardness variation within a plate, the second is the variation plate to plate which are manufactured within the same batch. The third, is batch to batch variation, while the fourth source is supplier to supplier variation of nominally the same plate. A single steel plate has a relatively small hardness distribution as has been shown in section 3.2 & 3.3.

Notwithstanding, a pseudo random drilling array has been applied to the drill test methodology to minimise any heterogeneous effects of the workpiece on tool life across all drills tested. However, the work completed within this thesis has shown that batch to batch and more significantly supplier to supplier mean plate hardness variability exists and is significant. Therefore, the effect of batch to batch mean plate hardness for one supplier of D2 (Schmolz and Bickenback) on tool life was characterised, so long term comparisons may be made.

Taylor's tool life model was developed to empirically model the effect of cutting speed on tool life for hardened carbon steel and HSS cutters. This was primarily used for calculating a set of cutting parameters which would result in the most productive use of a cutting tool [29]. Since its inception just over a century ago, many researches have expanded this model for drilling and milling [99] as well as the effect of cutting parameters such as the effect of minimum quantity lubricant on tool life [56]. Empirical modelling has been shown to approximate tool life well, however, only for the particular system the tool life data was collected from.

Hoffman [100], Wang and Wysk [101] have reported an empirical method of characterising the effect of workpiece hardness on tool life by expanding the Taylor's tool life model [29]. It is claimed to be a good approximation for tool life ranges between 10-60 minutes. Therefore, the aim of this work was to model the effect of batch to batch mean plate hardness on tool life by expanding the Taylor's tool life model, therefore providing a solution to the effect of batch to batch plate hardness of tool life.

### 3.5.2 Experimental Procedure

Uncoated Jobber drills at a single feed rate and a range of cutting speeds were drilled to failure in various D2 steel plates. All plates were from a single supplier and over a range of supplied batches. The boundary conditions of the cutting speeds were set at the upper and intermediate cutting speed limits of uncoated M2 HSS drills, applicable to drill testing of the Schmolz and Bickenbach supplied D2 cold work tool steel. The three cutting speeds chosen were 20, 25, and 30m/min. One set of drills were tested at 35m/min in the 467HL D2 plate. The three plate hardnesses chosen had a mean hardness of 467, 492 and 511 Leeb D hardness. See Table 3.31 for experimental design and Table 3.32 for plate hardness measurements. T-tests were applied to the plate hardness measurements to confirm that the plates were significantly different.

Tool life results were first converted from no. of holes to minutes spent drilling and plotted on a log-log graph (Figure 3.42). The data was first applied to the classic Taylor's tool life formula (Eq.1) exponents constants were first calculated and the correlation coefficient  $R^2$ . Octave was then used (a numerical computation software for solving linear and non-linear problems) to fit a 3 dimensional plane to the tool life data, to generate the extended Taylor's tool life formula (Eq. 14). Due to the limited supply of the three different plate hardnesses, sample sizes were first limited to 4, however, plate 2 492 HLD allowed two more drills to be tested.

$$C = V_c T^n HL^m \quad \text{Eq. 14}$$

Where:

C = Cutting speed for a lifetime of 1min.

$V_c$  = Cutting speed in m/min

T = Tool Life in min

n = Exponent which depends on the machining system, tool material, workpiece material etc.

HL = Mean plate hardness in Hardness Leeb D.

m = Exponent which depends on the effect of plate hardness on tool life.

Table 3.31. Drill test design, showing the number of samples to be tested at each cutting condition and plate hardness.

Cutting conditions	Plate hardness HLD	No. of drills
20m/min 0.125mm/rev	467	4
	492	4
	511	4
25m/min 0.125mm/rev	467	4
	492	5
	511	4
30m/min 0.125mm/rev	467	4
	492	5
	511	4
35m/min 0.125mm/rev	467	4

### 3.5.2.1 Workpiece Material

Table 3.32. Sample statistics for plate hardness measurements measured using a Leeb D hardness tester.

Plate hardness Leeb D								
Variable	N	Mean	St Dev	Min	Q1	Median	Q3	Max
Plate 1	30	511.6	9.6	497	503	510	521	530
Plate 2	30	492.5	4.2	486	490	492	494	508
Plate 3	30	467.6	7.3	454	463	466	471	486

## 3.5.3 Results

### 3.5.3.1 Workpiece Material

Results from t-tests applied to the three workpiece hardness measurements, revealed that all plates were statistically different with 95% confidence. Plate 1 was compared against plate 2 and found to have a difference of 19 HLD while plate 2 was tested against plate 3 and found to have a difference of 25 HLD see Appendix F for Minitab output.

### 3.5.3.2 Taylor's Tool Life Model

The tool life results plotted on a log-log graph, shown in Figure 3.42, reveals that for the cutting conditions chosen (20, 25, 30 and 35m/min at 0.125mm/rev) each plot which represents a particular mean plate hardness has a high correlation coefficient to a power curve for all three plate hardness used (Table 3.33) 0.976, 0.994 and 0.991 for plate hardness

of 467, 492 and 511HLD respectively. The tool life relationship with cutting speed is observed to be linear besides the uncoated drills tested at 20m/min in the 467HLD plate. As the cutting speed reduces, tool lifetime increases, except in the softest plate where the tool life has significantly reduced at 20m/min compared to 25m/min, as the tool life at 20m/min in the softest plate is not linear, this point was not used in the regression line as a region of linearity was the focus of this work. The characteristic cutting speed for 1 minute tool life shows that for the hardest plate (511HL) the cutting speed needed is 29.94m/min, for the D2 plate with a mean hardness of 492 HLD the cutting speed is 31.15 and for the softest plate (467HLD) the cutting speed is 37.95m/min.

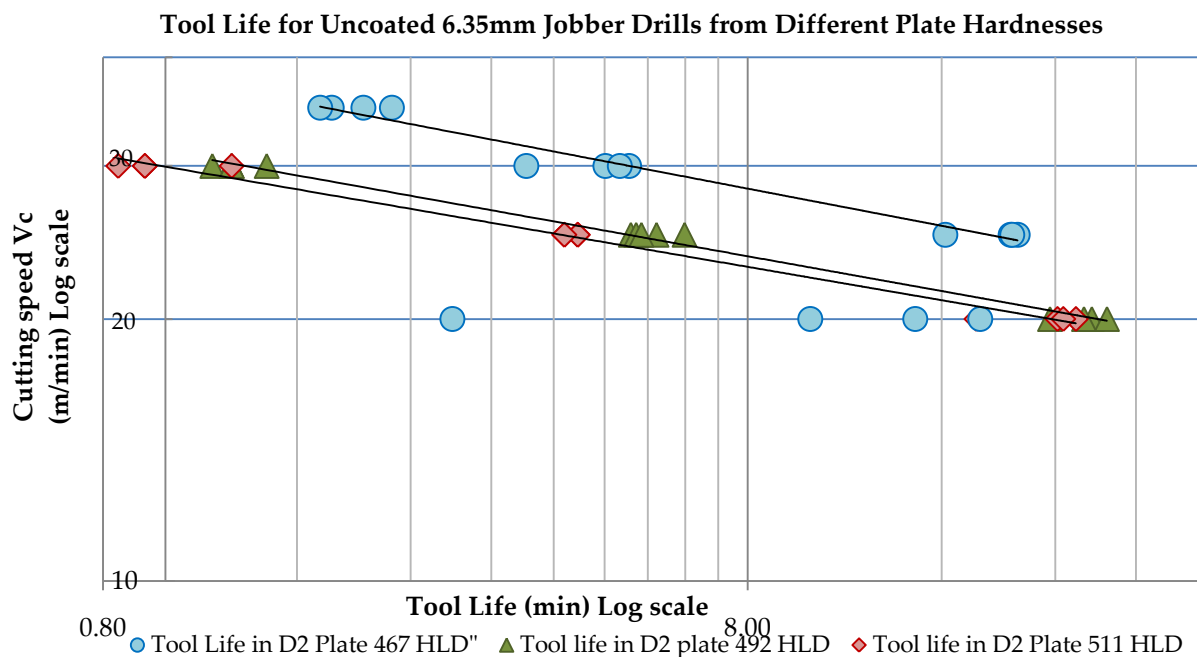


Figure 3.42. Log-log plot of the life time data collected from D2 plate with average hardness of 467, 492 and 511 Leeb D.

Table 3.33. Coefficients calculated for the Taylors tool life equation for three different plate hardness and the corresponding correlation coefficient R<sup>2</sup>.

Description	Cutting speed 1min life (m/min) 'C'	Characteristic exponent 'n'	R <sup>2</sup>
Plate HL 467	37.95	0.142	0.976
Plate HL 492	31.15	0.133	0.994
Plate HL 511	29.94	0.127	0.991




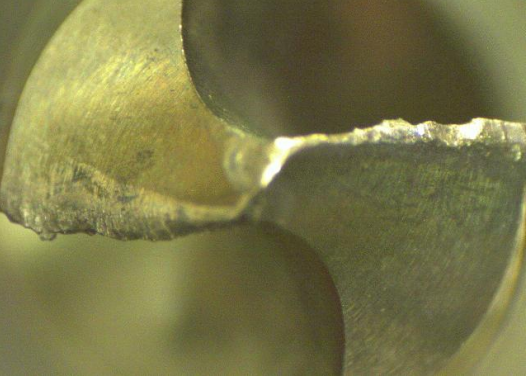
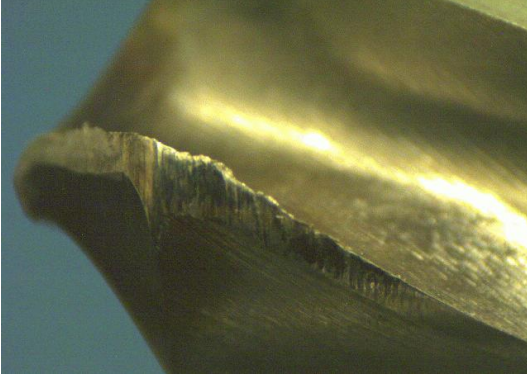
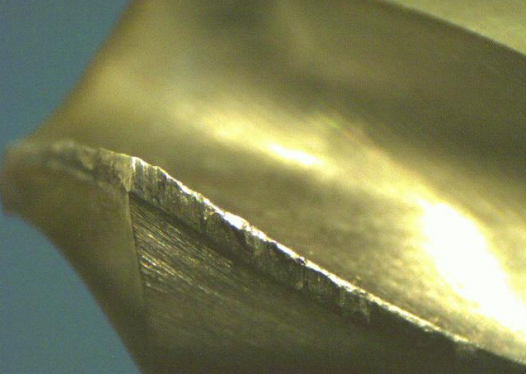
	
<p>(a) Drill no. 46. Screech failure. Chisel completely worn, nose flank wear excessive. Small BUE along cutting edges.</p>	<p>(b) Drill no. 7. Screech failure. Minimal chisel wear, minimal nose flank wear. Large BUE along both cutting edges.</p>
	
<p>(c) Drill no. 46. Screech failure. Outer corner margin completely worn. Minimal pick up of work piece material.</p>	<p>(d) Drill no. 7. Screech failure. Minimal outer corner wear. Significant material pickup along the entire margin.</p>

Figure 3.43 (a,b,c,d). Images of two failed drills tested to screech failure. Drill no. 46 (a & c) shows a normal screech failure, while drill no. 7 (b & d) non-standard failure.

Comparing drill no. 46 (figure 3.43 (a) & (c)), normal screech failure which represents the failure type of the majority of drills tested in this work, to drill no. 7 (figure 3.43 (b) & (d)), non-normal screech failure which represent the four drills tested at 20m/min in the softest plate (467 HLD). The differences between the two failed drills are the amount of BUE formation and material transfer. Drill no. 46 has large amounts of flank wear on the point flank and margin flank faces, also the chisel has been completely worn off. In stark contrast, drill no. 7 has minimal wear on the chisel and point flank and intermediate wear on the outer corner margin flank but the amount of BUE on both cutting lips and the margin is significantly more than drill no. 46.

### 3.5.3.3 Extended Taylor's Tool Life Model

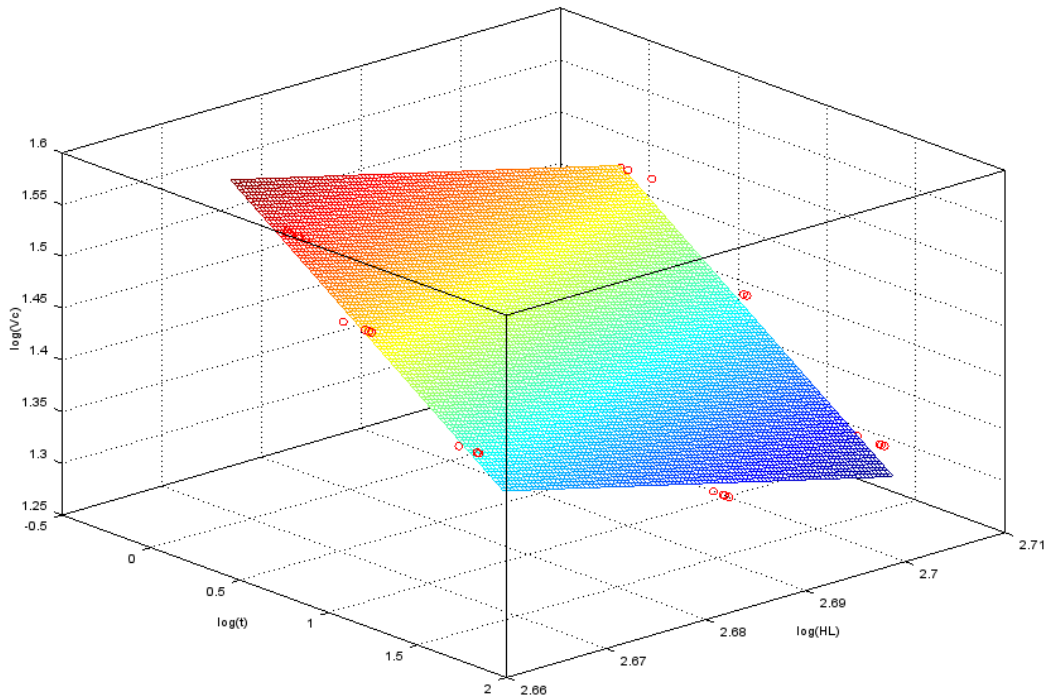


Figure 3.44. 3 axis graph showing a plane fit to the tool life data (min), cutting speed (m/min) and plate hardness (HLD). All data has been logged to the base 10.

Table 3.34. Coefficients from a plane fit performed using Octave software with corresponding lower and upper 95% confidence limits.

Coefficient	Value	Lower 95% confidence	Upper 95% confidence
b(1)	8.09201	7.23633	8.94768
b(2)	-0.13315	-0.14293	-0.12337
b(3)	-2.44526	-2.76313	-2.12736

Table 3.35 Correlation coefficient F-value and P value output from plane fit using Octave.

R <sup>2</sup>	F	P
0.96461	477.008	0.00

The tool life data showed a high correlation to the plane fit (Figure 3.44) applied using the Octave software, R<sup>2</sup> 0.964 (Table 3.35). The coefficients for the developed tool life model are shown in Table 3.34 labelled b(1), b(2) and b(3) with the corresponding upper and lower 95% confidence intervals. Eq.15 shows the coefficients substituted in a log form of the tool life equation. Eq.15 was then rearranged to the form of the Taylor's tool life equation, first by Logging all terms by Log<sub>10</sub> (Eq.16), followed by transposing the equation to have b(2), b(3) and V<sub>c</sub> terms on one side (Eq.17). The extended Taylor's tool life equation with coefficients substituted is shown in Eq.18. Equation 18 represents the goal of this work, that is, an

extended Taylor's tool life equation for the effect of plate hardness in D2 cold work tool steel between the mean hardness of 467-511 HLD.

$$\text{Log}(V_c) = b(1) + b(2)\text{Log}(T) + b(3)\text{Log}(HL) \quad \text{Eq. 15}$$

$$V_c = T^{b(2)}HL^{b(3)}10^{b(1)} \quad \text{Eq. 16}$$

$$V_c T^{-b(2)}HL^{-b(3)} = 10^{b(1)} \quad \text{Eq. 17}$$

Where:

$$\begin{aligned} b(1) &= 8.09201 \\ b(2) &= -0.13315 \\ b(3) &= -2.44526 \end{aligned}$$

Now from Eq. 14 it is seen that:

$$\begin{aligned} n &= 0.13315 = -b(2) \\ m &= 2.44526 = -b(3) \\ C &= 10^{8.09201} \\ 10^{8.09201} &= V_c T^{0.13315} HL^{2.44526} \end{aligned} \quad \text{Eq. 18}$$

### 3.5.4 Discussion

The results of the present study show that for the cutting conditions examined the tool life data fits a plain well, with a correlation coefficient value of 0.964. One cutting condition, 20m/min in 467 HLD mean plate hardness, did not follow the linear behaviour as the rest of the cutting conditions did. This cutting condition had significantly lower mean tool life and large scatter. This is the boundary of where tool life begins to no longer follow a linear relationship with cutting speed on a log-log graph. According to Shaw [4], tool life will exhibit a region of linearity for a particular range of cutting speeds (Figure 2.14). The region of linearity is bound on the left hand side by BUE formation (low cutting speed) and on the right hand side by thermal softening (high cutting speed). The images of the failed drills show that at this cutting condition (20m/min 467HLD) the amount of BUE formation on the cutting edges and margin faces was significantly more than a drill (no. 46) which represented the majority of failure type within this study. Therefore, a cutting condition has been identified where BUE formation significantly affects the failure mode of uncoated M2 HSS 6.35mm Jobber drills in 467HLD annealed D2 steel.

The tool life results from this work also correlate with the trend found by Vogel and Bergmann [12], where the tool life of drills tested in 42CrMo4 exponentially fell as the hardness was increased from 28HRC to 36HRC. Examining Vogel and Bergmann's data

revealed that an increase in plate hardness from 28 HRC to 33HRC, which converted to Leeb D is 561HLD to 593HLD a 5.7% increase, resulted in a 55% decrease in drill life. Results from this study show that at a cutting speed of 25m/min an increase in plate hardness from 467HLD to 492HLD, an increase of 5.3%, decreased drill life by 70.9%. This result reveals that a similar percentage increase in hardness of D2 steel has a larger effect on decreasing tool life than 42CrMo4 steel. Revealing just how sensitive tool life is to hardness. The percentage change in hardness is similar but the absolute value of hardness of the two materials is significantly different. If the relationship between tool life and hardness would continue at the same rate for D2, tool life would be even more sensitive to hardness variations.

This study still requires further work. Firstly the model will need to be evaluated for its ability to approximate tool life of uncoated 6.35mm HSS Jobber drills. Further work would then consist of expanding the model for a number of drill diameters, so a degree of flexibility in what size drills can be tested. However, this methodology of expanding the model for every factor leads to large data sets which need to be collected which is costly and time consuming. Venkatesh [102] reported his model which needed the combination of eight constants and coefficients to model the effect of all cutting parameters (speed, feed and depth of cut) as well as the effect of workpiece hardness. The alternative solution to using an empirical model for comparing tool life performance over time is the use of a large batch of reference drills (a control sample group). Each time a test would be conducted, a small reference sample would be used. This would allow tool life comparisons to be made over time, instead of using the empirical model solution which will have its tool life approximation questioned if the plate hardness is out by a few percent from the collected data plate hardness range.

### **3.5.5 Conclusions**

Taylor's tool life equation has been expanded for the effect of batch to batch mean plate hardness for D2 steel, supplied by Schmolz and Bickenbach, trade name Cryodur, between the range of 467-511HLD. The data collected fitted a plane well with a 0.964 correlation coefficient. For the softest plate at the lowest speed the plain fit was no longer valid. It has been shown that the cause of the non-linearity was due to large amounts of BUE formation on the cutting edges and margins, also the curve in the Taylor's tool life graph matches well with work published by Shaw. This work also revealed that within this range of plate hardnesses a small increase of 5.3% can decrease the life of uncoated 6.35mm M2 HSS Jobber drills by 70.9%. Further work that is definitely required is the evaluation of the model to approximate tool life for uncoated M2 HSS 6.35mm Jobber drills. Optional work would be to expand the model for the effect drill diameter and wear resistant coatings. However, this would require calculating the validity of this approach compared to using reference drills.

## 4 Discussion: The Developed Accelerated Drill Test

Tool life has been shown by other researchers [12, 25, 26], as well as within this work, to be a stochastic process with many complex behaviours and sources of variance which detrimentally affects the scatter in tool life results. Empirical testing is still the preferable method for cutting tool development especially in an industrial environment, as models are currently unable to replicate the complex interaction between cutting tool and workpiece as tool wear is the result of several mechanisms working simultaneously. The use of low value Jobber drills has been used as a vehicle for cutting tool development beyond the scope of specific drill design features, specifically for the purpose of coating research and development [12]. Accepting that the drive for productivity is constant and universal, manufactures must not only continually increase the productivity and quality of their manufacturing capability but their research and development methods as well. Hence within the arena of cutting tool manufacturing a robust, sensitive, rapid and low cost cutting tool test was found to not only be necessary but essential. The objective of this research was to design and develop a destructive accelerated drill test.

It was found, that although sources of machining complexity and variance which affects the scatter in tool life data, specifically in context of drill testing, have been identified, such as the effect of plate hardness, a solution to deal with it has not yet been provided. Using a systems approach facilitated the management of the complex behaviours so a machining regime could be identified which offered a repeatable and mono-modal tool failure, a robust test, as well as, where possible, to minimise or empirically model the effect of machining variance on tool life scatter, a sensitive test. A statistical approach was also adopted for the drill test methodology so tool life data generated would be able to resolve differences in tool life, using small samples, so that conclusions could be made with a high level of confidence on whether a change in the population of drills had occurred.

It was found that specific aspects of the accelerated drill test design and methodology can be adopted for wider cutting tool testing applications. Features such as, rigid workpiece fixturing and cutting tool holders so as to minimise the effect of vibration on tool life variance. The detrimental effect of machining system vibration is already well known and is an active area at the forefront of machining research. For example, Song *et al* [103] in June of 2014 determined chatter free machining regions and optimal cutting parameters for stable milling of aerospace aluminium using a shrink-fit tool holder.

The data analysis methodology used throughout this work (see chapter 2.7) can also be incorporated into wider cutting tool testing and non-cutting testing[66] applications. Weibull analysis is known to be able to determine failure distributions and was used within this work to determine the type and number of failure distributions during the accelerated drill testing into D2 and P20 steel. However, a limitation was found when applying the  $b$  slope test and characteristic life test used to distinguish mixed failure distributions. Small

amounts of curvature or offsets in the data may be hard to distinguish or be completely insignificant by observation of the data on a Weibull graph alone. In fact, the literature suggests that a sample size of 50 or greater be used when determining mixed failures using these tests. A specific example in this work was the mixed failure of the 760HV<sub>30</sub> drills tested in D2. This mixed failure was initially identified, through the preliminary appraisal of the failure data on a Weibull graph, to be an offset in the characteristic life; however, this was not the case. Applying the *b* slope test, to be thorough, revealed that there were two significantly different slopes within the original data set. The results from the ANOVA and Mood's median test suggests that the Mood's median test is more sensitive to the larger standard deviation caused by there being a sample size of 5 for drills tested at 35m/min, as the results from ANOVA show a significant difference in tool life for this same data. Even though the result for the Mood's median test was just below 95%, it can still be interpreted as a significant change, as the significance in comparison to the sample size is large, as Rupert Miller points out [98]. The metrology tools used to characterise macro geometry, Toolmakers microscope, can obviously be used for wider cutting tool testing applications than drills alone (it was designed for this reason). However, The surface roughness characterised using the Alicona IFM, plate hardness measured using a Leeb D hardness tester and Vickers 30Kg load, as well as the coating thickness measured using a XRF with a proportional counter detector, can all be incorporated into a wide variety of cutting tool tests as they were found to provide a suitable level of control, repeatability and accuracy needed to characterise these associated drill design variances so the determination of any correlation existing between tool life could be determined.

The microstructural examination of D2 and P20 steel showed that the D2 equivalent steel plate on a microscopic scale is an inhomogeneous material. However, the D2 steels inhomogeneity was uniformly distributed. Therefore, the samples of drills were interacting with notionally the same microstructure during a test. Small hardness variation within a plate was measured in D2, however the average chromium carbide size and spatial distribution across a plate was not characterised. This should also be investigated in future work as the American Society for Metal [24] reports that a non-uniform carbide distribution will affect the tool life scatter significantly, as these particles play a major role in the abrasive wear characteristic of D2 steel. In comparison the P20 plate examined was found to be homogeneous with a martensitic micro structure and a small amount of inclusions distributed sparingly throughout. The standard deviation in plate hardness was also small.

However, the use of boxplots and Weibull slope and characteristic life tests for mixed failure distributions revealed that when drilling into D2 it was able to offer a low tool life standard deviation and mono-modal tool life distribution. Hence this is why differences were able to be distinguished between sample groups using D2 and not P20. This work also suggests that the use of a pseudo random drilling array allowed the small variation in plate hardness to be distributed among all drills sampled. This solution may also distribute any potential chromium carbide spatial non-uniformity among all drills to a certain extent.

D2 steel was more difficult to machine due mainly to the chromium carbides and did not require high cutting speed or feed rate in comparison to P20 to accelerate wear. For accelerated testing of HSS cutting tools, which are thermally sensitive in comparison to WC-Co and Cermet materials, an abrasive wear test is preferable over a thermo-chemical wear mechanism. The exact mechanism for abrasive wear encountered while machining annealed D2 was difficult to identify through the literature. The 2 body abrasion model as described by Misra and Finnie [77] does not entirely match the description reported by Leed [78] which stated that while machining annealed D2 the cutting edge is able to “plough through the soft [ferritic] matrix and literally push the hard carbides aside”. This description may be interpreted as a closed three body abrasion model as defined by Misra and Finnie [77] where the hard particles are free to move between two closely mating surfaces. The questions that require further research are, whether the chromium carbides are truly fixed, free to move or somewhere in between at the interface between D2 and the HSS drill? How do the carbides interact with the cutting tool as the chip flows across the rake face and as the flank face of the cutting tool moves across the freshly machined surface under intimate contact? This lack of knowledge may not enhance the ability of the drill test to distinguish differences between tool life samples, as this has already been shown in this work via a predominantly single wear mechanism and mono-modal failure distribution; however, it does identify a gap in the current literature of this complex wear behaviour between annealed D2 and HSS cutting tools.

A certain percentage of Jobber drills sampled from a population of 500 were found to have key geometrical features that NAS [16] identified were crucial to tool life performance and dimensional accuracy outside tolerances, the percentage would change depending on what standard was used to compare. However, it is reasonable to assume that the percentage of drills outside of tolerance would be randomly distributed among samples. Therefore it does not matter that a number of those drills will be outside of tolerance because their influence on the scatter in tool life will also be randomly distributed. What does matter is that the effect of those drills on the standard deviation in tool life is relative to sample size [104]. If the sample mean between two samples is large than the standard deviation is not required to be small when determining a change in population mean but if there is only a small difference between the two sample means than the standard deviation is required to be small, especially when using small sample sizes (Eq.3).

The cutting torque was found to potentially offer a suitable measure to describe the performance of a drill. The resultant cutting force can be calculated from the torque and thrust, however where would be a suitable point on a drill to calculate the resultant cutting force if, the rake angle on a standard Jobber drill changes from a low negative rake angle to a high positive angle from the chisel region to along the cutting edge, as well as the cutting velocity increasing from near zero at the centre to its maximum at the periphery outer corner [19, 86]. A solution to these issues has been provided by Abele et al [87] and Chen et al [88] who used the solution of breaking the cutting edge and chisel into small elements to

calculate individual resultant forces. Notwithstanding, in regard to this work a specific value cutting force to describe a drill is not possible, however, once a drill has entered the steady state regime, a specific torque value may be used to describe a drills performance because it was shown to vary little over this stage of life, however further work would need to be conducted to test this hypothesis. This methodology may allow drill testing to be stopped once the steady state region has been reached. At which point the drilling torque can be compared against to distinguish if a design feature made a change.

There was evidence that drag polishing significantly affected the  $R_p$  surface roughness  $3xD$  up the flute, however the effect on tool life was not resolved in the current drill test regime. Balzers[69] have published data showing that coated drills, using the cathodic arc process, which have received post polishing have better chip removal properties due to the decrease in flute surface roughness by removing large macro particles. By using torque measurements, chip removal was shown to become a problem and a potential source of tool life variance when drilling deeper holes. However, in order to achieve the goal of low tool life scatter one drill test design feature was to drill to  $2.5xD$  hole depths. Torque and thrust results confirmed that when drilling to  $2.5xD$  hole depths using uncoated 6.35mm Jobber drills the cutting torque and thrust are constant when the outer corners are engaged in the material, therefore, this feature removed the effect of chip removal. Notwithstanding, this drill test design factor has now been shown to limit which drill design features can be tested, such as the effect of post coating polishing of the flute. Therefore, the notion of a universal drill test which can adequately test for tool life differences for all design features is not possible because the required application of the cutting tool would need to be taken into consideration before conducting a drill test. Put simply, if the effect of post coating flutes polishing on tool life is the intended aim then deep holes would need to be drilled. This hypothesis would require testing.



The life of uncoated M2 HSS 6.35mm Jobber drills was found to be sensitive to small changes in plate hardness. At a cutting speed of 25m/min an increase in plate hardness from 467HLD to 492HLD, an increase of 5.3%, decreased drill life by 70.9%. In this work the effect of plate hardness on tool life was modelled using empirical methods; however, empirical modelling has its limitations but empirical modelling is not the problem, the complex behaviours and associated sources of machining variance is. Tool life has been shown to change disproportionately if a small change is made to the machining system, specifically workpiece hardness. An alternative solution to empirically modelling every machining factor and expanding the models boundaries is the use of a large population of reference test drills which could be sampled each time a new test plate or batch of test plates were supplied. This methodology would allow a constant reference to be used to correct for the difference in plate hardness. For example if treatment 'A' is applied to a sample set of drills and tested alongside a sample of reference drills in a soft plate and the mean tool life result for both was 100 holes then it can be concluded that treatment 'A' made no effect to tool life. Now treatment 'B' is applied to a sample set of drills and tested alongside a set of reference drills but now in a harder plate then the last test. The tool life results show that the drills with treatment 'B' had a mean tool life of 60 holes while the reference set had a mean tool life of 50 holes. By comparing the ratios of the two separate tests it can be concluded that treatment 'B' increased too life by 20%.

## 5 Conclusions and Recommendations for Further Work

### 5.1 Conclusions

A destructive accelerated drill test has been designed, characterised and applied. A solution is now provided which can deal with the detrimental effect batch-to-batch plate hardness has on tool life scatter and long term tool life comparisons. A systems approach has facilitated the management of the complex behaviours so a machining regime could be identified which offered a repeatable and mono-modal tool failure, a robust test, as well as, where possible, to minimise or empirically model the effect of machining variance on tool life scatter, a sensitive test. The statistical approach adopted for the drill test methodology has allowed tool life data generated by the drill test to be able to resolve differences in tool life, using small sample sizes, with conclusions being drawn with a high level of confidence that a population change has occurred. However, a universal drill test which can adequately test for tool life differences for all design features at the same cutting conditions is not possible because the required application of the cutting tool would need to be taken into consideration before conducting a drill test.

Specific aspects of the accelerated drill test design and methodology can be adopted for wider cutting tool testing applications, such as using rigid workpiece fixturing and tool holders, tool life data analysis methods and the metrology tools used to characterise cutting tool design features and workpiece hardness.

D2 cold work tool steel in the annealed condition was found to have a small hardness distribution within a plate and be an inhomogeneous material on a microscopic scale with large chromium carbides embedded in a ferritic matrix, notwithstanding, the inhomogeneity was uniformly distributed. While the alternative material investigated, P20 plastic mould steel in the quenched and tempered condition was found to be a homogenous material with a martensitic microstructure and also have a small hardness distribution within a plate. D2 was able to offer a low tool life standard deviation and a mono-modal tool failure mode. In stark contrast P20 showed a larger standard deviation and a bi-modal failure mode. Therefore, D2 was able to fulfil the robustness requirement that the drill test was identified to need. This work also showed that for accelerated testing of HSS cutting tools, which are thermally sensitive, an abrasive wear test is preferable over a thermo-chemical wear mechanism.

If the difference between two sample means is large then the standard deviation is not required to be small when determining a change in population mean. However, if there is only a small difference between the two sample means then the standard deviation is required to be small, especially when using small sample sizes. Pre inspection of drill geometries for the rejection of Jobber drills outside of tolerance was found to be less of an issue when distinguishing the difference between sample means. It was assumed that the

drills outside of tolerance will be randomly distributed, along with the effect on tool life. It is important however, that the effect of those drills on the standard deviation in tool life is small relative to the sample size and small relative to the sample means.

It was found that the specific torque value may be used to describe a drills performance because it was shown to vary little over the steady state phase of life. However further work would need to be conducted to test this hypothesis. This methodology may allow drill testing to be stopped once the steady state region has been reached. At which point the drilling torque can be compared with a reference or base line to distinguish if a design feature has made a change. The  $R_p$  surface roughness measure is the most suitable for detecting changes to the surface roughness for a treatment which is applied to remove macro particles.

An extended Taylor's tool life model was generated which modelled the effect of batch to batch plate hardness between the range of 467HLD to 511HLD for annealed D2 cold work tool steel. This work showed that the life of uncoated M2 HSS 6.35mm Jobber drills is sensitive to small changes in plate hardness. At a cutting speed of 25m/min an increase in plate hardness from 467HLD to 492HLD, an increase of 5.3%, decreased drill life by 70.9%. The complexity of machining imposes limitations on the justification for how many machining factors should be modelled using an empirical methods. Tool life has been shown to change disproportionately if a small change is made to the machining system, specifically workpiece hardness and the large number of factors which contribute to tool life would require larger data sets to be collected. An alternative solution to empirically modelling every machining factor and expanding the models boundaries is the use of a large population of reference test drills which could be sampled each time a new test plate or batch of test plates were supplied. This methodology would allow a constant reference to be used to correct for the effect different plate hardness have on tool life.

## 5.2 Recommendations for Further Work

The average chromium carbide size and spatial distribution across a plate was not characterised. This should be investigated in future work as it has been discussed that a non-uniform carbide distribution will affect the tool life scatter significantly, as these particles play a major role in the abrasive wear characteristic of D2 steel.

The abrasive wear mechanism found while drilling D2 should be characterised for HSS cutting tools as this is lacking in the current literature due to a lack of knowledge of what happens to the chromium carbides during cutting. The following question needs answering. How do the chromium carbides interact with the cutting tool as the freshly generated chip, flows across the rake face but also as the flank face of the cutting tool moves across the freshly machined surface under intimate contact?

A specific torque value may be used to describe a drills performance because it was shown to vary little over the steady state stage of life. Further work would need to be conducted to test this hypothesis. This methodology may allow drill testing to be stopped once the steady state region has been reached. At which point the drilling torque can be compared against to distinguish if a design feature made a change.

The hypothesis that, in order to test the effect of post coating polishing in the flute on drill life can only be resolved by drilling deep holes is required to be tested.

An experiment to evaluate the prediction capability of the extended Taylor's tool life model for D2 plate hardnesses between the range of 467HLD and 511HLD is required.

# Appendix A – VMC Setup and Programming for Drill Testing

In order to investigate the machining mechanics in drilling as well as test cutting tools in an industrial environment a drill testing methodology was required which would be robust to variation such as test plate and cutting speed and sensitive to resolve tool life improvements through surface engineering techniques, such as polishing treatments and PVD coating architectures using small sample sizes. Any drill test designed for industrial use would also have constraints such as time and money. The following sections discuss the cutting tool testing methodology designed for an industrial environment.

## Programming a VMC Using G and M Code with Global and System Variables

Below is a list of the CNC programs which were used to preform drill tests in D2 and P20 test plate material. In order to use the global variables, separate programs were needed to be programmed in order to conduct testing using the two test plates but also separate programs to test drills with a 1-3mm diameter and 4-8mm diameter so as to use as much of the plate as possible.

The drill test programs were designed to function using a main program and a subroutine program shown in Table A.3, the program labelled "Drill Test Program 4mm-8mm" prepares the CNC for drilling; holding all X and Y positions for each group of holes as well as performing important internal checks to make sure the CNC will run safely. The program labelled "Drill Test Subroutine 4mm-8mm" would be called up at the beginning of every group of holes and would perform all drilling operations through a G81 canned cycle code. This subroutine is also where all cutting conditions are imputed such as cutting speed in terms of rpm, Feed rate in terms of millimetres per minute and hole depth in millimetres. The subroutine also has its own internal checks using global variables and simple counting logic to verify which holes have already been drilled, to prevent the spindle crashing into the workpiece.

Listing all main programs and subroutines used in the study

Main Programs	Subroutines
Drill Test Program D2 4mm-8mm	Drill Test Subroutine D2 4mm-8mm
Drill Test Program P20 4mm-8mm	Drill Test Subroutine P20 4mm-8mm
Drill Test Program D2 1mm-3mm	Drill Test Subroutine D2 1mm-3mm
Drill Test Program P20 1mm-3mm	Drill Test Subroutine P20 1mm-3mm

### Global variables for D2 plate

Table A.1. Shows the variable number and its corresponding meaning in the drill testing program and possible values during execution of a drill test into D2.

Variable No.#	Variable description	Possible values
#103	Hole number counter 4-8mm drills	1 to 10
#104	Group number counter	1 to 90
#105	Work coordinate system (G58 and G59)	0 or 1
#107	Hole number counter 3mm drills	1 to 32
#108	Logic controller, 3mm drills in same plate as 4-8mm	0 or 1

### Global variables for P20 plate

Table A.2. Shows the variable number and its corresponding meaning in the drill testing program and possible values during execution of a drill test into P20.

Variable No.#	Variable description	Possible values
#100	Hole number counter 4-8mm drills	1 to 10
#101	Group number counter	1 to 90
#102	Work coordinate system (G56 and G57)	0 or 1
#106	Hole number counter 3mm drills	1 to 32
#108	Logic controller, 3mm drills in same plate as 4-8mm	0 or 1

Table A.3. Shows the main program (O9004) and subroutine programs (O9005 & O9006) used in testing 6.35mm Jobber drills into D2.

<p>%  O9004 (Accelerated Drill Test Program D2 4mm-8mm. This program prepares the CNC for drill testing and holds the coordinates of the first hole from 90 groups with 10 holes in each, it ends by resetting the global variables, resetting and homing the machine)  G103 P1 (Limit block look ahead, P1 CNC will read one line of code at a time)  G90 (Absolute positioning command)  G21 G94 G43 (Metric coordinate system, Feed per minute, Tool length composition in + direction)  T01 M06 (Tool no. 1, change tool command)  H01 (Tool no. 1, tool settings coolant nozzle direction, value of compensation length)  G00 X-100. (Rapid motion to machine coordinate</p>	<p>%  O9005 (Accelerated Drill Test Subroutine D2 4mm-8mm. This subroutine holds the cutting parameter settings and the coordinates of the ten holes within the G52 work coordinate system)  #198 = #5201 (record the value of the system variable #5201 'value of x coordinate' to the global variable #198)  #199 = #5202 (record the value of the system variable #5202 'value of y coordinate' to the global variable #198)  S1754 M42 (the spindle is set to a 1754rpm and the high gear is overridden.)  M03 (rotate spindle in the clockwise direction)  G00 Z20. (move spindle to Z 20mm above plate within local coordinate system)</p>
---	--

<p>X-100) Z120. (Rapid motion to machine coordinate Z120) N100 (Used as a reference for pointer logic) IF [#105] THEN G59 (If the global variable #105 is not equal to zero then use local coordinate system G59) IF [#105 LT 1] THEN G58 (If the global variable #105 is less than 1 then use local coordinate system G58 otherwise move to the next line of code) IF [#104 GT 90] THEN #104 = 1 (If global variable #104 is greater than 90, then #104 is equal to 1, otherwise move to the next line of code) GOTO#104 (Go to the line of code with the value of this variable) N1 G52 X165.4 Y-124.1 (line of code no. 1 move to X165.4 Y124.1 then go into local coordinate system G52) M98 P9005 (Read the subroutine program P9004) N2 G52 X64.5 Y-239.1 (see line N1) M98 P9005</p> <p>(this area has 87 repeats of the same code with different X and Y coordinates covering the whole plate)</p> <p>N90 G52 X39.3 Y-239.1 M98 P9005 #105 = #105 + 1 IF [#105 EQ 1] GOTO100 (If the global variable is equal to 1 then go to line N100 other wise move to the next line of code) G28 (home the CNC machine) #103=1 ( reset the global variable to 1) #104=1 ( reset the global variable to 1) #105=0 ( reset the global variable to 0) M30 (program end and reset) %</p>	<p>M08 G81 F219.3 R5. Z-15.87. L0 (Turn on coolant, drill canned cycle with a feed rate of 219.3 mm/min to a hole depth of 15.87mm) IF [#103 GT 9] THEN #103 = 1 ( If global variable is greater than 10, then #103 is equal to 1 otherwise move to the next line of code) GOTO#103 (Move to the line of code with the value of #103) N1 X0. Y0.0 #103 = #103 + 1 M98 P9006 (drill hole at X0 Y0, plus one to the global variable #103 and open subroutine P9006) N2 X6.3 Y-5.8 #103 = #103 + 1 M98 P9006 (see N1) N3 X0. Y-11.6 #103 = #103 + 1 M98 P9006 N4 X6.3 Y-17.4 #103 = #103 + 1 M98 P9006 N5 X0. Y-23.2 #103 = #103 + 1 M98 P9006 N6 X0. Y-29.0 #103 = #103 + 1 M98 P9006 N7 X6.3 Y-34.8 #103 = #103 + 1 M98 P9006 N8 X0. Y-40.6 #103 = #103 + 1 M98 P9006 N9 X6.3 Y-46.4 #103 = #103 + 1 M98 P9006 N10 X0. Y-52.2 #104 = #104 + 1 M98 P9006 (Drill hole at the XY coordinates and plus 1 to global variable #104 then open program P9006) #103 = #103 + 1 G00 Z20.(Bring spindle to Z20 M99 (Go back to main program P9004) %</p>
<p>% O9006 (Drill Test Subroutine X,Y DPRNT. This program sends the X-Y coordinates of every hole a specific drill has drilled in the plate) #189 = #198 + #5041 #190 = #199 + #5042 DPRNT[X#189[13]*Y#190[13]] (sends the value via RS-232 to the PC) %</p>	

## Network Infrastructure

To send and receive data from a PC to a CNC the following network infrastructure needed to be implemented due to the fact that the CNC receives data signals across a RS-232 serial port. A router was used to connect PC's to a network, the router is then connected to a TRP-C32 serial to Ethernet device which would convert IP addresses to physical serial ports shown in Figure A.1.

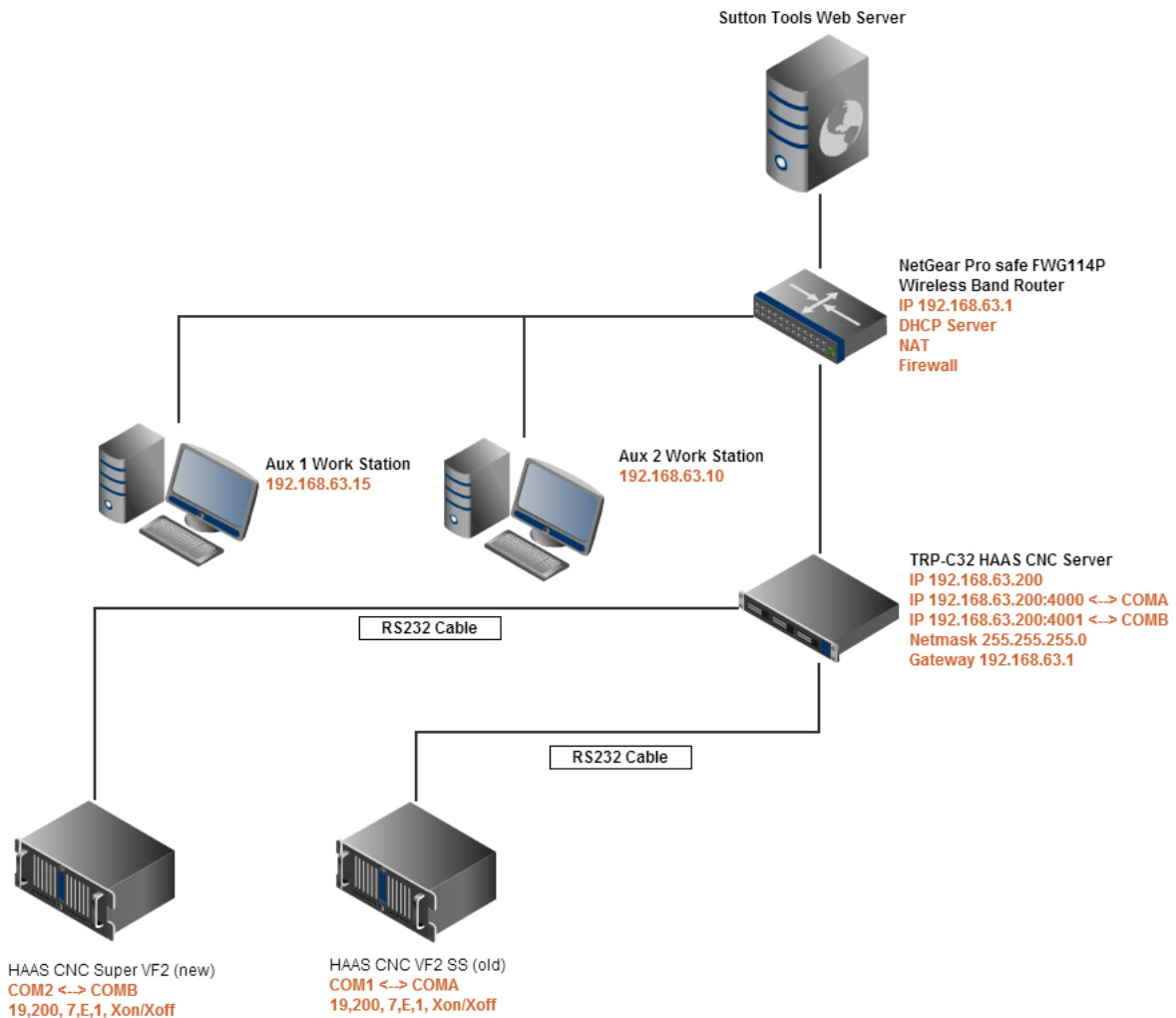


Figure A.1. Schematic showing the network configuration for Ethernet to serial communication between PC's and CNC's for cutting tool testing.



## **Appendix B - Designing an Automated Drill Test and DAQ System for Spindle Current Collection**

In any commercial industrial environment it is important to maintain and whenever possible improve efficiency. It may also be necessary to improve upon current systems. A situation arose after completion of the drill test, with the following questions being asked, would it be possible to automate this system and can any more information be collected from the drill test. The following sections discuss the design of an automated drill testing system as well the collection of the spindle motor current as a means of calculating the power consumed during metal cutting. This system would be potentially able to stop testing at a predefined limit, change drill and continue testing all the while recording spindle current in order to calculate power consumption during drilling.

### **Automated Drill Testing**

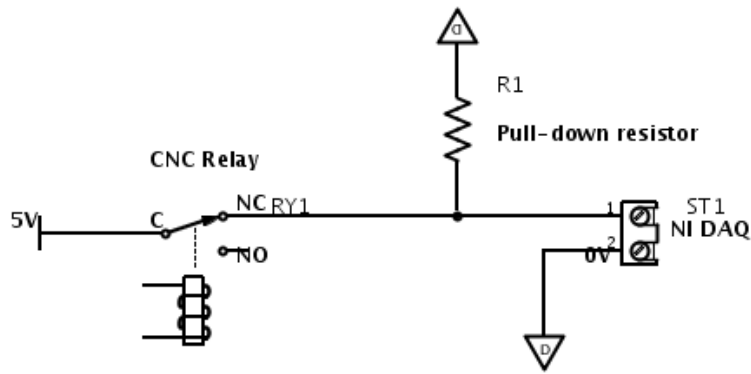
An automated drill test would need to be able to reliably execute the following three steps. Firstly, the system would require knowing when a tool has failed and stop drilling. Secondly, be able to change to the next tool in the tool carousel and record this change. Thirdly, restart the drilling program and continue on with the next hole in the test plate. A secondary goal of this study was to modify the drill test developed in the previous sections and make it an automated system. However, not all three steps were possible in the HAAS VF2. The first step to stop drilling at a predefined limit was possible through the "Tool overload" option designed into the HAAS VF2 CNC. This option allows for a user to define a spindle load limit as a percentage of total spindle output, once this limit is reached the CNC will perform one of the following options, it may trigger an alarm which will stop the axis motors and the spindle motor, turn off the coolant and disable servos. The CNC may also perform a "feed hold" action which stops the feed motor and alerts the operator with a message on the screen, the spindle motor is still running using this option. Lastly the CNC may simply beep with a message on the screen and continue drilling. The "tool overload" option was tested and found to be adequate in stopping drilling at the point of failure. The second step needed to transform the drill test to an automated system is the tool change. This step was found to be outside the capability of the HAAS VF2 for the following reasons. To accomplish a tool change while using a programme an operator must first either be in Manual Data Input (MDI) mode and input the correct command or press the tool change up/down button found on the interface while in MDI mode, the CNC must not be running a programme for this action to take place, if for example a "tool overload" alarm occurred the operator must first "RESET" the CNC before any further action may take place. Secondly, the tool number must be updated inside the program; if the tool number has not been updated once the program begins again the CNC will change the tool to whatever tool number has been programmed this of course being the failed tool. The third step was taken care of in the initial program design by using global variables to count the hole number and

group number on the plate, nevertheless without a solution to step two the automated drill test would not be possible in a HAAS VF2. The important reason why an operator cannot change a tool during a program is for safety, a "RESET" must first be initialised to stop all motors and servos. The reason why the manufactures of the HAAS VMC implement this safety feature, is due to the fact that the VMC is designed to do more machining operations than just drilling. For example if a tap fails during a hole and the feed and spindle motors stop, then the tap is rapidly withdrawn from the hole, it will damage to the machined part.

## **DAQ System for Spindle Current Collection**

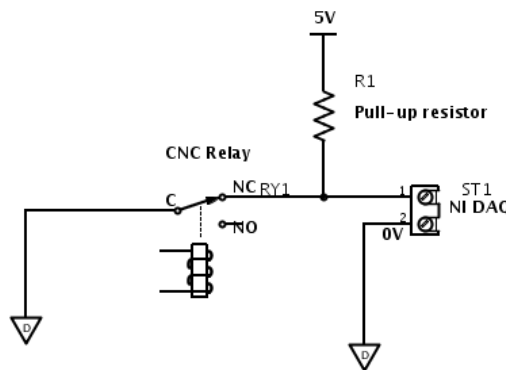
A DAQ system to collect spindle current for the calculation of power consumed during drilling was also a goal of this study. A National Instruments USB-6008 DAQ device would be connected to the spindle motor controller which is an inverter drive. The inverter drive generates an adjustable voltage/frequency three phase output for complete cutting speed or rpm control, by adjusting the frequency of the signal it allows the control of the voltage across the spindle motor and is why inverter drives are termed variable-frequency drives. The inverter drive provides a 0-10Vdc signal which is proportional to either output frequency, output current, output voltage reference or output power between terminals 21 & 22 inside the inverter. Why this is a useful signal to measure has already been stated the ability to calculate the power consumed during drilling, but it also allows analysis of tool wear across the tool life due to the feedback loop that the inverter uses to maintain a particular rpm. During a drill test or normal cutting operations the cutting edges and outer corners will wear, consequently the power needed to cut at a particular cutting speed will need to be increased, forcing the inverter drive to supply a higher current output to maintain the desired rpm. Taking advantage of this fact allows the tool wear and life to be examined as a change in spindle current.

Spindle current collection can be triggered while a drill test program is running. a digital signal may be used to trigger the DAQ to stop and start acquisition according to the physical state of a relay on the HAAS CNC controller board, the relays used on the CNC are Single Pole Double Throw (SPDT) 120V 1A. To ensure that the logic state signal connected to the DAQ is steady, a pull-up or a pull down resistor set-up will be arranged in the circuit as can be seen below. Pull-up/down resistors are used in electronic logic circuits to ensure that the signal inputs to logic devices settle at their desired levels, in this case either at 0 or 5 volts. A pull-up resistor will pull the voltage towards its voltage source, while a pull down resistor, which is connected to ground, will pull down the voltage to zero.



Pull-down orientation	Logic state	Voltage
Switch closed	1	5
Switch open	0	0

Figure B.1. Circuit diagram showing a pull-down resistor setup with a table explaining the logic states and voltage levels.



Pull-up orientation	Logic state	Voltage
Switch closed	0	0
Switch open	1	5

Figure B.2. Circuit diagram showing a pull-up resistor setup with a table explaining the logic states and voltage levels.

Switch bouncing is a problem found in circuitry designed to alter the state of a digital signal, high or low. Physically, the problem is that the contacts within a switch do not make contact cleanly but slightly bounce which may cause the signal to trigger a number of times. Below is a signal trace demonstrating this phenomenon. There are many solutions that deal with switch bouncing, for example, de-bouncing circuits, software de-bouncing and integrated de-bouncing chips. Below is an example of a de-bouncing circuit. While the switch is open the capacitor will charge via resistor 1 and diode 1, once the capacitor has charged the point of  $V_b$  will reach within 0.7V of VCC and the Schmitt trigger will be at a logic state of 0.

When the switch is closed the capacitor will discharge via resistor 2 and eventually the point at  $V_b$  will reach 0V therefore the Schmitt trigger will be at a logic state of 1. A Schmitt trigger retains its logic state until the voltage input sufficiently changes, when the input is higher than a certain chosen threshold, the output is high; when the input is below a chosen threshold, the output is low; when the input is between the two, the output retains its state. The Schmitt trigger allows for the voltage to rise and drop during the switch bouncing without altering the logic state of the signal.

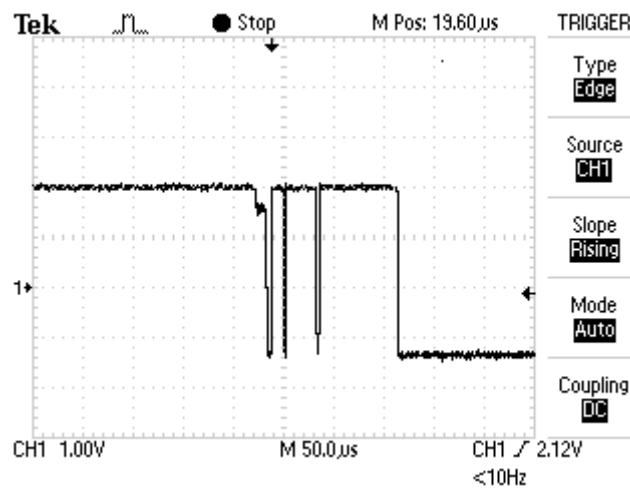


Figure B.3. Signal trace showing the effect of a switch bouncing.  
<http://www.labbookpages.co.uk/>

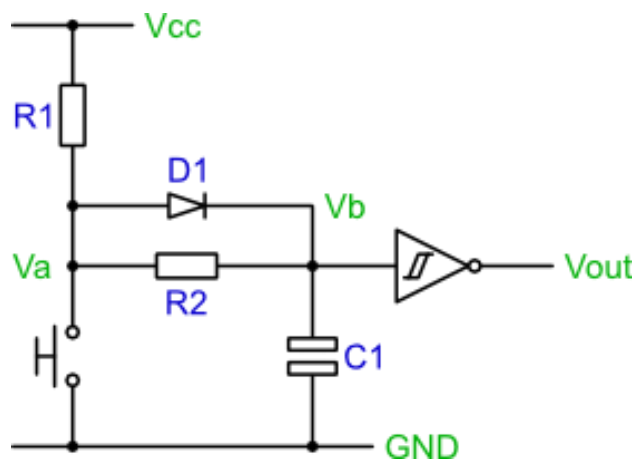
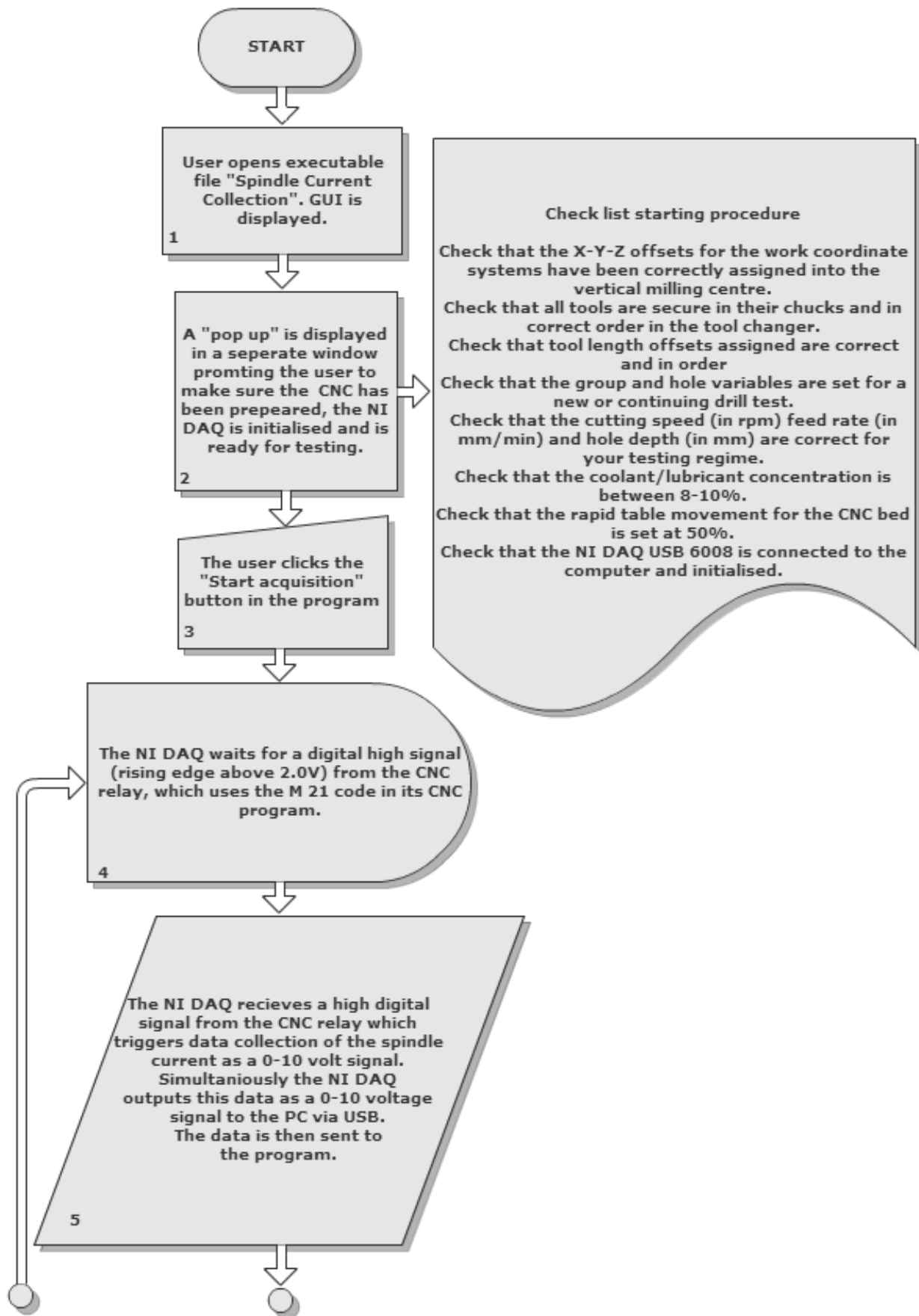


Figure B.4. Circuit diagram showing a de-bouncing circuit. <http://www.labbookpages.co.uk/>

A flow chart was created for the spindle current collection system so as to understand the steps required. This flowchart covers the steps involved from the data acquisition perspective, not the CNC drill testing.



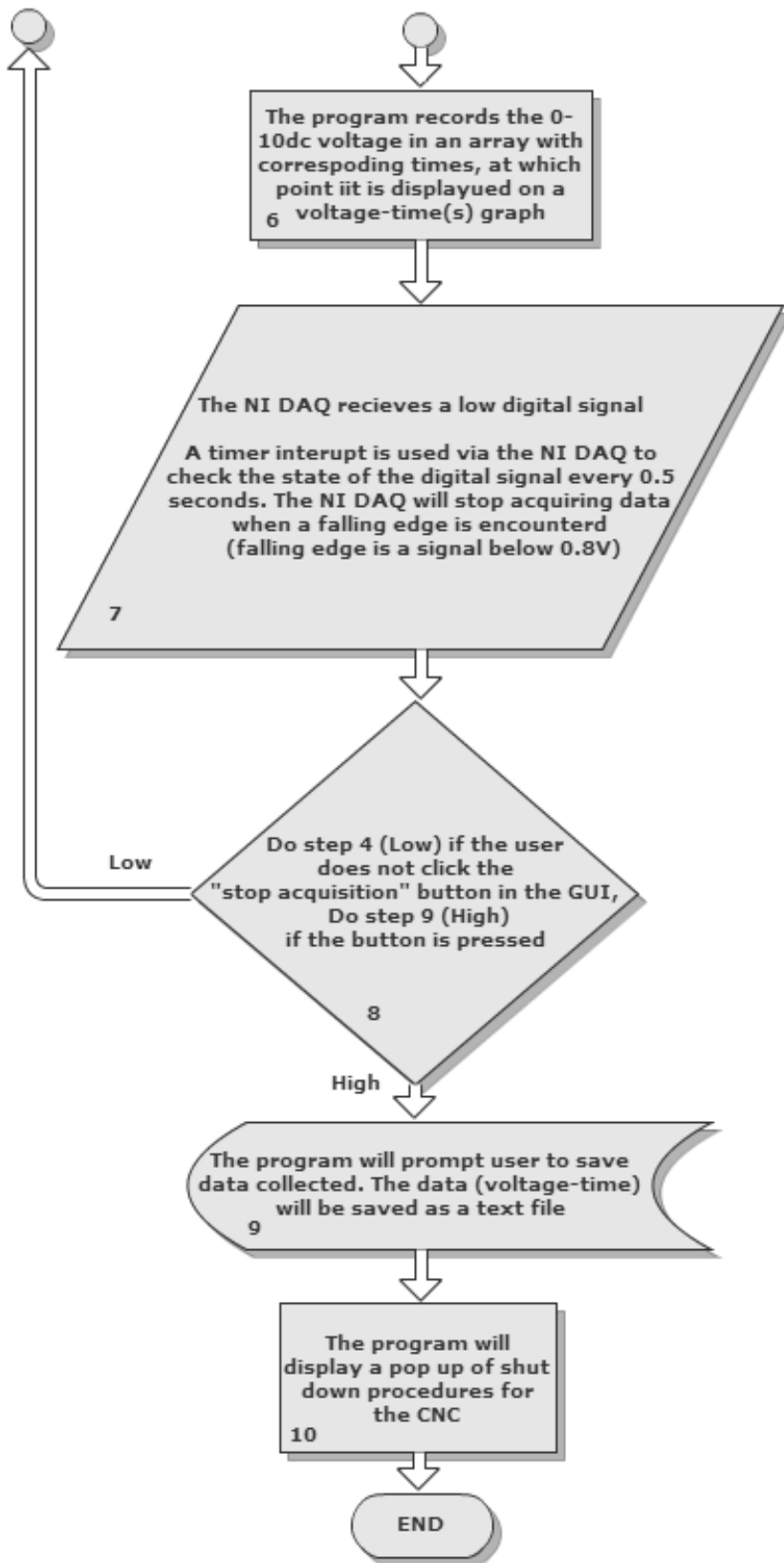


Figure 0.5. Flowchart showing step one to five in the data acquisition system for spindle current collection.

## Appendix C – Chapter 3.2 Data

### D2 and P20 workpiece hardness

D2 Plate Hardness (HV)	P20 Plate Hardness (HV)	D2 Plate Hardness (HLD)	P20 Plate Hardness (HLD)
217	291	467	564
220	240	471	560
220	288	471	561
217	293	467	565
219	286	470	559
217	284	467	556
220	285	471	557
223	287	474	560
221	285	473	557
221	282	473	554
222	288	474	561
221	291	473	564
219	301	470	573
220	286	471	559
219	293	470	565
220	291	471	564
219	291	470	564
221	292	473	565
225	283	476	555
213	276	463	549
211	280	461	552
217	283	467	555
221	288	473	561
223	280	474	552
223	291	474	564
219	283	470	555
210	287	460	560
217	288	467	561

### R40 Drill Hardness and Tool Life

<b>Tool Life No. of 2.5xD Holes in P20 HV<sub>30</sub>760</b>	<b>Drill Hardness Average HV<sub>30</sub></b>	<b>Tool Life No. of 2.5xD Holes in P20 HV<sub>30</sub>860</b>	<b>Drill Hardness Average HV<sub>30v</sub></b>
100	778	6	857
303	780	304	869
39	750	745	871
47	755	1114	874
160	755	15	855
93	759	261	867
66	756	13	852
318	762	7	861
363	755	9	869
98	767	4	851

<b>Tool Life No. of 2.5xD Holes in D2 HV<sub>30</sub>760</b>	<b>Drill Hardness Average HV<sub>30</sub></b>	<b>Tool Life No. of 2.5xD Holes in D2 HV<sub>30</sub>860</b>	<b>Drill Hardness Average HV<sub>30</sub></b>
154	773	158	878
105	744	163	865
208	761	188	861
160	761	126	863
180	767	290	866
70	742	83	864
75	767	104	865
99	761	153	867
120	763	191	872
168	751	383	863



## Appendix D – Chapter 3.3 Data

### Jobber Drill Measurements

Drill No.	Chisel Angle (°)	Chisel Angle (°)	Point Centrality (µm)	Primary Lip relief (°)	Point Angle (°)
Measurement device	Mowhawk	Mowhawk	Mowhawk	Mowhawk	Mowhawk
1	127	37	94.5	13	122
2	129	39	67.5	13	122
3	128	38	121.5	10	122
4	129	39	94.5	11	120
5	128	38	121.5	13	120
6	117	27	27.0	14	118
7	119	29	40.5	12	120
8	127	37	81.0	16	122
9	119	29	94.5	14	120
10	122	32	54.0	14	120
11	118	28	81.0	14	122
12	122	32	40.5	14	120
13	120	30	27.0	13	120
14	122	32	13.5	12	120
15	121	31	0.0	13	122
16	121	31	40.5	12	120
17	122	32	0.0	13	122
18	128	38	81.0	13	120
19	128	38	94.5	14	122
20	129	39	148.5	13	122
21	122	32	40.5	14	120
22	127	37	81.0	13	122
23	121	31	40.5	14	120
24	129	39	81.0	13	122
25	128	38	94.5	14	122
26	129	39	121.5	13	120
27	124	34	54.0	13	120
28	120	30	0.0	12	120
29	120	30	0.0	13	118
30	127	37	108.0	14	122
31	128	38	108.0	15	122
32	128	38	67.5	13	122
33	120	30	81.0	14	120
34	127	37	135.0	14	120
35	121	31	40.5	12	120
36	128	38	94.5	14	120
37	126	36	94.5	13	122
38	121	31	67.5	15	120
39	128	38	67.5	14	122

40	129	39	67.5	14	122
41	124	33.5	21.0	9	122
42	127	37.4	195.0	12.5	120
43	119	29.45	92.0	11.5	120
44	127	37.1	157.0	13	122
45	127	37.1	19.0	12	119
46	129	39.1	101.0	13	122
47	126	36.3	60.0	13	121
48	128	38.4	90.0	14.5	122
49	122	32	119.0	14	121
50	128	38.1	66.0	15	122
51	128	38	92.0	13.5	122
52	128	38.3	5.0	13.5	122

<b>Drill No.</b>	<b>Web thickness (mm)</b>	<b>Helix Angle 1 (°)</b>	<b>Helical Angle 2 (°)</b>	<b>Mean Helical Angle (°)</b>
Measurement device	Pin micrometre	Euro-Tech	Euro-Tech	Euro-Tech
1	1.02	31.75	31.47	31.61
2	1.01	31.30	31.49	31.40
3	0.99	31.51	31.51	31.51
4	1.02	31.50	31.55	31.53
5	1.00	31.66	31.70	31.68
6	0.99	31.92	31.85	31.89
7	0.96	31.71	31.27	31.49
8	1.01	31.47	31.77	31.62
9	1.00	31.92	31.69	31.81
10	0.98	31.86	31.40	31.63
11	1.03	31.45	31.65	31.55
12	1.01	31.17	31.58	31.38
13	0.99	31.35	31.46	31.41
14	1.02	31.48	31.16	31.32
15	1.04	31.10	30.97	31.04
16	0.99	31.67	31.26	31.47
17	0.97	31.35	31.61	31.48
18	1.01	31.24	30.74	30.99
19	0.98	31.43	31.50	31.47
20	1.00	31.28	31.43	31.36
21	0.98	31.29	31.64	31.47
22	0.99	31.52	31.31	31.42
23	1.01	31.66	31.39	31.53
24	1.00	31.50	31.44	31.47
25	1.01	31.32	31.69	31.51
26	0.98	32.24	31.77	32.01
27	1.01	31.55	31.47	31.51
28	1.02	31.31	31.58	31.45

29	1.02	31.31	31.85	31.58
30	1.06	31.93	32.12	32.03
31	1.02	31.53	32.37	31.95
32	0.99	32.01	32.30	32.16
33	1.02	31.94	31.74	31.84
34	1.04	32.03	31.04	31.54
35	1.00	31.57	31.69	31.63
36	1.00	31.14	31.50	31.32
37	0.98	31.48	31.82	31.65
38	1.00	31.44	31.15	31.30
39	1.00	31.62	31.31	31.47
40	1.01	31.75	31.60	31.68
41	1.03	31.75	30.92	31.34
42	1.06	33.00	31.25	32.13
43	1.11	30.96	31.77	31.37
44	1.04	32.23	32.47	32.35
45	0.98	32.74	32.04	32.39
46	1.11	31.74	33.40	32.57
47	1.09	33.72	32.22	32.97
48	1.10	32.49	32.74	32.62
49	1.07	31.23	33.29	32.26
50	1.08	33.18	31.26	32.22
51	1.04	32.11	31.72	31.92
52	1.06	32.07	31.91	31.99

<b>Drill No.</b>	<b>Margin Width 1 (mm)</b>	<b>Margin Width 2 (mm)</b>	<b>Mean Margin Width (mm)</b>	<b>Relative Lip Height (µm)</b>
Measurement Device	Euro-Tech	Euro-Tech	Euro-Tech	Euro-Tech
1	0.577	0.597	0.587	62
2	0.482	0.563	0.523	22
3	0.561	0.578	0.569	35
4	0.591	0.547	0.569	53
5	0.530	0.505	0.517	56
6	0.486	0.531	0.509	20
7	0.459	0.476	0.467	13
8	0.600	0.563	0.581	38
9	0.543	0.522	0.533	21
10	0.442	0.520	0.481	49
11	0.592	0.574	0.583	48
12	0.533	0.487	0.510	52
13	0.507	0.457	0.482	13
14	0.497	0.481	0.489	28
15	0.587	0.544	0.565	51
16	0.503	0.477	0.490	61
17	0.571	0.452	0.511	7

18	0.578	0.488	0.533	39
19	0.517	0.470	0.493	37
20	0.472	0.541	0.507	61
21	0.455	0.517	0.486	36
22	0.478	0.522	0.500	56
23	0.504	0.531	0.517	41
24	0.536	0.592	0.564	50
25	0.590	0.553	0.572	34
26	0.528	0.480	0.504	49
27	0.471	0.527	0.499	30
28	0.605	0.523	0.564	11
29	0.530	0.504	0.517	14
30	0.608	0.551	0.580	59
31	0.554	0.482	0.518	50
32	0.523	0.494	0.508	57
33	0.492	0.536	0.514	19
34	0.622	0.563	0.592	49
35	0.488	0.540	0.514	35
36	0.618	0.557	0.587	60
37	0.509	0.479	0.494	27
38	0.483	0.547	0.515	38
39	0.473	0.523	0.498	58
40	0.548	0.606	0.577	47
41	0.524	0.540	0.532	13
42	0.669	0.562	0.616	125
43	0.591	0.639	0.615	66
44	0.573	0.699	0.636	110
45	0.746	0.770	0.758	33
46	0.653	0.680	0.667	133
47	0.666	0.563	0.615	59
48	0.659	0.602	0.631	40
49	0.625	0.571	0.598	38
50	0.586	0.601	0.594	84
51	0.683	0.576	0.630	20
52	0.697	0.718	0.708	14

## D2 Workpiece Hardness Measurements

Leeb D measurements

x(cm)	y(cm)	M 1 (HLD)	M2 (HLD)	M 3 (HLD)	M4 (HLD)	Average M (HLD)
4.5	5	428	436	435	442	435
4.5	10	435	435	436	437	436
4.5	15	434	435	436	439	436
4.5	20	430	433	442	437	436
4.5	25	429	426	439	426	430
4.5	30	428	433	438	434	433
4.5	35	429	426	436	435	432
4.5	40	431	420	441	427	430
9	5	433	440	436	440	437
9	10	441	444	442	441	442
9	15	436	436	440	440	438
9	20	440	444	440	437	440
9	25	438	437	437	439	438
9	30	437	437	441	436	438
9	35	437	441	438	425	435
9	40	441	429	440	431	435
13.5	5	433	446	431	443	438
13.5	10	442	444	443	450	445
13.5	15	443	441	445	446	444
13.5	20	440	442	436	441	440
13.5	25	442	443	439	441	441
13.5	30	438	437	445	436	439
13.5	35	443	443	440	435	440
13.5	40	438	428	443	430	435
18	5	428	440	430	447	436
18	10	444	440	440	445	442
18	15	446	446	447	444	446
18	20	444	442	443	438	442
18	25	440	435	440	439	439
18	30	444	443	442	444	443
18	35	437	445	442	443	442
18	40	430	430	445	435	435
22.5	5	432	442	431	447	438
22.5	10	447	442	443	440	443
22.5	15	446	444	446	440	444
22.5	20	445	443	444	440	443
22.5	25	442	442	443	440	442
22.5	30	445	442	441	444	443
22.5	35	444	445	442	442	443

22.5	40	444	431	440	427	436
27	5	427	440	434	447	437
27	10	441	438	443	446	442
27	15	441	439	447	447	444
27	20	445	443	445	438	443
27	25	445	442	442	438	442
27	30	443	447	441	442	443
27	35	443	437	443	441	441
27	40	442	437	447	431	439
31.5	5	437	444	433	445	440
31.5	10	445	439	442	443	442
31.5	15	445	443	444	437	442
31.5	20	438	440	443	441	441
31.5	25	443	441	441	441	442
31.5	30	441	443	445	442	443
31.5	35	449	444	444	441	445
31.5	40	449	439	440	435	441
36	5	434	445	420	439	435
36	10	446	442	437	440	441
36	15	443	443	435	435	439
36	20	439	442	436	434	438
36	25	440	442	438	435	439
36	30	443	447	441	435	442
36	35	442	441	438	436	439
36	40	446	430	437	428	435

Vickers 30Kg Measurements

<b>x(cm)</b>	<b>y(cm)</b>	<b>M 1 (HV<sub>30</sub>)</b>	<b>M2 (HV<sub>30</sub>)</b>	<b>M 3 (HV<sub>30</sub>)</b>	<b>M4 (HV<sub>30</sub>)</b>	<b>Average (HV<sub>30</sub>)</b>
4.5	5	205	211	205	208	207
4.5	10	207	211	207	200	206
4.5	15	208	207	206	206	207
4.5	20	217	206	207	203	208
4.5	25	208	204	203	207	206
4.5	30	209	208	206	209	208
4.5	35	211	215	210	207	211
4.5	40	210	211	206	207	209
9	5	205	208	207	212	208
9	10	204	206	204	204	205
9	15	207	207	208	207	207
9	20	207	206	209	207	207
9	25	212	212	207	204	209
9	30	208	207	208	211	209

9	35	206	207	208	211	208
9	40	212	207	210	207	209
13.5	5	211	206	209	210	209
13.5	10	207	210	206	208	208
13.5	15	209	207	209	211	209
13.5	20	207	207	208	207	207
13.5	25	208	211	209	211	210
13.5	30	207	207	211	207	208
13.5	35	208	206	208	206	207
13.5	40	207	207	208	207	207
18	5	209	209	212	213	211
18	10	211	209	207	208	209
18	15	214	207	214	215	213
18	20	207	209	212	211	210
18	25	209	212	211	211	211
18	30	209	209	209	209	209
18	35	208	208	208	209	208
18	40	209	208	207	207	208
22.5	5	213	213	207	210	211
22.5	10	208	209	208	214	210
22.5	15	211	209	211	209	210
22.5	20	213	210	210	210	211
22.5	25	210	210	209	208	209
22.5	30	214	210	211	210	211
22.5	35	211	211	211	213	212
22.5	40	214	211	208	213	212
27	5	204	207	208	208	207
27	10	211	207	210	207	209
27	15	210	209	207	209	209
27	20	206	211	207	206	208
27	25	208	206	210	209	208
27	30	211	212	215	210	212
27	35	210	215	212	211	212
27	40	212	211	212	210	211
31.5	5	211	211	209	210	210
31.5	10	210	210	211	211	211
31.5	15	211	211	208	210	210
31.5	20	209	208	207	207	208
31.5	25	207	208	212	208	209
31.5	30	208	211	207	210	209
31.5	35	211	207	209	216	211
31.5	40	212	212	210	211	211
36	5	213	215	214	213	214
36	10	210	214	210	211	211

36	15	211	211	211	211	211
36	20	208	208	207	210	208
36	25	207	207	207	211	208
36	30	208	207	209	207	208
36	35	208	210	208	210	209
36	40	208	208	209	212	209

### Cutting Force measurements

Hole 1

Cutting condition (m/min_mm/rev)	Torque Ncm	pC/Ncm	pC	error ± %	error ± pC	error ± Ncm
30_0.15	264	1.66	438.24	0.01	4.4	2.6
35_0.15	261	1.66	433.26	0.01	4.3	2.6
40_0.15	276	1.66	458.16	0.01	4.6	2.8
30_0.125	243	1.66	403.38	0.01	4.0	2.4
35_0.125	225	1.66	373.5	0.01	3.7	2.3
40_0.125	230	1.66	381.8	0.01	3.8	2.3
30_0.1	196	1.66	325.36	0.01	3.3	2.0
35_0.1	197	1.66	327.02	0.01	3.3	2.0
40_0.1	204	1.66	338.64	0.01	3.4	2.0

Hole 1

Cutting condition (m/min_mm/rev)	Thrust N	pC/N	pC	error ± %	error ± pC	error ± N
30_0.15	1340	3.46	4636.4	0.01	46.4	13.4
35_0.15	1273	3.46	4404.58	0.01	44.0	12.7
40_0.15	1399	3.46	4840.54	0.01	48.4	14.0
30_0.125	1215	3.46	4203.9	0.01	42.0	12.2
35_0.125	1150	3.46	3979	0.01	39.8	11.5
40_0.125	1192	3.46	4124.32	0.01	41.2	11.9
30_0.1	1081	3.46	3740.26	0.01	37.4	10.8
35_0.1	1048	3.46	3626.08	0.01	36.3	10.5
40_0.1	1061	3.46	3671.06	0.01	36.7	10.6

Point of steady state

Cutting condition (m/min_mm/rev)	Torque Ncm	pC/Ncm	pC	error ± %	error ± pC	error ± Ncm
30_0.15	286	1.66	474.76	0.01	4.7	2.9
35_0.15	282	1.66	468.12	0.01	4.7	2.8
40_0.15	288	1.66	478.08	0.01	4.8	2.9
30_0.125	263	1.66	436.58	0.01	4.4	2.6
35_0.125	249	1.66	413.34	0.01	4.1	2.5
40_0.125	252	1.66	418.32	0.01	4.2	2.5
30_0.1	217	1.66	360.22	0.01	3.6	2.2



35_0.1	217	1.66	360.22	0.01	3.6	2.2
40_0.1	211	1.66	350.26	0.01	3.5	2.1

Point of steady state

Cutting condition (m/min_mm/rev)	Thrust N	pC/N	pC	error ± %	error ± pC	error ± N
30_0.15	1488	3.46	5148.48	0.01	51.5	14.9
35_0.15	1469	3.46	5082.74	0.01	50.8	14.7
40_0.15	1665	3.46	5760.9	0.01	57.6	16.7
30_0.125	1349	3.46	4667.54	0.01	46.7	13.5
35_0.125	1307	3.46	4522.22	0.01	45.2	13.1
40_0.125	1438	3.46	4975.48	0.01	49.8	14.4
30_0.1	1190	3.46	4117.4	0.01	41.2	11.9
35_0.1	1211	3.46	4190.06	0.01	41.9	12.1
40_0.1	1234	3.46	4269.64	0.01	42.7	12.3

Hole 20

Cutting condition (m/min_mm/rev)	Torque Ncm	pC/N	pC	error ± %	error ± pC	error ± Ncm
30_0.15	305	1.66	506.3	0.01	5.1	3.1
35_0.15	294	1.66	488.04	0.01	4.9	2.9
40_0.15	298	1.66	494.68	0.01	4.9	3.0
30_0.125	266	1.66	441.56	0.01	4.4	2.7
35_0.125	258	1.66	428.28	0.01	4.3	2.6
40_0.125	262	1.66	434.92	0.01	4.3	2.6
30_0.1	224	1.66	371.84	0.01	3.7	2.2
35_0.1	225	1.66	373.5	0.01	3.7	2.3
40_0.1	231	1.66	383.46	0.01	3.8	2.3

Hole 20

Cutting condition (m/min_mm/rev)	Thrust N	pC/N	pC	error ± %	error ± pC	error ± N
30_0.15	1624	3.46	5619.04	0.01	56.2	16.2
35_0.15	1625	3.46	5622.5	0.01	56.2	16.3
40_0.15	1870	3.46	6470.2	0.01	64.7	18.7
30_0.125	1437	3.46	4972.02	0.01	49.7	14.4
35_0.125	1408	3.46	4871.68	0.01	48.7	14.1
40_0.125	1556	3.46	5383.76	0.01	53.8	15.6
30_0.1	1226	3.46	4241.96	0.01	42.4	12.3
35_0.1	1268	3.46	4387.28	0.01	43.9	12.7
40_0.1	1389	3.46	4805.94	0.01	48.1	13.9

## Appendix E – Chapter 3.4 Data & Results

### Surface roughness data outer corner rake face

Lc 800  $\mu\text{m}$

Drill ID	Ra Average roughness (nm)	Rt Max peak to valley height ( $\mu\text{m}$ )	Rz Mean peak to valley height ( $\mu\text{m}$ )	Rp Max peak height ( $\mu\text{m}$ )	Rv Max valley height ( $\mu\text{m}$ )
3_1_1	597.95	5.94	3.98	3.92	2.02
3_1_2	804.77	5.48	4.97	2.59	2.89
3_1_3	693.38	6.17	4.81	3.49	2.68
3_1_4	654.25	4.53	3.95	2.63	1.89
3_1_5	533.91	4.03	3.25	2.05	1.98
3_1_6	379.96	3.59	2.77	1.96	1.63
3_1_7	651.31	4.86	4.10	2.17	2.69
3_1_8	428.05	4.13	3.35	2.61	1.52
3_1_9	493.20	5.53	3.88	2.67	2.86
3_1_10	421.86	4.40	3.09	1.73	2.67
3_1_11	532.93	5.55	3.95	3.24	2.30
3_1_12	540.13	5.39	4.15	2.45	2.93
<b>Average</b>	<b>560.98</b>	<b>4.97</b>	<b>3.85</b>	<b>2.63</b>	<b>2.34</b>
3_2_1	738.68	6.39	5.03	4.17	2.22
3_2_2	678.68	6.05	5.17	3.44	2.61
3_2_3	464.94	6.41	4.24	3.69	2.72
3_2_4	478.39	5.44	3.61	3.42	2.01
3_2_5	634.75	5.42	4.41	2.71	2.70
3_2_6	863.46	10.32	7.23	6.53	3.78
3_2_7	820.48	6.17	5.35	3.58	2.58
3_2_8	657.73	5.00	4.14	2.50	2.50
3_2_9	527.93	5.29	4.38	2.50	2.78
3_2_10	599.81	4.61	3.85	2.66	1.94
3_2_11	670.74	4.51	3.94	2.52	1.98
3_2_12	437.90	4.66	3.66	2.63	2.02
<b>Average</b>	<b>631.12</b>	<b>5.86</b>	<b>4.58</b>	<b>3.36</b>	<b>2.49</b>
3_3_1	545.71	3.98	3.41	1.93	2.03
3_3_2	578.05	4.51	4.25	2.27	2.24
3_3_3	631.26	5.47	4.46	2.19	3.28
3_3_4	712.52	5.54	4.51	2.86	2.67
3_3_5	496.41	4.57	3.69	2.53	2.03

3_3_6	604.82	4.92	4.09	1.92	2.99
3_3_7	704.38	5.07	4.69	2.53	2.54
3_3_8	540.36	4.51	4.15	1.69	2.28
3_3_9	769.81	5.45	4.85	2.55	2.90
3_3_10	588.09	4.81	4.35	2.56	2.25
3_3_11	686.39	5.80	5.28	2.27	3.52
3_3_12	659.51	6.35	4.74	3.43	2.92
<b>Average</b>	<b>626.44</b>	<b>5.08</b>	<b>4.37</b>	<b>2.39</b>	<b>2.64</b>
3_4_1	562.31	6.42	5.10	3.26	3.16
3_4_2	905.57	8.86	6.80	5.98	2.88
3_4_3	719.26	9.30	6.30	5.73	3.57
3_4_4	957.94	8.70	6.86	4.97	3.72
3_4_5	626.41	6.94	5.37	3.97	2.96
3_4_6	742.48	6.97	5.33	3.82	3.15
3_4_7	788.89	10.27	7.04	2.80	4.20
3_4_8	625.02	6.76	5.21	3.45	3.31
3_4_9	607.91	8.66	6.13	5.87	2.78
3_4_10	549.98	5.36	4.24	2.74	2.62
3_4_11	496.70	8.63	5.66	5.95	2.67
3_4_12	667.74	7.62	6.44	3.92	3.69
<b>Average</b>	<b>687.52</b>	<b>7.87</b>	<b>5.87</b>	<b>4.37</b>	<b>3.23</b>

**Surface roughness data on flute 3 diameters away from chisel point**

Lc 800  $\mu\text{m}$

<b>Drill ID</b>	<b>Ra Average roughness (<math>\mu\text{m}</math>)</b>	<b>Rt Max peak to valley height (<math>\mu\text{m}</math>)</b>	<b>Rz Mean peak to valley height (<math>\mu\text{m}</math>)</b>	<b>Rp Max peak height (<math>\mu\text{m}</math>)</b>	<b>Rv Max valley height (<math>\mu\text{m}</math>)</b>
3_1_1	1.5624	9.68	8.39	6.01	3.66
3_1_2	1.7078	14.44	11.95	7.35	7.09
3_1_3	1.5402	12.51	9.96	7.77	4.74
3_1_4	1.8210	11.04	9.43	6.28	4.76
3_1_5	2.2100	11.61	9.97	7.24	4.36
3_1_6	1.8083	13.76	11.44	7.94	5.82
3_1_7	1.4630	10.43	8.58	6.26	4.17
3_1_8	1.6971	12.89	10.51	7.73	5.16
3_1_9	1.7033	14.05	11.93	7.48	6.57
3_1_10	1.6376	11.05	9.42	6.89	4.16

3_1_11	1.8380	11.97	10.03	7.15	4.81
3_1_12	1.9991	12.10	10.54	6.33	5.78
<b>Average</b>	<b>1.7490</b>	<b>12.13</b>	<b>10.18</b>	<b>7.04</b>	<b>5.09</b>
3_2_1	1.4764	10.15	8.51	6.49	3.66
3_2_2	1.7000	9.96	8.82	5.66	4.29
3_2_3	1.5513	9.96	8.25	5.90	4.06
3_2_4	2.0908	11.96	10.22	6.65	5.31
3_2_5	2.0623	12.71	10.46	7.55	5.15
3_2_6	1.7839	13.27	10.49	8.42	4.85
3_2_7	1.4857	10.32	8.82	6.37	3.96
3_2_8	1.9320	14.59	12.76	7.95	6.63
3_2_9	1.7934	10.91	8.84	6.92	3.99
3_2_10	1.6391	11.36	8.85	7.28	4.07
3_2_11	1.6066	11.94	9.93	7.19	4.75
3_2_12	2.0526	12.53	11.21	6.69	5.84
<b>Average</b>	<b>1.7645</b>	<b>11.64</b>	<b>9.76</b>	<b>6.92</b>	<b>4.71</b>
3_3_1	1.4140	11.45	8.95	7.29	4.16
3_3_2	1.8406	12.55	10.80	7.25	5.30
3_3_3	1.7279	13.60	10.96	8.43	5.18
3_3_4	1.8891	12.19	10.89	7.19	4.99
3_3_5	1.5580	12.93	10.27	7.65	5.28
3_3_6	1.7173	12.69	10.99	7.95	4.74
3_3_7	1.4282	10.62	9.19	6.62	4.01
3_3_8	2.0145	16.01	12.69	8.49	7.52
3_3_9	1.6375	12.25	10.65	7.20	5.05
3_3_10	1.6192	11.26	9.69	6.26	4.99
3_3_11	1.7923	9.82	8.79	5.51	4.31
3_3_12	2.0866	12.57	11.04	6.91	5.66
<b>Average</b>	<b>1.7271</b>	<b>12.33</b>	<b>10.41</b>	<b>7.23</b>	<b>5.10</b>
3_4_1	2.1996	14.22	11.95	7.12	7.10
3_4_2	2.0778	12.51	10.90	7.88	4.63
3_4_3	1.8275	12.48	10.22	7.44	5.05
3_4_4	1.9197	11.77	10.13	6.22	5.55
3_4_5	1.7255	11.32	10.06	5.79	5.53
3_4_6	1.9144	13.94	12.72	7.75	6.20
3_4_7	1.5034	9.77	8.01	6.40	3.37
3_4_8	1.3441	9.39	8.01	6.00	3.39
3_4_9	2.2141	15.57	13.46	7.91	7.66
3_4_10	1.6217	12.01	9.68	7.94	4.07

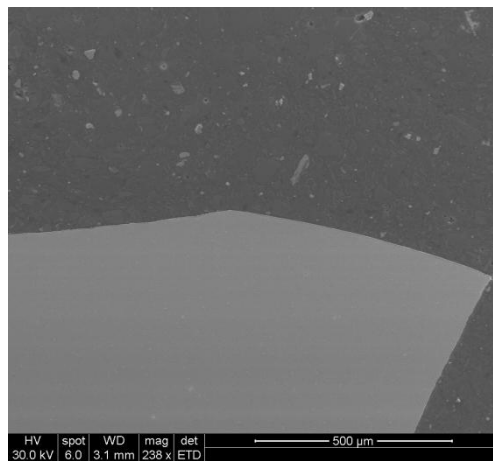
3_4_11	1.6022	10.97	9.79	6.39	4.58
3_4_12	1.5679	12.26	10.21	6.95	5.31
<b>Average</b>	<b>1.7932</b>	<b>12.18</b>	<b>10.43</b>	<b>6.98</b>	<b>5.20</b>

Lc 80  $\mu\text{m}$

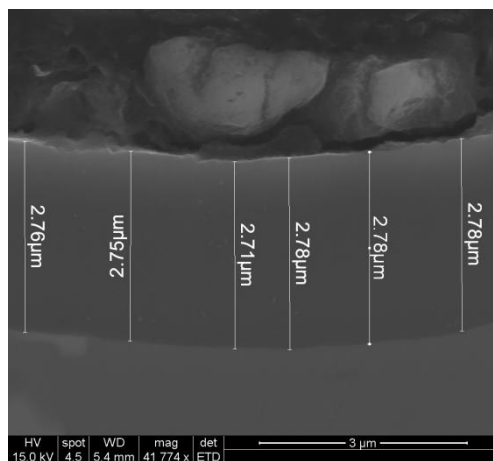
Drill ID	Ra Average roughness (nm)	Rt Max peak to valley height ( $\mu\text{m}$ )	Rz Mean peak to valley height ( $\mu\text{m}$ )	Rp Max peak height ( $\mu\text{m}$ )	Rv Max valley height ( $\mu\text{m}$ )
3_1_1	460.46	4.38	3.52	2.52	1.85
3_1_2	889.40	7.20	6.35	3.34	3.86
3_1_3	591.95	4.70	4.28	2.49	2.21
3_1_4	470.98	4.87	3.62	2.80	2.07
3_1_5	642.00	5.21	3.85	3.02	2.18
3_1_6	645.39	5.45	4.93	2.83	2.62
3_1_7	507.27	4.36	3.67	2.61	1.75
3_1_8	615.28	5.10	4.66	2.89	2.21
3_1_9	746.70	5.92	5.19	2.63	3.29
3_1_10	643.26	6.60	5.11	4.08	2.52
3_1_11	670.56	4.65	4.27	2.31	2.34
3_1_12	857.89	7.41	5.69	4.77	2.64
<b>Average</b>	<b>645.10</b>	<b>5.49</b>	<b>4.59</b>	<b>3.02</b>	<b>2.46</b>
3_2_1	565.62	8.58	4.69	5.22	3.36
3_2_2	532.04	4.76	4.16	2.61	2.15
3_2_3	527.07	4.23	3.82	2.11	2.11
3_2_4	613.39	5.16	4.45	2.78	2.38
3_2_5	600.44	6.89	5.15	5.04	1.85
3_2_6	746.90	6.12	4.87	4.16	1.95
3_2_7	669.09	5.05	4.35	2.99	2.06
3_2_8	1325.30	7.59	6.59	3.70	3.88
3_2_9	505.21	4.73	4.00	2.95	1.78
3_2_10	533.48	5.06	4.01	3.37	1.69
3_2_11	772.54	5.80	4.77	3.25	2.55
3_2_12	860.29	6.66	5.44	4.03	2.63
<b>Average</b>	<b>687.61</b>	<b>5.88</b>	<b>4.69</b>	<b>3.52</b>	<b>2.37</b>
3_3_1	436.90	4.63	3.67	2.65	1.98
3_3_2	736.85	6.19	4.96	3.54	2.65
3_3_3	705.97	5.47	4.65	2.95	2.52

3_3_4	960.79	5.72	5.06	3.49	2.25
3_3_5	566.62	5.66	4.98	2.62	3.04
3_3_6	706.15	5.63	4.90	3.15	2.48
3_3_7	513.89	5.04	4.30	2.89	2.15
3_3_8	1085.80	7.31	6.39	3.62	3.69
3_3_9	846.39	6.51	5.85	3.47	3.04
3_3_10	790.33	5.18	4.55	2.78	2.40
3_3_11	570.91	5.65	4.28	3.10	2.55
3_3_12	939.89	5.59	5.35	2.73	2.86
<b>Average</b>	<b>738.37</b>	<b>5.71</b>	<b>4.91</b>	<b>3.08</b>	<b>2.63</b>
3_4_1	860.52	6.21	5.82	2.62	3.59
3_4_2	764.62	6.23	5.47	4.10	2.13
3_4_3	763.83	6.64	5.16	3.45	3.19
3_4_4	590.24	4.23	3.89	2.59	1.64
3_4_5	757.38	6.76	5.84	3.48	3.27
3_4_6	777.93	6.87	5.54	4.08	2.80
3_4_7	414.28	4.64	3.29	3.05	1.59
3_4_8	484.28	7.39	4.49	5.27	2.13
3_4_9	790.27	7.07	6.17	3.79	3.28
3_4_10	562.45	5.67	4.43	3.41	2.27
3_4_11	806.96	6.97	5.67	4.54	2.43
3_4_12	693.58	5.29	4.78	2.86	2.43
<b>Average</b>	<b>688.86</b>	<b>6.17</b>	<b>5.04</b>	<b>3.60</b>	<b>2.56</b>

## Coating thickness data and results

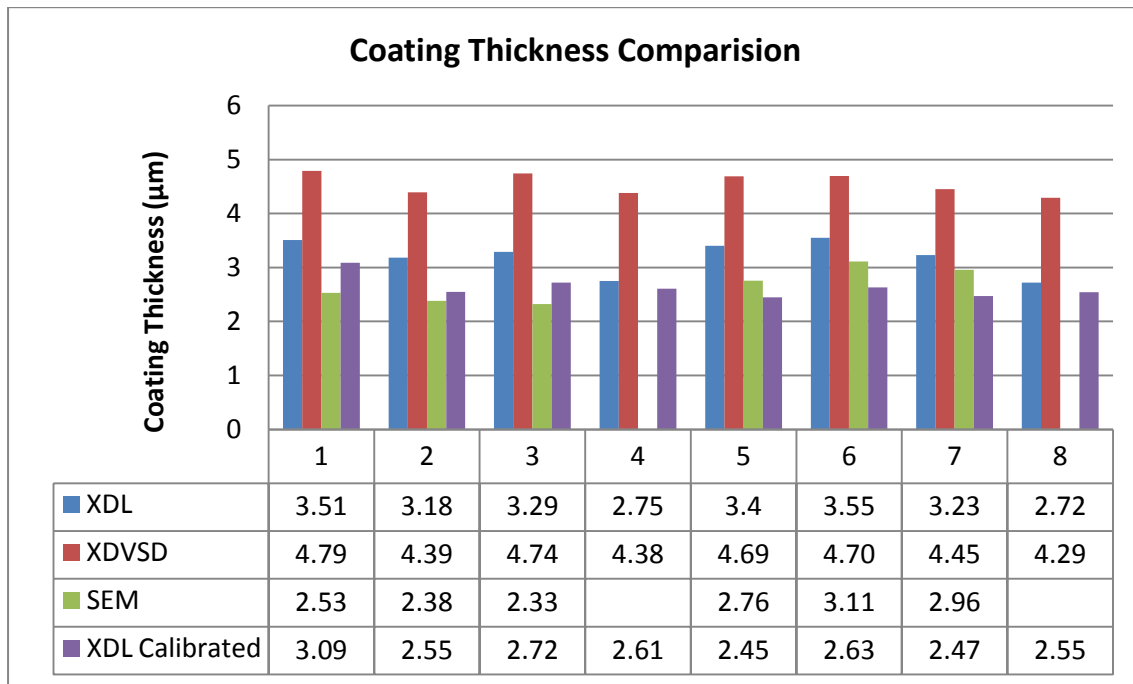


SEM image showing the margin of drill 3.1.11, all coating thickness measurements are taken from this point.



SEM image showing the PVD coating thickness measurements made on drill 3.3.5

The results from the comparative study of XRF detectors show coating thicknesses between  $2.72\mu\text{m}$  and  $3.55\mu\text{m}$ , while coating thicknesses from the XDV-SD were between  $4.29\mu\text{m}$  and  $4.79\mu\text{m}$ , prior to calibration. The coating thickness should be  $3.00\mu\text{m}$ , therefore the initial findings supported the XDL model with the proportional counter. SEM measurements correlated more closely with the XDL model. The samples were then used as calibration pieces and all eight drills were remeasured. Calibrated results laid even closer to the SEM measurements, hence the XDL was chosen to measure all forty eight drills.



Bar chart showing results comparing the XDL and XDVSD X-Ray Fluorescence measuring devices against measured thicknesses via SEM as well as the XDL results after calibrating the device with SEM samples.

### TiN Coating Thickness Measurements via XRF

#### Group 3.1

M1 (µm)	M2 (µm)	M3 (µm)	Average (µm)
3.081	3.062	3.117	3.087
3.021	3.020	3.011	3.017
2.393	2.411	2.382	2.395
2.433	2.490	2.435	2.453
3.190	3.162	3.164	3.172
3.188	3.133	3.147	3.156
2.789	2.561	2.687	2.679
2.837	2.811	2.808	2.819
2.473	2.487	2.504	2.488
2.802	2.799	2.771	2.791
2.796	2.794	2.755	2.782
2.551	2.545	2.545	2.547

#### Group 3.2

M1 (µm)	M2 (µm)	M3 (µm)	Average (µm)
2.784	2.761	2.796	2.780
2.542	2.612	2.575	2.576



2.631	2.423	2.542	2.532
2.776	2.773	2.749	2.766
3.119	2.480	2.590	2.730
3.122	2.640	2.750	2.837
2.715	2.634	2.875	2.741
2.798	2.799	2.780	2.792
3.114	3.069	3.106	3.096
2.791	2.834	2.852	2.826
2.593	2.619	2.612	2.608
2.726	2.720	2.734	2.727

Group 3.3

M1 (μm)	M2 (μm)	M3 (μm)	Average (μm)
2.485	2.486	2.523	2.498
2.700	2.669	2.613	2.661
2.624	2.655	2.670	2.650
2.654	2.660	2.669	2.661
2.452	2.413	2.471	2.445
2.618	2.565	2.580	2.588
2.676	2.694	2.658	2.676
2.559	2.580	2.555	2.565
2.541	2.469	2.488	2.499
2.621	2.631	2.641	2.631
2.570	2.601	2.591	2.587
2.518	2.538	2.500	2.519

Group 3.4

M1 (μm)	M2 (μm)	M3 (μm)	Average (μm)
2.545	2.519	2.566	2.543
2.594	2.608	2.691	2.633
2.576	2.579	2.487	2.545
2.723	2.765	2.745	2.744
2.722	2.628	2.630	2.660
2.613	2.539	2.559	2.570
2.695	2.642	2.669	2.669
2.506	2.405	2.383	2.431
2.459	2.617	2.562	2.546
2.456	2.492	2.467	2.472
2.545	2.616	2.566	2.576
2.431	2.503	2.478	2.471

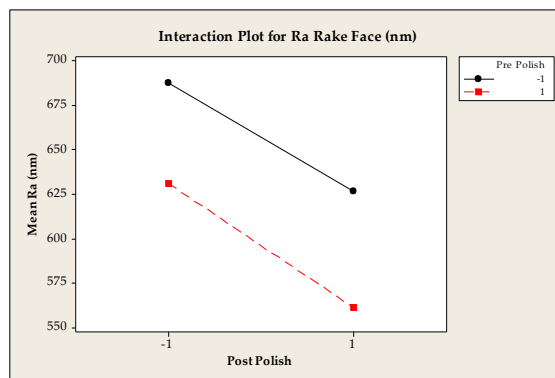
### Tool Life Data

Drill ID	Cutting parameters speed m/min feed mm/rev	No. of 2.5xD holes
3_1_1	45_0.125	
3_1_2	45_0.125	50
3_1_3	45_0.125	40
3_1_4	45_0.125	38
3_1_5	45_0.125	64
3_1_6	45_0.125	67
3_1_7	35_0.125	142
3_1_8	35_0.125	104
3_1_9	35_0.125	86
3_1_10	35_0.125	103
3_1_11	45_0.125	48
3_1_12	35_0.125	143
3_2_1	45_0.125	
3_2_2	45_0.125	60
3_2_3	45_0.125	59
3_2_4	45_0.125	43
3_2_5	45_0.125	67
3_2_6	45_0.125	50
3_2_7	35_0.125	146
3_2_8	35_0.125	127
3_2_9	35_0.125	152
3_2_10	35_0.125	122
3_2_11	45_0.125	40
3_2_12	35_0.125	129
3_3_1	45_0.125	
3_3_2	45_0.125	38
3_3_3	45_0.125	45
3_3_4	45_0.125	39
3_3_5	45_0.125	30
3_3_6	45_0.125	35
3_3_7	35_0.125	87
3_3_8	35_0.125	110
3_3_9	35_0.125	102
3_3_10	35_0.125	100
3_3_11	45_0.125	41
3_3_12	35_0.125	130
3_4_1	45_0.125	
3_4_2	45_0.125	40

3_4_3	45_0.125	33
3_4_4	45_0.125	50
3_4_5	45_0.125	45
3_4_6	45_0.125	41
3_4_7	35_0.125	100
3_4_8	35_0.125	106
3_4_9	35_0.125	95
3_4_10	35_0.125	104
3_4_11	45_0.125	36
3_4_12	35_0.125	110

### Surface Roughness Analysis Statistical Results: ANOVA tables, Interactions plots

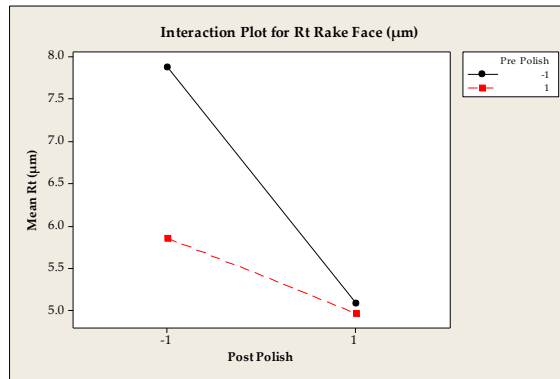
#### Analysis of surface data measured on the rake face at the outer corner



Interaction plot showing the effect of pre and post drag polishing on the mean value for the Ra average height of the profiles measured on the rake face adjacent to the cutting edge.

ANOVA results for the Ra average height of primary profile measured on the rake face adjacent to the cutting edge.

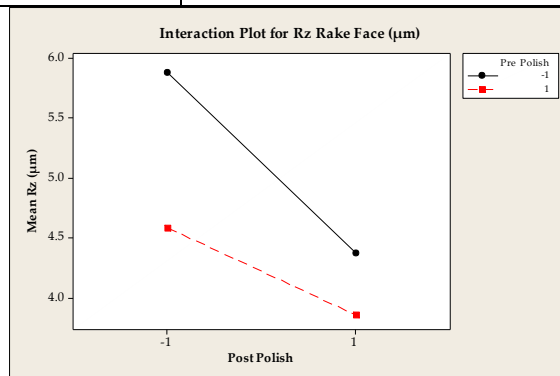
Rake Face Outer Corner Ra Lc 800µm						
	DF	Seq SS	Adj SS	Adj MS	F-Value	P-Value
<b>Main Effects</b>	2	96210	96210	48104.8	3.15	0.053
<b>Pre Polish</b>	1	44550	44550	44550.2	2.92	0.095
<b>Post Polish</b>	1	51659	51659	51659.3	3.38	0.073
<b>2 Way Interactions</b>	1	247	247	247	0.02	0.899
<b>Pre Polish +Post Polish</b>	1	247	247	247	0.02	0.899
<b>Residual error</b>	44	671615	671615	15264		
<b>Pure error</b>	44	671615	671615	15264		
<b>Total</b>	47	768071				



Interaction plot showing the effect of pre and post drag polishing on the mean value for the Rt maximum peak to valley height of the profiles measured on the rake face adjacent to the cutting edge.

ANOVA results for the Rt maximum peak to valley height of primary profile measured on the rake face adjacent to the cutting edge.

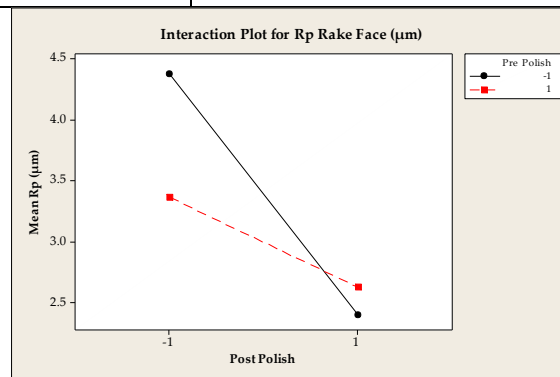
Rake Face Outer Corner Rt Lc 800µm						
	DF	Seq SS	Adj SS	Adj MS	F-Value	P-Value
<b>Main Effects</b>	2	54.32	54.32	27.16	19.51	0.000
<b>Pre Polish</b>	1	13.65	13.65	13.65	9.81	0.003
<b>Post Polish</b>	1	40.66	40.66	40.66	29.21	0.000
<b>2 Way Interactions</b>	1	10.87	10.87	10.87	7.81	0.008
<b>Pre Polish +Post Polish</b>	1	10.87	10.87	10.87	7.81	0.008
<b>Residual error</b>	44	61.26	61.26	1.39		
<b>Pure error</b>	44	61.26	61.26	1.39		
<b>Total</b>	47	126.44				



Interaction plot showing the effect of pre and post drag polishing on the mean value for the Rz mean peak to valley height of the profiles measured on the rake face adjacent to the cutting edge.

ANOVA results for the Rz mean peak to valley height of primary profile measured on the rake face adjacent to the cutting edge.

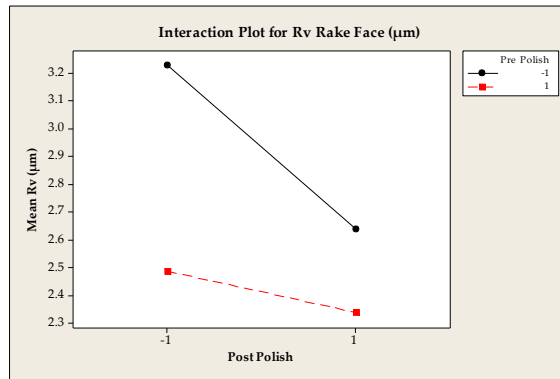
Rake Face Outer Corner Rz Lc 800 $\mu$ m						
	DF	Seq SS	Adj SS	Adj MS	F-Value	P-Value
<b>Main Effects</b>	2	24.73	24.73	12.36	20.22	0.000
<b>Pre Polish</b>	1	9.80	9.80	9.80	16.03	0.000
<b>Post Polish</b>	1	14.93	14.93	14.93	24.41	0.000
<b>2 Way Interactions</b>	1	1.78	1.78	1.78	2.91	0.095
<b>Pre Polish +Post Polish</b>	1	1.78	1.78	1.78	2.91	0.095
<b>Residual error</b>	44	26.91	26.91	0.61		
<b>Pure error</b>	44	26.91	26.91	0.61		
<b>Total</b>	47	53.42				



Interaction plot showing the effect of pre and post drag polishing on the mean value for the Rp maximum peak height of the profiles measured on the rake face adjacent to the cutting edge.

ANOVA results for the Rp maximum peak height of primary profile measured on the rake face adjacent to the cutting edge.

Rake Face Outer Corner Rp Lc 800 $\mu$ m						
	DF	Seq SS	Adj SS	Adj MS	F-Value	P-Value
<b>Main Effects</b>	2	23.91	23.91	11.956	13.52	0.000
<b>Pre Polish</b>	1	1.84	1.81	1.813	2.05	0.159
<b>Post Polish</b>	1	22.1	22.1	22.1	24.98	0.000
<b>2 Way Interactions</b>	1	4.61	4.16	4.619	5.22	0.027
<b>Pre Polish +Post Polish</b>	1	4.61	4.61	4.619	5.22	0.027
<b>Residual error</b>	44	38.92	38.92	0.8846		
<b>Pure error</b>	44	38.92	38.92	0.8846		
<b>Total</b>	47	67.45				

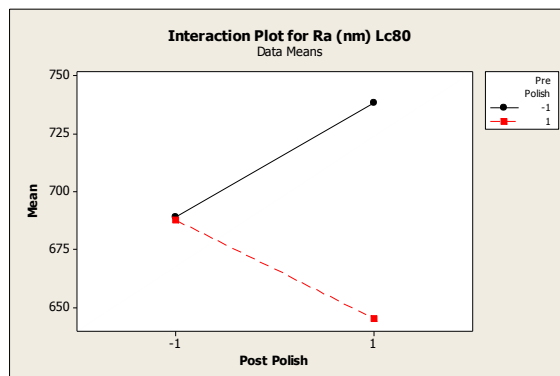


Interaction plot showing the effect of pre and post drag polishing on the mean value for the Rv maximum valley height of the profiles measured on the rake face adjacent to the cutting edge.

ANOVA results for Rv maximum valley height of primary profile measured on the rake face adjacent to the cutting edge.

Rake Face Outer Corner Rv Lc 800µm						
	DF	Seq SS	Adj SS	Adj MS	F-Value	P-Value
<b>Main Effects</b>	2	4.862	4.862	2.431	9.640	0.000
<b>Pre Polish</b>	1	3.234	3.234	3.234	12.830	0.001
<b>Post Polish</b>	1	1.62	1.628	1.62	6.460	0.015
<b>2 Way Interactions</b>	1	0.580	0.580	0.580	2.300	0.136
<b>Pre Polish +Post Polish</b>	1	0.580	0.580	0.580	2.300	0.136
<b>Residual error</b>	44	11.093	11.093	0.252		
<b>Pure error</b>	44	11.093	11.093	0.252		
<b>Total</b>	47	16.536				

Analysis of surface data measured 3 diameters up the flute from the chisel point.

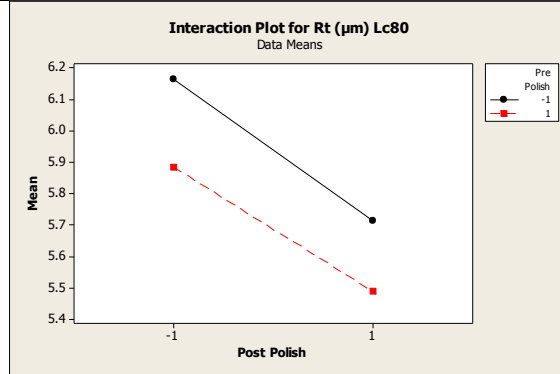


Interaction plot showing the effect of pre and post drag polishing on the mean value for Ra average height of the profiles measured 3 diameters up the flute from the chisel point.

ANOVA results for the Ra average height of primary profile measured 3 diameters up the flute from the chisel point.

Analysis of Variance for Ra (nm) 3xD up flute Lc80

Source	DF	Seq SS	Adj SS	Adj MS	F	P
Main Effects	2	26953	26953	13476.3	0.41	0.664
Pre Polish	1	26806	26806	26805.9	0.82	0.369
Post Polish	1	147	147	146.7	0.00	0.947
2-Way Interactions	1	25409	25409	25409.5	0.78	0.382
Pre Polish*Post Polish	1	25409	25409	25409.5	0.78	0.382
Residual Error	44	1432320	1432320	32552.7		
Pure Error	44	1432320	1432320	32552.7		
Total	47	1484682				

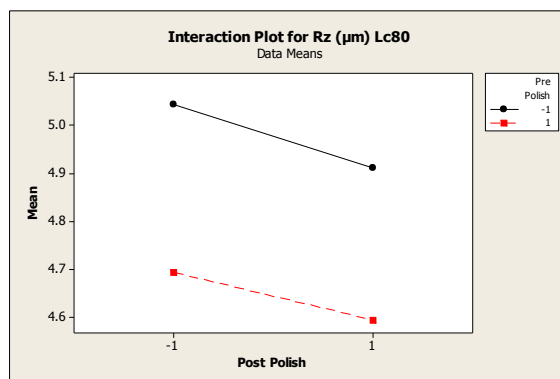


Interaction plot showing the effect of pre and post drag polishing on the mean value for the Rt maximum peak to valley height of the profiles measured 3 diameters up the flute from the chisel point.

ANOVA results for the Rt maximum peak to valley height of primary profile measured 3 diameters up the flute from the chisel point.

Analysis of Variance for Rz (µm) 3xD up flute Lc80

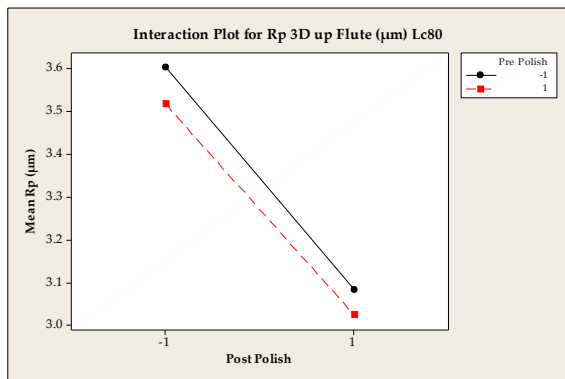
Source	DF	Seq SS	Adj SS	Adj MS	F	P
Main Effects	2	2.9248	2.9248	1.46242	1.34	0.273
Pre Polish	1	0.7693	0.7693	0.76935	0.70	0.406
Post Polish	1	2.1555	2.1555	2.15549	1.97	0.167
2-Way Interactions	1	0.0091	0.0091	0.00909	0.01	0.928
Pre Polish*Post Polish	1	0.0091	0.0091	0.00909	0.01	0.928
Residual Error	44	48.1303	48.1303	1.09387		
Pure Error	44	48.1303	48.1303	1.09387		
Total	47	51.0642				



Interaction plot showing the effect of pre and post drag polishing on the mean value for the Rz mean peak to valley height of the profiles 3 diameters up the flute from the chisel point.

ANOVA results for the Rz mean peak to valley height of primary profile measured 3 diameters up the flute from the chisel point.

Analysis of Variance for Rz ( $\mu\text{m}$ ) 3xD up flute Lc80						
Source	DF	Seq SS	Adj SS	Adj MS	F	P
Main Effects	2	1.5086	1.5086	0.75430	1.12	0.335
Pre Polish	1	1.3471	1.3471	1.34707	2.00	0.164
Post Polish	1	0.1615	0.1615	0.16153	0.24	0.627
2-Way Interactions	1	0.0033	0.0033	0.00332	0.00	0.944
Pre Polish*Post Polish	1	0.0033	0.0033	0.00332	0.00	0.944
Residual Error	44	29.5921	29.5921	0.67255		
Pure Error	44	29.5921	29.5921	0.67255		
Total	47	31.1040				

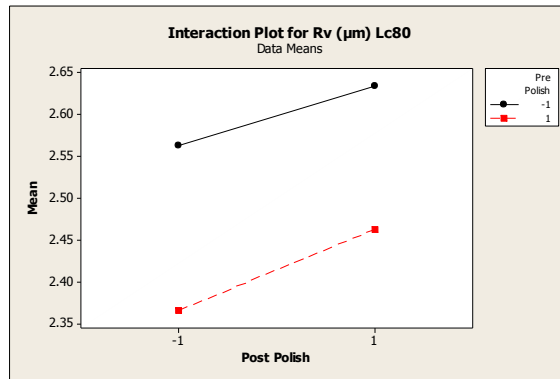


Interaction plot showing the effect of pre and post drag polishing on the mean value for the Rp maximum peak height of the profiles measured 3 diameters up the flute from the chisel point.

ANOVA results for Rp maximum peak height of primary profile measured 3 diameters up the flute from the chisel point.

3xD up Flute Rp Lc 80 $\mu\text{m}$						
	DF	Seq SS	Adj SS	Adj MS	F-Value	P-Value
Main Effects	2	3.1438	3.1438	1.5719	2.85	0.069
Pre Polish	1	0.0606	0.0606	0.0605	0.11	0.742
Post Polish	1	3.0832	3.0832	3.0832	5.58	0.023
2 Way Interactions	1	0.0024	0.0024	0.0024	0.00	0.948
Pre Polish +Post Polish	1	0.0024	0.0024	0.0024	0.00	0.948
Residual error	44	24.2987	24.2987	0.55224		
Pure error	44	24.2987	24.2987	0.55224		
Total	47	27.4449				





Interaction plot showing the effect of pre and post drag polishing on the mean value for the Rv maximum valley height of the profiles measured 3 diameters up the flute from the chisel point.

ANOVA results for Rv maximum valley height of primary profile measured 3 diameters up the flute from the chisel point.

Analysis of Variance for Rv (µm) 3xD up flute Lc80

Source	DF	Seq SS	Adj SS	Adj MS	F	P
Main Effects	2	0.4918	0.4918	0.245924	0.68	0.514
Pre Polish	1	0.4069	0.4069	0.406916	1.12	0.296
Post Polish	1	0.0849	0.0849	0.084933	0.23	0.631
2-Way Interactions	1	0.0021	0.0021	0.002079	0.01	0.940
Pre Polish*Post Polish	1	0.0021	0.0021	0.002079	0.01	0.940
Residual Error	44	16.0004	16.0004	0.363645		
Pure Error	44	16.0004	16.0004	0.363645		
Total	47	16.4943				

## Tool Life Statistical Results: ANOVA and Mood Median Tests

Analysis of Variance for Tool Life No. of 2.5xD Holes 35m/min

Source	DF	Seq SS	Adj SS	Adj MS	F	P
Main Effects	2	2557.8	2557.8	1278.9	4.62	0.026
Pre-Polish	1	2205.0	2205.0	2205.0	7.96	0.012
Post-Polish	1	352.8	352.8	352.8	1.27	0.276
2-Way Interactions	1	627.2	627.2	627.2	2.26	0.152
Pre-Polish*Post-Polish	1	627.2	627.2	627.2	2.26	0.152
Residual Error	16	4432.8	4432.8	277.0		
Pure Error	16	4432.8	4432.8	277.1		
Total	19	7617.8				

Minitab output: ANOVA using raw tool life data (No. of 2.5xD Holes) at 35m/min 0.125mm/rev testing the significance of pre polishing, post polishing and interaction.

Analysis of Variance for Tool Life No. of 2.5xD Holes/Micron 35m/min

Source	DF	Seq SS	Adj SS	Adj MS	F	P
Main Effects	2	200.633	200.633	100.316	3.31	0.062
Pre Polish	1	192.820	192.820	192.820	6.37	0.023
Post Polish	1	7.812	7.812	7.812	0.26	0.618
2-Way Interactions	1	1.104	1.104	1.104	0.04	0.851
Pre Polish*Post Polish	1	1.104	1.104	1.104	0.04	0.851
Residual Error	16	484.248	484.248	30.265		
Pure Error	16	484.248	484.248	30.266		
Total	19	685.985				

Minitab output: ANOVA using Tool life No. of 2.5xD holes/micron data at 35m/min 0.125mm/rev testing the significance of pre polishing, post polishing and interaction.

Analysis of Variance for Tool Life No. of 2.5xD Holes 45m/min

Source	DF	Seq SS	Adj SS	Adj MS	F	P
Main Effects	2	1010.42	1010.42	505.208	6.31	0.008
Pre-Polish	1	975.38	975.38	975.375	12.17	0.002
Post-Polish	1	35.04	35.04	35.042	0.44	0.516
2-Way Interactions	1	1.04	1.04	1.042	0.01	0.910
Pre-Polish*Post-Polish	1	1.04	1.04	1.042	0.01	0.910
Residual Error	20	1602.50	1602.50	80.125		
Pure Error	20	1602.50	1602.50	80.125		
Total	23	2613.96				

Minitab output: ANOVA using raw tool life data (No. of 2.5xD Holes) at 45m/min 0.125mm/rev testing the significance of pre polishing, post polishing and interaction.

Analysis of Variance for Tool Life No. of 2.5xD Holes/Micron 45m/min

Source	DF	Seq SS	Adj SS	Adj MS	F	P
Main Effects	2	101.604	101.604	50.802	6.89	0.005
Pre Polish	1	88.550	88.550	88.550	12.02	0.002
Post Polish	1	13.054	13.054	13.054	1.77	0.198
2-Way Interactions	1	1.654	1.654	1.654	0.22	0.641
Pre Polish*Post Polish	1	1.654	1.654	1.654	0.22	0.641
Residual Error	20	147.392	147.392	7.370		
Pure Error	20	147.392	147.392	7.370		
Total	23	250.650				

Minitab output: ANOVA using Tool life No. of 2.5xD holes/micron data at 45m/min 0.125mm/rev testing the significance of pre polishing, post polishing and interaction.

Mood median test for Tool Life No. of 2.5xD Holes 35m/min Pre Polish  
 Chi-Square = 3.20 DF = 1 P = 0.074

Pre Polish	N<=	N>	Median	Q3-Q1
No	7	3	103.0	11.3
Yes	3	7	128.0	40.0

Individual 95.0% CIs  
 (---\*---)  
 (-----\*-----)

Overall median = 108.0

A 95.0% CI for median(-1) - median( 1): (-43.0,6.0)

Minitab output: Mood median test using raw tool life data (No. of 2.5xD Holes) at 35m/min 0.125mm/rev testing the significance of pre polishing.

Mood median test for Tool Life No. of 2.5xD Holes/Micron 35m/min Pre Polish  
 Chi-Square = 3.20 DF = 1 P = 0.074

Pre Polish	N<=	N>	Median	Q3-Q1
No	7	3	41.5	6.4
Yes	3	7	46.4	11.0

Individual 95.0% CIs  
 (-----\*-----)  
 (-----\*-----)

Overall median = 43.1

A 95.0% CI for median(No) - median(Yes): (-15.5,0.6)

Minitab output: Mood median test using Tool life No. of 2.5xD holes/micron data at 35m/min 0.125mm/rev testing the significance of pre polishing.

Mood median test for Tool Life No. of 2.5xD Holes 35m/min Post Polish  
 Chi-Square = 0.80 DF = 1 P = 0.371

Post-Polish	N<=	N>	Median	Q3-Q1
-1	4	6	116.0	30.3
1	6	4	103.5	36.3

Individual 95.0% CIs  
 (-----\*-----)  
 (-----\*-----)

Overall median = 108.0

A 95.0% CI for median(-1) - median( 1): (-26.0,29.0)

Minitab output: Mood median test using raw tool life data (No. of 2.5xD Holes) at 35m/min 0.125mm/rev testing the significance of post polishing.

Mood median test for Tool Life No. of 2.5xD Holes/Micron 35m/min Post Polish  
 Chi-Square = 3.20 DF = 1 P = 0.074

Post Polish	N<=	N>	Median	Q3-Q1
No	3	7	44.0	6.8
Yes	7	3	41.8	10.2

Individual 95.0% CIs  
 (-----\*-----)  
 (-----\*-----)

Overall median = 43.1

A 95.0% CI for median(No) - median(Yes): (-4.8,9.0)

Minitab output: Mood median test using Tool life No. of 2.5xD holes/micron data at 35m/min 0.125mm/rev testing the significance of post polishing.

Mood median test for Tool Life No. of 2.5xD Holes 45m/min Pre Polish  
 Chi-Square = 6.00 DF = 1 P = 0.014

```

Pre
Polish N<= N> Median Q3-Q1 Individual 95.0% CIs
No 9 3 39.5 8.8 (-----*-----)
Yes 3 9 50.0 22.3 (-----*-----)
-----+-----+-----+-----+
40.0 48.0 56.0 64.0

Overall median = 42.0

A 95.0% CI for median(-1) - median( 1): (-24.0,-2.0)

```

Minitab output: Mood median test using raw tool life data (No. of 2.5xD Holes) at 45m/min 0.125mm/rev testing the significance of pre polishing.

```

Mood median test for Tool Life No. of 2.5xD Holes/Micron 45m/min Pre Polish
Chi-Square = 6.00 DF = 1 P = 0.014

Pre
Polish N<= N> Median Q3-Q1 Individual 95.0% CIs
No 9 3 14.95 3.05 (-----*-----)
Yes 3 9 17.45 7.00 (-----*-----)
-----+-----+-----+-----+
15.0 17.5 20.0 22.5

Overall median = 16.30

A 95.0% CI for median(No) - median(Yes): (-7.20,-0.60)

```

Minitab output from a Mood median test using Tool life No. of 2.5xD holes/micron data at 45m/min 0.125mm/rev testing the significance of pre polishing.

```

Mood median test for Tool Life No. of 2.5xD Holes 45m/min Post Polish
Chi-Square = 0.67 DF = 1 P = 0.414

Post-Polish N<= N> Median Q3-Q1 Individual 95.0% CIs
-1 5 7 44.0 16.8 (-----*-----)
1 7 5 40.5 11.5 (-----*-----)
-----+-----+-----+-----+
42.0 48.0 54.0

Overall median = 42.0

A 95.0% CI for median(-1) - median( 1): (-8.0,12.0)

```

Minitab output: Mood median test using raw tool life data (No. of 2.5xD Holes) at 45m/min 0.125mm/rev testing the significance of post polishing.

```

Mood median test for Tool Life No. of 2.5xD Holes/Micron 45m/min Post Polish
Chi-Square = 0.00 DF = 1 P = 1.000

Post
Polish N<= N> Median Q3-Q1 Individual 95.0% CIs
No 6 6 16.45 6.80 (-----*-----)
Yes 6 6 16.20 2.82 (-----*-----)
-----+-----+-----+-----+
15.0 17.5 20.0 22.5

Overall median = 16.30

A 95.0% CI for median(No) - median(Yes): (-1.70,3.50)

```

Minitab output: Mood median test using Tool life No. of 2.5xD holes/micron data at 45m/min 0.125mm/rev testing the significance of post polishing.

## Appendix F – Chapter 3.5 Data & Results

### Plate Hardness Data

D2 Plate 1 511 (HLD)	D2 Plate 2 492 (HLD)	D2 Plate 3 467 (HLD)
515	493	463
505	493	457
508	496	454
502	493	461
503	491	477
530	493	466
521	492	458
508	486	459
514	492	463
516	488	464
523	496	471
508	486	466
521	488	461
522	490	470
523	488	486
529	489	469
505	491	467
524	492	469
519	494	466
518	491	481
509	493	472
505	508	469
500	492	464
499	491	465
511	491	476
511	493	469
502	494	471
497	498	471
503	495	463
498	498	480

### 2 Sample t-Tests Plate Hardness

Two-sample T for Plate 1 511 HLD vs Plate 2 492 HLD

	N	Mean	StDev	SE Mean
511 HL D	30	511.63	9.60	1.8
492 HL D	30	492.50	4.21	0.77

Difference = mu (511 HL D) - mu (492 HL D)

Estimate for difference: 19.13  
 95% CI for difference: (15.26, 23.00)  
 T-Test of difference = 0 (vs not =): T-Value = 10.00 P-Value = 0.000 DF = 39

Two-sample T for Plate 2 492 HLD vs Plate 3 467 HLD

	N	Mean	StDev	SE Mean
492 HL D	30	492.50	4.21	0.77
467 HL D	30	467.60	7.32	1.3

Difference = mu (492 HL D) - mu (467 HL D)  
 Estimate for difference: 24.90  
 95% CI for difference: (21.80, 28.00)  
 T-Test of difference = 0 (vs not =): T-Value = 16.16 P-Value = 0.000 DF = 46

## Tool Life Data

### D2 Plate 1 511 HLD

Drill No.	Cutting parameters (speed m/min_feed rate mm/rev)	No. of 2.5xD holes at failure	Tool Life Time spent drilling (min)
22	30_0.125	10	0.84
12	30_0.125	11	0.93
19	30_0.125	15	1.27
23	30_0.125	11	0.93
	average tool life	12	0.99
9	25_0.125	41	4.15
29	25_0.125	43	4.36
18	25_0.125	43	4.36
39	25_0.125	41	4.15
	average tool life	42	4.26
4	20_0.125	204	25.82
6	20_0.125	191	24.18
14	20_0.125	143	18.10
11	20_0.125	195	24.68
	average tool life	183	23.20

### D2 Plate 2 492 HLD

Drill No.	Cutting parameters (speed m/min_feed rate mm/rev)	No. of 2.5xD holes at failure	Tool Life Time spent drilling (min)
1	30_0.125	15	1.27
10	30_0.125	14	1.18
13	30_0.125	15	1.27
27	30_0.125	17	1.44

16	30_0.125	15	1.27
	average tool life	15	1.28
15	25_0.125	57	5.78
8	25_0.125	52	5.27
24	25_0.125	53	5.37
3	25_0.125	54	5.47
20	25_0.125	63	6.38
	average tool life	56	5.65
25	20_0.125	186	23.54
5	20_0.125	216	27.34
2	20_0.125	228	28.86
26	20_0.125	210	26.58
	average tool life	210	26.58

D2 Plate 3 467 HLD

<b>Drill No.</b>	<b>Cutting parameters (speed m/min_feed rate mm/rev)</b>	<b>No. of 2.5xD holes at failure</b>	<b>Tool Life Time spent drilling (min)</b>
52	35_0.125	25	1.81
49	35_0.125	28	2.03
45	35_0.125	31	2.24
48	35_0.125	24	1.74
	average tool life	27	1.95
41	30_0.125	57	4.81
44	30_0.125	43	3.63
54	30_0.125	62	5.23
53	30_0.125	60	5.06
	average tool life	56	4.69
42	25_0.125	202	20.47
51	25_0.125	207	20.97
46	25_0.125	160	16.21
50	25_0.125	203	20.57
	average tool life	193	19.56
21	20_0.125	79	10.00
7	20_0.125	22	2.78
47	20_0.125	145	18.35
43	20_0.125	115	14.56
	average tool life	90	11.42

## References

1. Astakhov, V.P., *Geometry of Single-point Turning Tools and Drills Fundamentals and Practical Applications*. Springer Series in Advanced Manufacturing, 2010: Springer. 565.
2. Kopač, J. and S. Dolinšek, *ADVANTAGES OF EXPERIMENTAL RESEARCH OVER THEORETICAL MODELS IN THE FIELD OF METAL CUTTING*. *Experimental Techniques*, 1996. **20**(3): p. 24-28.
3. Kopac, J., M. Sokovic, and S. Dolinsek, *Tribology of coated tools in conventional and HSC machining*. *Journal of Materials Processing Technology*, 2001. **118**(1-3): p. 377-384.
4. Shaw, M.C., *Metal Cutting Principles*. Second Edition ed. 2005: Oxford University Press.
5. Astakhov, V.P., *On the inadequacy of the single-shear plane model of chip formation*. *International Journal of Mechanical Sciences*, 2005. **47**(11): p. 1649-1672.
6. Suri, R., *World Machine Tool Cutting Tool Markets*. 2000.
7. Analysts, G.I. *High Speed Steel (HSS) Metal Cutting Tools 2009*; Available from: [http://www.strategy.com/HighSpeedSteel\(HSS\)MetalCuttingToolsMarketReport.aspx](http://www.strategy.com/HighSpeedSteel(HSS)MetalCuttingToolsMarketReport.aspx).
8. Quinto, D. *The Tool Company Executive Decision on All This PVD Stuff in World Markets and Technology for Advanced Coatings and Surface Treatments for Cutting Tools and Wear Parts*. 2000. Atlanta USA: Gorham.
9. Atkins, T., *The science and engineering of cutting: the mechanics and processes of separating and puncturing biomaterials, metals and non-metals*. 2009: Butterworth-Heinemann.
10. Iyer, R., P. Koshy, and E. Ng, *Helical milling: An enabling technology for hard machining precision holes in AISI D2 tool steel*. *International Journal of Machine Tools and Manufacture*, 2007. **47**(2): p. 205-210.
11. Gardner, T.a.W.S., *USA 2011 Breakdown of Cutting Tools by Category*. 2010.
12. Vogel, J. and E. Bergmann, *Problems encountered with the introduction of ion plating to large-scale coatings of tools*. *J. VAC. SCI. & TECHNOL. A*, 1986. **4**(6 , Nov.-Dec. 1986): p. 2731-2739.
13. Davim, J.P., *Machining Fundamentals and Recent Advances* 2008: Springer.
14. Trent, E, W.P., *Metal Cutting* 4th edition ed. 2000: Butterworth-Heinemann.
15. Carter, A.D.S., *Mechanical reliability*. Vol. 1. 1986: Macmillan London.
16. Barish, H.B., *Split-point twist drill*. 1985, Google Patents.
17. Lyman, T., *METALS HANDBOOK; ; VOL. 3; MACHINING*. 1967.
18. Kang, D., *Geometrical analysis and CAD/CAM software for twist drills*. 1997: University of Melbourne (Department of Mechanical and Manufacturing Engineering).
19. Galloway, D., *Some experiments on the influence of various factors on drill performance*. *Trans. ASME*, 1957. **79**(2): p. 191.
20. Harris, S.G., *Improving the dry machining performance of advanced physical vapour deposited coatings with particular reference to applications in the automotive industry*, in *School of Engineering and Science*. 2003, Swinburne University of Technology: Melbourne.
21. Sproul, W.D. and R. Rothstein, *High rate reactively sputtered TiN coatings on high speed steel drills*. *Thin Solid Films*, 1985. **126**(3-4): p. 257-263.
22. Jamal, T., R. Nimmagadda, and R.F. Bunshah, *Friction and adhesive wear of titanium carbide and titanium nitride overlay coatings*. *Thin Solid Films*, 1980. **73**(2): p. 245-254.



23. Doyle, E.D. and D.M. Turely, *Microstructural Behaviour - Its Influence on Machining* The American Society of Mechanical Engineers, 1982.
24. Committee, A.I.H., *Properties and selection: irons, steels, and high-performance alloys*. 1990.
25. Holmberg, K. and A. Mathews, *Coatings Tribology - Properties, Techniques and Applications in Surface Engineering*. 1994, Elsevier Amsterdam.
26. Astakhov, V.P., M.O.M. Osman, and M. Al-Ata, *Statistical Design of Experiments in Metal Cutting - Part One: Methodology*. Journal of Testing and Evaluation, 1997. **25**(3): p. 322-327.
27. Radhakrishnan, T., S. Wu, and C. Lin, *A mathematical model for split point drill flanks*. Journal of Engineering for Industry, 1983. **105**(3): p. 137-142.
28. Linman, R. *Carbide Inserts: Price vs. Productivity - You Be the Judge*. 2004 2007.
29. Taylor, F.W., *On the Art of Cutting Metals*, in *Proceeding of The American Society of Mechanical Engineers*. 1906, The American Society of Mechanical Engineers New York.
30. Ulutan, D. and T. Ozel, *Machining induced surface integrity in titanium and nickel alloys: A review*. International Journal of Machine Tools and Manufacture, 2011. **51**(3): p. 250-280.
31. Choudhury, I.A. and M.A. El-Baradie, *Machinability of nickel-base super alloys: a general review*. Journal of Materials Processing Technology, 1998. **77**(1-3): p. 278-284.
32. Smith, G.T., *Advanced Machining - The Handbook of Cutting Technology* 1989: Springer - Verlag.
33. Gumpel, P.H., E. , TETB, 1983. **13**.
34. Giménez, S., et al., *Sintering behaviour and microstructure development of T42 powder metallurgy high speed steel under different processing conditions*. Materials Science and Engineering: A, 2008. **480**(1-2): p. 130-137.
35. Kumar, A.K.N., M. Watabe, and K. Kurokawa, *The sintering kinetics of ultrafine tungsten carbide powders*. Ceramics International, 2011. **37**(7): p. 2643-2654.
36. Aramcharoen, A., et al., *Evaluation and selection of hard coatings for micro milling of hardened tool steel*. International Journal of Machine Tools and Manufacture, 2008. **48**(14): p. 1578-1584.
37. Cozza, R.C., D.K. Tanaka, and R.M. Souza, *Micro-abrasive wear of DC and pulsed DC titanium nitride thin films with different levels of film residual stresses*. Surface and Coatings Technology, 2006. **201**(7): p. 4242-4246.
38. ISO, *Tool-life testing with single-point turning tools*. 1993.
39. von Tunzelmann, N., *Historical coevolution of governance and technology in the industrial revolutions*. Structural Change and Economic Dynamics, 2003. **14**(4): p. 365-384.
40. Lugscheider, E., K. Bobzin, and K. Lackner, *Investigations of mechanical and tribological properties of CrAlN+C thin coatings deposited on cutting tools*. Surface and Coatings Technology, 2003. **174-175**(0): p. 681-686.
41. Posti, E. and I. Nieminen, *Influence of coating thickness on the life of TiN-coated high speed steel cutting tools*. Wear, 1989. **129**(2): p. 273-283.
42. ME/10, c.A.N.Z., *Drills and reamers*. 1994: Standards Australia.
43. Time, I., *Resistance of Metals and woods to cutting* Dermacow, St.Petersberg, Russia, 1870.

44. Doyle, E.D., J.G. Horne, and D. Tabor, *Frictional interactions between chip and rake face in continuous chip formation* Proceedings of the Royal Society London 1978. **366**: p. 173-183.
45. Merchant, M.E., *Mechanics of the Metal Cutting Process. II. Plasticity Conditions in Orthogonal Cutting*. Journal of Applied Physics, 1945: p. 7.
46. Atkins, T., *Toughness and processes of material removal*. Wear, 2009. **267**(11): p. 1764-1771.
47. Atkins, T., *Chapter 3 - Simple Orthogonal Cutting of Floppy, Brittle and Ductile Materials*, in *The Science and Engineering of Cutting*. 2009, Butterworth-Heinemann: Oxford. p. 35-74.
48. Trent, E.M., *Conditions of Seizure at the Tool Work Interface*. Iron and Steel Institute 1967. **special report 94**.
49. Hogmark, S. and M. Olsson, *Wear Mechanisms of HSS Cutting Tools*, The Angstrom Laboratory. p. 14.
50. Söderberg, S. and S. Hogmark, *Wear mechanisms and tool life of high speed steels related to microstructure*. Wear, 1986. **110**(3-4): p. 315-329.
51. *Wear of cutting tools : G. Barrow*, Tribology, 5 (1) (1972) 22-30; 12 figs., 18 refs. Wear, 1972. **21**(2): p. 415.
52. Cselle, T., *Influence of Edge Preparation on the Performance of Coated Cutting Tools*, in *International Conference Metalurgical Coatings Thin Coatings 2007*: San Diego. p. 34.
53. Williams, J., E. Smart, and D.R. Milner, *Metallurgia: the British Journal of Metals*, 1970. **81**(3): p. 51-89.
54. Astakhov, V.P., M. O. M. Osman, *An analytical evaluation of the cutting forces in self-piloting drilling using the model of shear zone with parallel boundaries* International Journal of Machine Tools and Manufacture, 1996. **36**.
55. Gómez, M.P., et al., *Tool wear evaluation in drilling by acoustic emission*. Physics Procedia, 2010. **3**(1): p. 819-825.
56. Marksberry, P.W. and I.S. Jawahir, *A comprehensive tool-wear/tool-life performance model in the evaluation of NDM (near dry machining) for sustainable manufacturing*. International Journal of Machine Tools and Manufacture, 2008. **48**(7-8): p. 878-886.
57. Niebel, B.W., A.B. Draper, and R.A. Wysk, *Modern manufacturing process engineering*. 1989: McGraw-Hill New York.
58. Boston, O.W., *Metal processing*. 1941, New York, NY: Wiley.
59. Lau, W., P. Venuvinod, and C. Rubenstein, *The relation between tool geometry and the Taylor tool life constant*. International Journal of Machine Tool Design and Research, 1980. **20**(1): p. 29-44.
60. Logothetis, N., *Managing for Total Quality From Deming to Taguchi and SPC*. The Manufacturing Practitioner Series. 1992: Prentice Hall.
61. Devore, J.L., *Probability and Statistics for Engineering and the Sciences*. 7th ed. 2007: Thomson Brooks/Dale.
62. Salkind, N.J., *Statistics for People who (think They) Hate Statistics: Excel 2010 Edition*. 2012: Sage.
63. Milliken, G.A., Johnson, D.E., *Analysis of Messy Data*. Vol. Volume 1. 1984: Van Nostrand Reinhold.
64. Ronniger, C., *Reliability Analyses with Weibull*. 2012: [www.crgraph.com](http://www.crgraph.com).
65. Dowey, S.J., et al., *Life analysis of coated tools using statistical methods*. Surface and Coatings Technology, 1999. **116-119**: p. 654-661.

66. Dowey, S.J., B. Rähle, and A. Matthews, *Performance analysis of coated tools in real-life industrial experiments using statistical techniques*. Surface and Coatings Technology, 1998. **99**(1-2): p. 213-221.
67. Sutton, T., *Training Module for the Mowhawk 1999*, Sutton Tools: Melbourne.
68. Hoyle, G., *High Speed Steels*. 1988: Butterworths.
69. Balzers, O. *Balinit Futura Top, Reliability to the doph.*
70. Davis, J.R., K. Mills, and S. Lampman, *Metals Handbook. Vol. 1. Properties and Selection: Irons, Steels, and High-Performance Alloys*. ASM International, Materials Park, Ohio 44073, USA, 1990. 1063, 1990.
71. Bickenbach, S., *Cryodur 2379 Technical Data Sheet*.
72. Uddeholm, B., *Uddenholm Impax Supreme*, Uddeholm, Editor. 2011.
73. Boubekri, N., J. Rodriguez, and S. Asfour, *Development of an aggregate indicator to assess the machinability of steels*. Journal of Materials Processing Technology, 2003. **134**(2): p. 159-165.
74. Tukey, J.W., *Exploratory data analysis*. 1977. Massachusetts: Addison-Wesley, 1976.
75. Roberts, G.A., Cary, R, A,, *Tool Steels*. 4th ed. 1980: American Society for metals.
76. Brandt, D.A., Warner, J. C., *Metallurgy Fundamentals*. 4th ed. 2005, Illinois: The Goodheart-Willcox Company, Inc.
77. Misra, A. and I. Finnie, *A classification of three-body abrasive wear and design of a new tester*. Wear, 1980. **60**(1): p. 111-121.
78. Leed, R.M., *Tool and Die Making Troubleshooter*. 2003: SME.
79. Dolodarenko, A. and I. Ham, *Effects of built-up edge in drilling*. Journal of Engineering for Industry, 1976. **98**(1): p. 287-292.
80. Uddeholm, B., *Bohler K110 Cold Work Tool Steel*.
81. Sutton, T., *Sutton Tools Industrial Catalogue*. 2011: Melbourne.
82. Machinability Data Center, *Machining Data Handbook*. 2nd ed. 1972, Cincinnati: Machinability Data Centre Metcut Research Associates Inc.
83. Armarego, E.J.A., *Some fundamental and practical aspects of twist drills and drilling*. Journal of Materials Processing Technology, 1994. **44**(3-4): p. 189-198.
84. Czopor, E.J., *Twist Drills*, in *ASME B94.11M-1993*. 1993, The American Society of Mechanical Engineers: New York.
85. Leeb, D., *Dynamic hardness testing of metallic materials*. NDT International, 1979. **12**(6): p. 274-278.
86. Haggerty, W., *Effect of point geometry and dimensional symmetry on drill performance*. International Journal of Machine Tool Design and Research, 1961. **1**(1): p. 41-58.
87. Abele, E. and M. Fujara, *Simulation-based twist drill design and geometry optimization*. CIRP Annals - Manufacturing Technology, 2010. **59**(1): p. 145-150.
88. Chen, W.-C., et al., *Design optimization of a split-point drill by force analysis*. Journal of Materials Processing Technology, 1996. **58**(2): p. 314-322.
89. Sugihara, T. and T. Enomoto, *Crater and flank wear resistance of cutting tools having micro textured surfaces*. Precision Engineering, 2013. **37**(4): p. 888-896.
90. Sarwar, M., *Application of advanced surface engineering treatments to multi-point cutting edges*. Surface and Coatings Technology, 1998. **108-109**(0): p. 612-619.
91. Arunachalam, R.M., M.A. Mannan, and A.C. Spowage, *Surface integrity when machining age hardened Inconel 718 with coated carbide cutting tools*. International Journal of Machine Tools and Manufacture, 2004. **44**(14): p. 1481-1491.

92. Lalwani, D.I., N.K. Mehta, and P.K. Jain, *Experimental investigations of cutting parameters influence on cutting forces and surface roughness in finish hard turning of MDN250 steel*. Journal of Materials Processing Technology, 2008. **206**(1–3): p. 167-179.
93. Bradbury, S.R., D.B. Lewis, and M. Sarwar, *The effect of product quality on the integrity of advanced surface engineering treatments applied to high speed steel circular saw blades*. Surface and Coatings Technology, 1996. **85**(3): p. 215-220.
94. Bradbury, S.R., et al., *Impact of surface engineering technologies on the performance and life of multi-point cutting tools*. Surface and Coatings Technology, 1997. **91**(3): p. 192-199.
95. Handbook, A., *Vol. 5: Surface Engineering*. ASM International, Materials Park, OH, 1994: p. 345-347.
96. Fischerscope, X.-R., *Fischerscope X-Ray Product Line* <http://pdf.directindustry.com/pdf/fischer/fischerscope-x-ray/54320-66428.html>, Fischer.
97. Bouzakis, K.D., et al., *Effect of dry micro-blasting on PVD-film properties, cutting edge geometry and tool life in milling*. Surface and Coatings Technology, 2009. **204**(6–7): p. 1081-1086.
98. Miller, R.G., *Beyond ANOVA, Basics of Applied Statistics* 1986, New York: John Wiley & Sons.
99. Armarego, E., et al., *An appraisal of empirical modeling and proprietary software databases for performance prediction of machining operations*. Machining science and technology, 2000. **4**(3): p. 479-510.
100. Hoffman, E.G., *Fundamentals of tool design*. 1984: Society of Manufacturing Engineers Dearborn, Mich.
101. Wang, H.-P.b. and R.A. Wysk, *An expert system for machining data section*. Computers & Industrial Engineering, 1986. **10**(2): p. 99-107.
102. Venkatesh, V. *Computerised machinability data*. in *Proceedings of Automach*. 1986. Australia, Sydney,: SME.
103. Song, Q., et al., *Subdivision of chatter-free regions and optimal cutting parameters based on vibration frequencies for peripheral milling process*. International Journal of Mechanical Sciences, 2014. **83**(0): p. 172-183.
104. Tomas, P. and R. Smith. *The wear failure of titanium nitride coated drills*. in *Third International Conference on Manufacturing Engineering 1986: Technology for Manufacturing Growth; Preprints of Papers, The*. 1986: Institution of Engineers, Australia.